Escuela Politécnica Superior de

Grado en Ingeniería Geomática y Topográfica

UNIVERSIDAD DE JAÉN

ESCUELA POLITÉCNICA SUPERIOR de Jaén

Trabajo Fin de Grado

GENERATION OF DIGITAL TERRAIN AND SURFACE MODELS FROM INFORMATION CAPTURED BY LIDAR SENSOR

Student Mohamed Amine Shil

Supervisor : Professor Jorge Delgado García

Dpto Ingeniería Cartográfica, Geodésica y Fotogrametría

September, 2023

UNIVERSIDAD DE JAÉN

ESCUELA POLITÉCNICA SUPERIOR

Departamento Ingeniería Cartográfica, Geodésica y Fotogrametría

Dr. Jorge Delgado García, Supervisor of the BSc Thesis entitled

GENERATION OF DIGITAL TERRAIN AND SURFACE MODELS FROM INFORMATION CAPTURED BY LIDAR SENSOR

That presents Mohamed Amine Shil, authorizes its presentation for defense and evaluation at the Escuela Politécnica Superior de Jaén (Spain), September 2023

Student **Supervisor**

Mohamed Amine Shil **Prof. D. Jorge Delgado García**

ACKNOWLEDGMENTS

First, I would like to express my warmest thanks to **Dr. Jorge Delgado Garcia**, my supervisor, and teacher at **the University of Jaén**, who did not spare any effort to support me and guide me all throughout the period of the IEP, for his gracious help, as well as for his advice and kindness and for the chance he gave me to carry out this project.

I exceptionally thank **Dr. Mohamed Khaled Bouzid**, my supervisor and Teacher at **the Higher School of Aeronautics and Technologies (ESAT)**, who prompted me to come up with my ideas with her relevant suggestions, encouragement, directives, and support.

I would also like to thank the Jury President for accepting the heavy task of judging my work and chairing the Jury for my Defense.

I would also like to thank the Reviewer for accepting the onerous task of judging my work and Graduation Project report.

I would also like to thank all the staff of **the University of Jaén**, who helped me directly or indirectly in the development of this work and the smooth running of my internship.

Finally, I would like to extend my warm thanks to all my trainers and the administration leaders of the Higher School of Aeronautics and Technologies (ESAT)

Table of Content

List of figures

List of tables

Abbreviation list

3D: Three Dimension

ASCII: American Standard Code for Information Interchange

ATM: Aerial Topographic Mapper

CNIG: Centro Nacional de Informacion Geografica

DSM: Digital Surface Model

DTM: Digital Terrain Model

EPSG: European Petroleum Survey Group

ETRS: European Terrestrial Reference System

GIS: Geographic Information System

GNSS: Global Navigation Satellite System

GPS: Global Positioning System

GRS: Geodetic Reference System

IDW: Inverse Distance Weighting

IGN: Institut géographique national

IMU: Inertial Metric Unit

INS: Inertial Navigation System

LAS: LiDAR Aerial Survey

LAZ: LiDAR Aerial Survey Zip

LiDAR: Light Detection And Ranging

NASA: National Aeronautics and Space Administration

NEON: National Ecological Observatory Network

NOAA: National Oceanic and Atmospheric Administration

PNG: Portable Network Graphics

PNOA: Plan Nacional de Ortofotografía Aérea (National Aerial Orthophotography Plan)

RMSE: Root Mean Square Error

SIA: Simplified Isohyetal Adjustement

TIN: Triangulated Irregular Network

UAV: Unmanned Aeronautical Vehicle

UTM: Universal Transverse Mercator

General introduction

The airborne LiDAR methodology is a pivotal invention in modern reality capture approaches, exemplifying cutting-edge technology that has received widespread recognition in a variety of scientific and practical sectors. Its implementation represents a paradigm change in spatial data collecting, transforming fields such as architecture, urban planning, archaeology, agriculture, bathymetry, and military operations. LiDAR technology has grown into an invaluable tool, permitting the painstaking collection, analysis, and modeling of three-dimensional surroundings with unprecedented precision, thanks to its intrinsic aptitude for high-resolution point cloud creation. In the next chapters of this thesis, we will dive deep into the multiple uses of airborne LiDAR, diving into the complexities of its deployment and the revolutionary impact it has on reality capture. This research intends to shed light on the deep scientific contributions of LiDAR technology as well as its key position in the current landscape of spatial data collecting and processing.

In order to obtain the engineering degree in geomatics and topography and to finalize our studies, we have to do a project in which we will use our academic knowledge and professional experience acquired along these five years of studies and internships. Based on my End of the Year Project entitled “Difference between terrestrial and airborne LiDAR”, in which I detailed various aspects of the airborne LiDAR (Light Detection And Ranging) systems, I decided to continue to dive in this powerful system and explain this technology and to have a real case study.

IGN (National Geographic Institution) of Spain have lunched a national LIDAR acquisition of all the Spain territory under the PNOA project. This acquisition is obtained regularly in order to keep the data updated, and our study area project is located in the southern west of Castilla La Mancha and it’s limited to an area of 1:50000 sheet. the actual data were submitted to the University Of Jaén as they presented problems between passes.

The main goal of this project is to create Digital Surface and Terrain models from the acquired point cloud data. A primary aim is to establish a well-defined pipeline and process for processing LiDAR data with an emphasis on quality control and debugging errors.

The methodology consists of running a data quality checking, debugging errors, filtering and classifying the point cloud and then generate the DTM (Digital Terrain Model) and the DSM (Digital Surface Model).

How does LiDAR work, and what is an airborne LiDAR sensor? Furthermore, what processes should be put in place to assure the utility and quality of the data obtained by this sensor, as well as how Digital Terrain Models (DTM) and Digital Surface Models (DSM) are created from LiDAR data?

This Manuscript will be divided in two basic parts:

- The first part presents the LIDAR technology and its different components. In addition to presenting the PNOA project in which the mission have took place.
- The second part will talk about the national LiDAR projects and PNOA project as an example.
- The third part will present and illustrate the practical component in generating DSM and DTM from quality control, debugging errors, to delivering the required products.

Chapter 1 Theoretical component LiDAR technology

I. Introduction

In this chapter, we are going to represent first of all: the background of the technology used during our project by defining the LIDAR technology and its different components. Secondly, the sources of error of a LiDAR system. Thirdly, the surface and terrain digital models and their mathematical aspects. Finally, we are going to talk about the quality control and its importance in big projects.

II. LiDAR

1. Introduction to LiDAR

LiDAR, which is commonly spelled LiDAR and also known as LADAR or Laser altimetry, is an acronym for Light Detection And Ranging. It refers to a remote sensing technology that emits intense, focused beams of light and measures the time it takes for the reflections to be detected by the sensor. This information is used to compute ranges, or distances, to objects. In this manner, LiDAR is analogous to radar (radio detecting and ranging), except that it is based on discrete pulses of Laser light. The three-dimensional coordinates (e.g., x,y,z or latitude, longitude, and elevation) of the target objects are computed from

- ❖ The time difference between the Laser pulse being emitted and returned
- ❖ The angle at which the pulse was "fired"
- ❖ The absolute location of the sensor on or above the surface of the Earth.

There are two classes of remote sensing technologies that are differentiated by the source of energy used to detect a target passive systems and active systems. Passive systems detect radiation that is generated by an external of energy, such as the sun, while active systems generate and direct energy toward a target and subsequently detect the radiation. LiDAR systems are active systems because they emit pulses of light (i.e. the Laser beams) and detect the reflected light. This characteristic allows LiDAR data to be collected at night when the air is usually clearer and the sky contains less air traffic than in the daytime. In fact, most LiDAR data are collected at night. Unlike radar, LiDAR cannot penetrate clouds, rain, or dense haze and must be flown during fair weather. **(National Oceanic and Atmospheric Administration (NOAA) Costal Services Center, 2012)**

At sampling rates greater than 6 MHz (i.e., 150,000 pulses per second), LiDAR devices can swiftly monitor the Earth's surface. The end result is a densely spaced network of very precise georeferenced elevation points (figure 1) that may be used to build three-dimensional representations of the Earth's surface and its features.

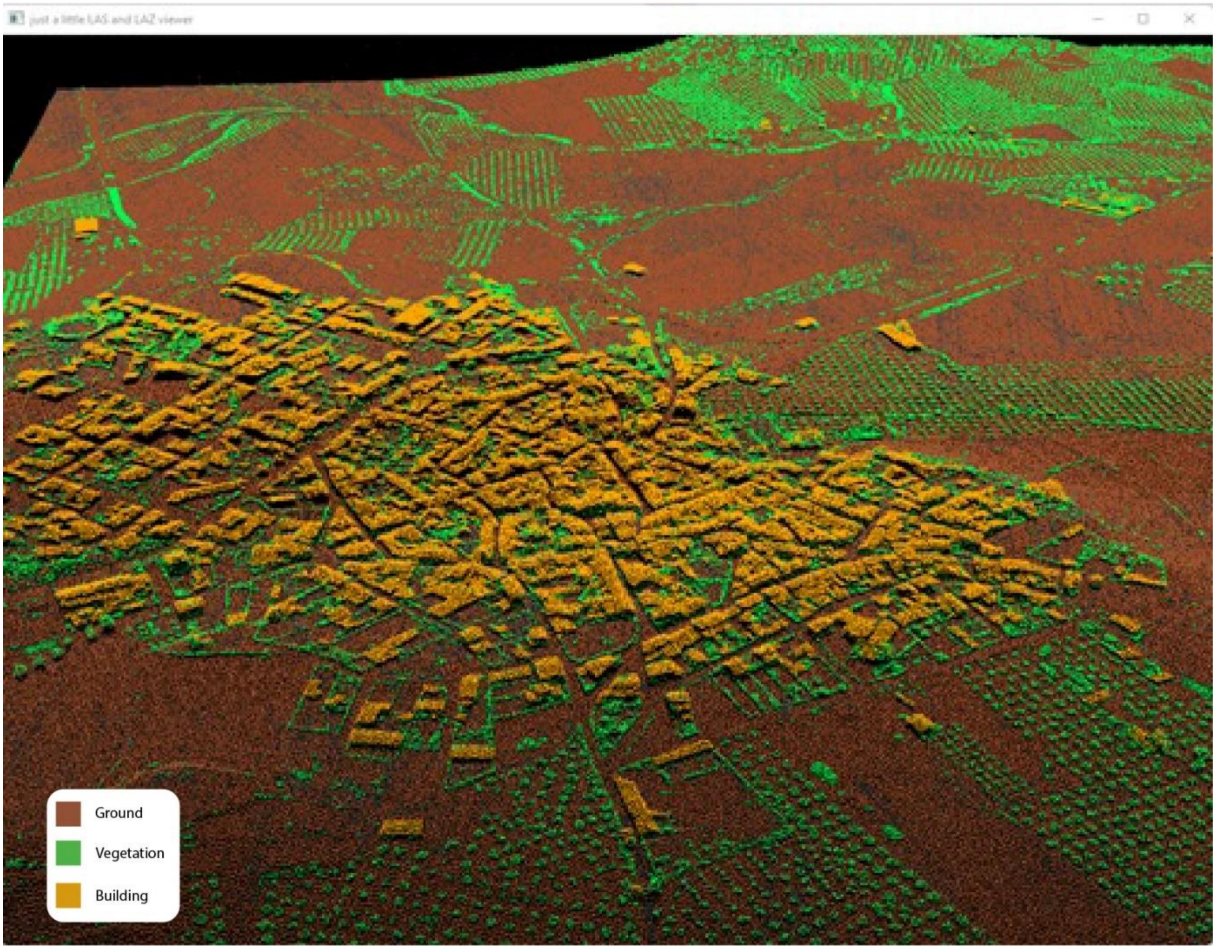

Figure 1 : LiDAR dense cloud example from the study area

Many LiDAR systems operate in the near-infrared area of the electromagnetic spectrum, while some sensors can also penetrate water and detect bottom structures in the green band, you can see the two electromagnetic spectrum in the figure 2. Bathymetric LiDAR devices can be used to estimate seabed heights in locations with generally clear water. LiDAR-derived heights typically have absolute accuracies of 6 to 12 inches (15 to 30 cm) for older data and 4 to 8 inches for newer data and for older data and 4 to 8 inches (10 to 20 centimeters) for more recent data; relative accuracies (e.g., heights of roofs, hills, banks, and dunes) are even better.

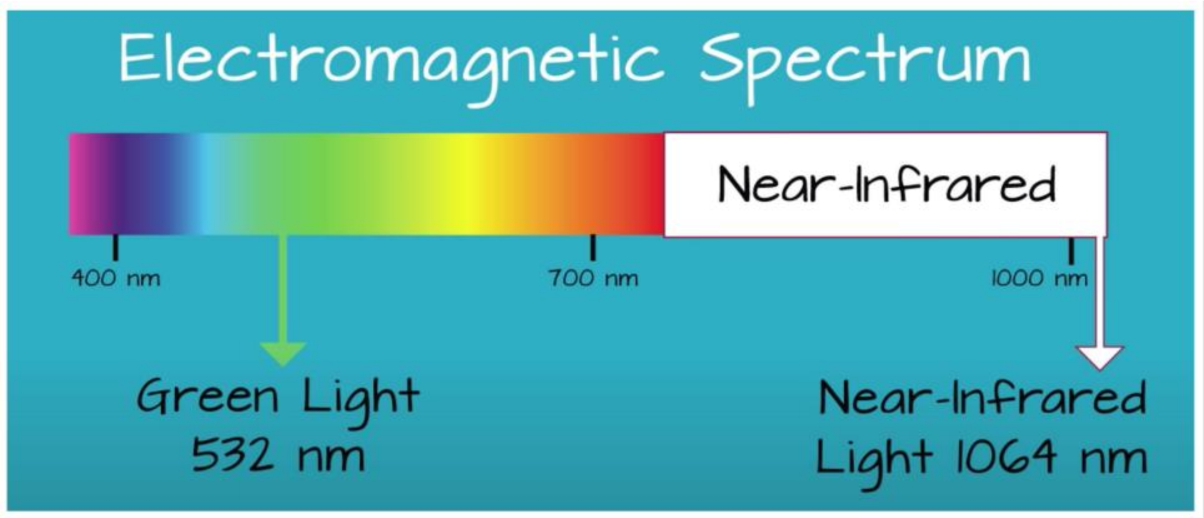

Figure 2 : wavelength of the electromagnetic spectrum (NEON)

When gathering elevation data using remote sensing data gathered from above the Earth's surface (e.g., airplanes or satellites), the capacity to "see under trees" is a repeating aim. The majority of the larger scale elevation data sets were created utilizing remote sensing methods that are unable to penetrate vegetation. LiDAR is no exception; nonetheless, there are usually enough individual "points" to give enough coverage in wooded regions, even if only a tiny number of them reach the ground via the trees. LiDAR, in effect, can see through gaps in the canopy or vegetation. Dense woods or locations with total covering (such as a rain forest), on the other hand, sometimes have few "openings" and hence poor ground representation. A rule of thumb is that if you can look up and see the sky through the trees, then that location can be measured with LiDAR. For this reason, collecting LiDAR in “leaf off” conditions is advantageous for measuring ground features in heavily forested areas.

2. Historical review

The history of LiDAR technology is long and colourful, spanning several decades. Its beginnings may be found in the early 20th century, when scientists started experimenting with light-based ranging methods. The first Laser ranging device, which used reflected Laser pulses to measure distances to the moon, was created by Hughes Aircraft Company in 1961, heralding the infancy of what would later grow into LiDAR technology.

Following then, LiDAR established itself in a number of uses. It became widely used in atmospheric research in the 1960s and 1970s, allowing researchers to precisely monitor cloud height and density. Due to improvements in Laser technology, LiDAR systems have been integrated into aerial platforms for topographic mapping and forestry surveys.

The 1980s saw substantial advances in LiDAR remote sensing. NASA's aerial LiDAR devices, such as the aerial Topographic Mapper (ATM), were critical in mapping the topography of the Earth and gathering significant data for scientific study. These breakthroughs cleared the path for LiDAR integration onto satellite platforms, enabling global-scale mapping and opening up new opportunities for Earth observation.

In the 1990s, the combination of LiDAR and GPS technologies constituted a watershed moment in the area of geospatial mapping. Because of LiDAR's unrivalled precision and resolution, very detailed point clouds were created, resulting in exact 3D digital elevation models (DEMs) and surface reconstructions. This invention changed the way applications like topography mapping, urban modelling, and infrastructure planning were done.

Another key milestone for LiDAR technology in the twenty-first century was its incorporation into autonomous cars. The capacity of LiDAR to gather real-time 3D information became crucial for object identification and perception systems as the quest of self-driving automobiles gained traction. Autonomous driving capabilities improved as solid-state LiDAR and the merging of LiDAR with other sensor technologies advanced, bringing us closer to a future of safer and more efficient transportation**.(Florant Petit. (2019)).**

LiDAR has found applications in environmental monitoring and conservation initiatives beyond from mapping and autonomous cars. LiDAR systems, both airborne and satellite-based, have proven useful in analyzing forest changes, measuring biodiversity, monitoring shoreline erosion, and tracking the effects of climate change. These large-scale data collecting skills have been critical in understanding and maintaining our natural res.

Finally, LiDAR technology has progressed from its inception to become a ubiquitous and vital tool in a variety of sectors. Its evolution from laser range systems to mapping, autonomous cars, and environmental monitoring shows the constant pursuit of innovation and the transformational potential of scientific advances. As technology advances, LiDAR's potential expands, suggesting even more possibilities in domains yet to be explored.

Figure 3 : Chronological approach to LIDAR development (mvtgeosolutions.com)

The figure 3 describes perfectly the different phases and important dates for the advancement of the LIDAR technology.

3. Components

3.1. Laser

The Laser is the main component in the LiDAR system. It emits beam of laser light in the form of infrared or sometimes green wavelength. The wavelength of the laser is determined by the application and the desired properties, such as the ability to penetrate vegetation or the reflectivity of the target surface. There are two types of laser wave, discrete and full waveform.

There are a lot of types in laser, which depend on the cost, wavelength, pulse duration, pulse repetition rate, energy output, beam divergence, beam quality stability, size and weight, power consumption and safety. All of these factors differ from one sensor to another, and usually they differ in their application.

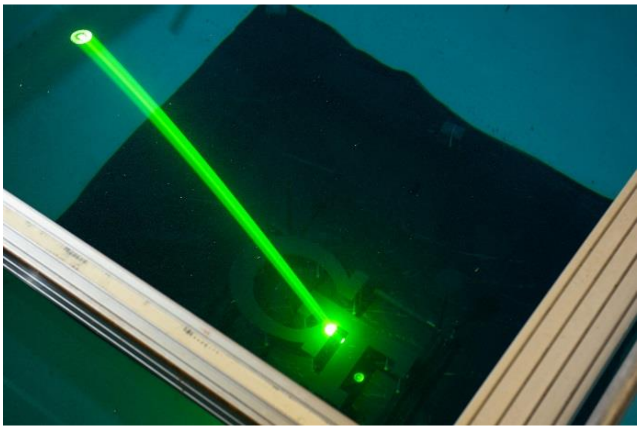

Figure 4 : laser beam in green wavelength (opli.net)

3.2. Scanner or Mirror system

Scanning LiDARs have beam deflecting units or scanner units that deflect the laser beam in different directions to perform ranging measurements, creating unique patterns in the point cloud. These patterns have different characteristics such as number of scan lines or dot density. Depending on the application in which the LiDAR will be used, the characteristics of the scan pattern can be important. For example, in a people counting application, depending on the number of people present in a certain area, a high resolution point cloud can be crucial. In order to achieve the required resolution, a high number of scan lines is required. laser scanners can be rotating or non-rotating, using different deflecting optical elements such as prisms, gratings and mirrors creating specific scanning patterns. There are mainly four types of models which vary according to the type of optical elements

3.2.1. The oscillating mirror

Lasers using oscillating mirrors direct laser pulses in two directions across the web, creating a jagged pattern on the floor. The width of the band is given by the maximum angle of inclination of the mirror. The resulting dot density is not uniform because the laser pulses tend to accumulate at the edges of the web due to mirror deceleration, the figure 9 summarize the phenomena.

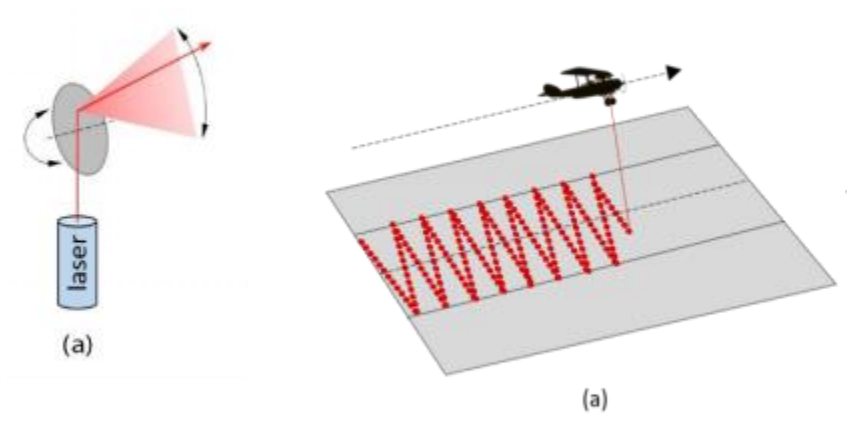

Figure 5 : Oscillating mirror (cours cartographie urbain)

3.2.2. The rotating polygone mirror

This system creates a sweeping pattern consisting of parallel lines oblique to the direction of platform progression. Here, the sweep is always in the same direction. The width of the strip depends on the width of the face of the polygonal mirror, the figure 10 summarize the phenomena.

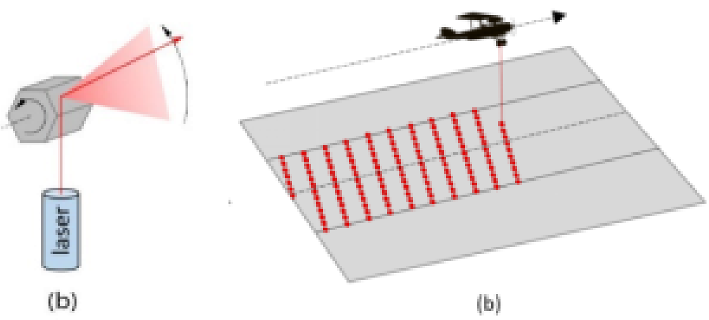

Figure 6 : Rotating mirror (cours cartographie urbain)

3.2.3. The rotating mirror

With its axis of rotation collinear with the direction of the laser beam emitted by the rotating mirror can scan almost 360°. As in the previous example, the scan pattern is composed of parallel lines oblique to the direction of system motion. This time, the size of the band depends on the maximum range of the LiDAR system.

3.2.4. Prisme or dispersive grating

Dispersive prisms as well as dispersive gratings rotate around the same axis to generate rose-like scanning patterns. For example, Risley prisms - also called wedge prisms - can form circles or sweeping rose-like patterns, the figure 11 summarize the phenomena.

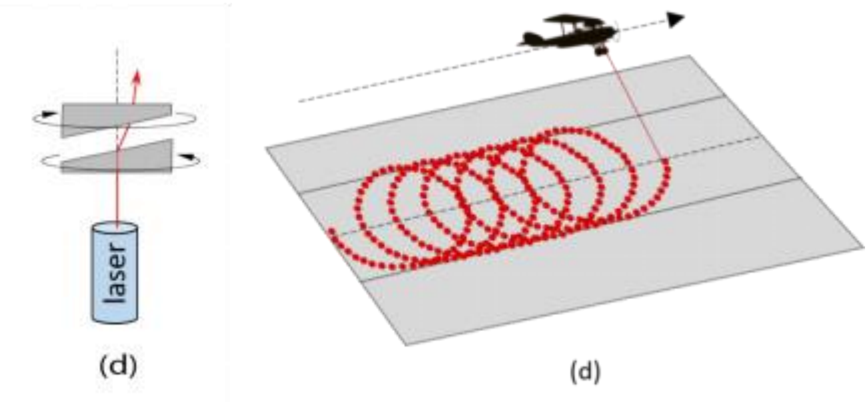

Figure 7 : Prisme (cours cartographie urbain)

3.3. Receiver

The receiver is a sensitive sensor that detects the reflected laser pulses from the target objects or surfaces. When a laser pulse collides with an item, it bounces back and is picked up by the receiver. The receiver records the time it takes for the pulse to return, as well as the angle at which it was reflected, in order to properly determine the distance to the object.

There are sensors that have two in one function, provides the source and receives the returns.

3.4. Global positioning system

In order to obtain georeferenced data, the sensor contains an inertial center records each of the movements (roll, pitch and yaw) in real time and with a very high frequency to understand what is the orientation, the direction and the movements or vibration produced in order to be able to correct the position of the measurements acquired in space, its accuracy depends on its frequency, the higher the frequency of the IMU the more precision we obtain. The system is connected with the GNSS satellite and a reference station through a receiver. (See figure) in addition to the flight height we can obtain, with a simple mathematical formula, the elevation of the ground or the objects. The distance between the receiver antenna of the GPS and the sensor is calculated with a very high precision and it is controlled every flight. It is also preferable to have at least one GPS station on the ground, close to the flight zone, to improve the geographical precision of the sensor.

The mathematical formula used to calculate the position of each point is:

$$\vec{X}_p = \vec{X}_{GPS} + \vec{X}_{IMU-GPS} + \vec{X}_{IMU-LiDAR} + \vec{\rho}_{LiDAR}$$

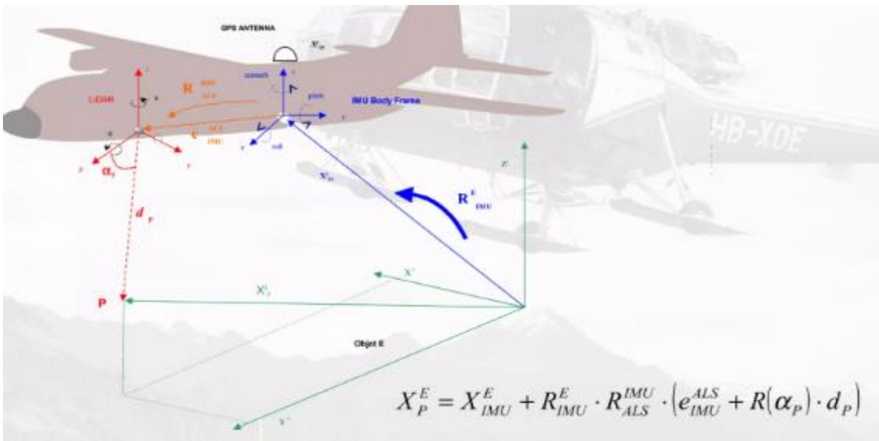

Figure 8 : Schema of the Georeferencing System in a plane for LiDAR sensor (National Geographic Institute)

The figure 8 represents a schema that simplify the phenomena and the relationships between the 3 components GPS, Sensor and ground reference.

3.5. Data acquisition and control unit

This device is in charge of controlling laser emission, scanner movement and data gathering. It synchronizes the laser firing with the scanner's location and captures the time-of-flight information, as well as the related angles, for each pulse.

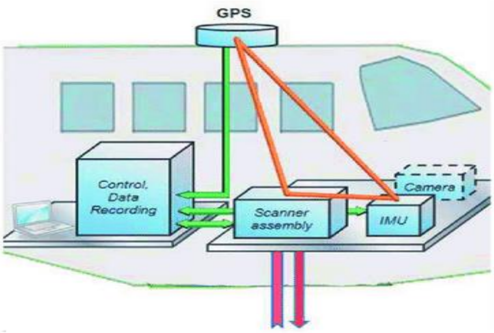

(a)

Figure 9 : Schema of information routes (google.com)

4. Source of Errors

Airborne LIDAR System is a complex integrated system, resulting in its accuracy affected by the interaction of the various components of the system. From Airborne LIDAR 'error sources being various even very complex, they can be divided into two major aspects: single error and integrated error, as shown in Figure.

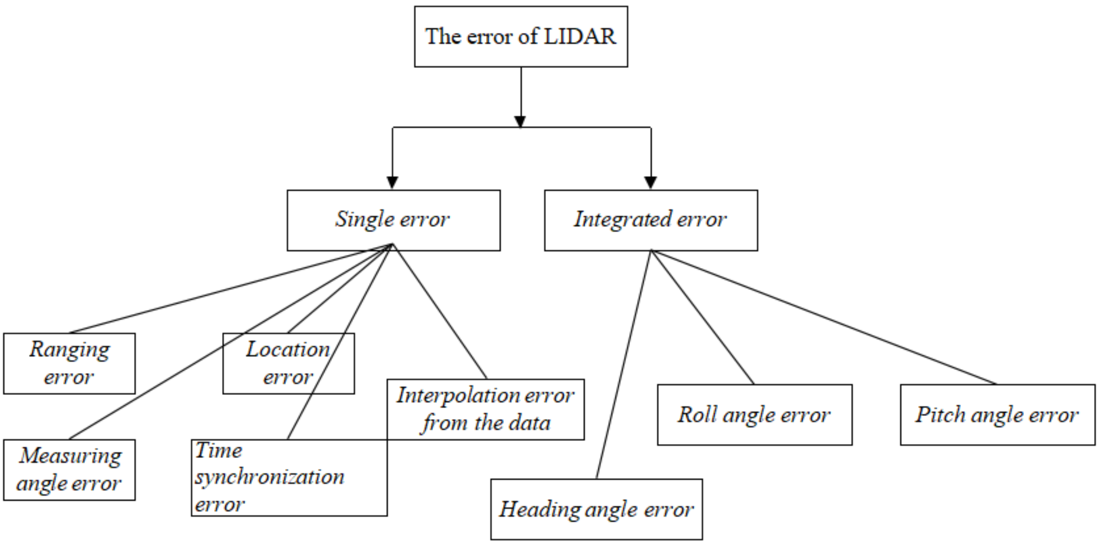

Figure 10: Error Category (H C Ren et al 2016 IOP Conf. Ser.: Earth Environ. Sci. 46 012030)

4.1. Single error

4.1.1. Ranging error

The core equipment used to be rangefinder about Airborne LIDAR System. All factors can affect the precision of laser pin point coordinates, but the ranging accuracy, which is the most complex. According to Schenk (2001), described the mathematical model, says that LIDAR point clouds no iuy;error geolocation equation:

$$P_w = P_{GPS} + R_w R_{GEO} R_{INS} (R_{lu} R_{LB} S + l_0) \quad (1)$$

Pw: laser target point coordinates in WGS84 ; PGPS : GPS antenna phase center coordinates in WGS84; RW : Local Ellipsoid System to the WGS-84 coordinate system transformation matrix; RGEO : Navigation frame transformation matrix to local ellipsoid system; RINS : IMU attitude where the carrier to coordinate the navigation frame transformation matrix; RLU: laser scanners IMU coordinate system to the coordinate transformation matrix carrier; RLB : The instantaneous position of the laser beam to the laser coordinate system coordinate system; S : laser spot position coordinates of the laser beam coordinate system; l0 : The eccentric amount of the emitted GPS antenna phase center to the center of the laser emission.

Be taken into account when RW, RGEO value is relatively small, LIDAR point cloud positioning equation can be rewritten as:

$$P^*_w = P_{GPS} + P_{GPS} + R_{INS}(R_{lu} R_{lu} R_{LB} R_{LB} (s + s) + l_0 + l_0) + p_s \quad (2)$$

△PGPS : the GPS positioning error; △RINS: Attitude IMU error; △RLU and △ RLB :placed foot error and laser scanning angle error; △s: laser point ranging error; △PS : Error laser point with GPS and INS; After the adoption of (1) and (2) added to the system error correction, laser ranging' error is between 2 centimeter and 4 centimeter (Lai X D 2009 Airborne laser Radar Fundamentals and Applications (Beijing: Electronic Industry press)).

Ranging error elimination can be carried out by various experiments in the room to eliminate, the residual error after calibration can reach centimeter level (Zhang X H 2007

Airborne laser Radar Measurement Technology Theory and Method (Wuhan: Wuhan University Press)).

4.1.2. Measuring angle error.

Angle measurement error is attitude angle error and scan angle error from the GPS and INS integrated. Attitude (IMU) error is mainly horizontal error except for Laser gyro sight deviation, acceleration allowed timing, complex measurement noise, the presence of non-orthogonal between the bearing and the like, mainly affecting roll angle, pitch angle, flight angle, which can by flying at low altitude to reduce the influence. Due to the installation, design and other reasons such scanning system axis direction and original state with a certain bias, leading to the starting angle scanning angle greater than 0 degrees, named scanning angle error, can be measured at the factory as long as the instruments prescribed time calibration to, but the actual work do not consider such errors generally (**Lai X D 2009** Airborne laser Radar Fundamentals and Applications (Beijing: Electronic Industry press)).

4.1.3. Location error.

The positioning errors of GPS are all kinds ,including satellite orbit error, satellite clock error, the receiver clock error, multipath, phase center of instability, and there is a constellation of satellites, observation noise, integer ambiguity resolution is whether is correct or not, etc. (Zhang Xiao Hong, 2001). GPS positioning uses a dynamic difference method, while recording the GPS carrier phase and pseudo distance from ground-based reference stations from the data in conjunction with data from the satellite carrier phase and pseudo-together after the flight to use Novatel Inertial Explorer8.6 (IE) solver, less than 50km in baseline length can reach between 23cm and 32 cm accuracy (**Jiang Y S 2001** Remote Sens.5 241-6). Some scholars use differential GPS real-time dynamic three-dimensional coordinate measurement target, up to centimeter-level accuracy (**Cong hui Feng, 2007**).

4.1.4. Time synchronization error

There are laser rangefinder, GPS differential positioning, IMU attitude, which interfere with each other, working independently of each other, with having their own time recording apparatus. In order to get a correct three-dimensional coordinates of the laser point in space, we must ensure that the laser ranging value at launch, and the attitude of observational position are at the same time, so they need to be imputed to the respective time uniform time UTC or GPS time. If the time is not, there will be positioning errors (**Zhang Y T 2012** Airborne LIDAR systems integration and precision calibration error assessment (Qingdao: Shandong University of Science and Technology). Interpolation can be linear or low-order polynomial fitting method to eliminate the time offset, but some tests shows that if the data updated rate GPS signal receiver is more than 2 times per second, two adjacent epoch GPS antenna location linear interpolated between two adjacent epochs GPS antenna position at a time, you can reduce the impact of the time synchronization error (**Da hai Guo etc., 2006**).

4.1.5. Interpolation error from the data

Interpolation error is due to various airborne LIDAR system having different sampling frequencies caused. At present, the frequency of the Laser ranging system can be up to 20 kHz, however, IMU data sampling frequency is generally 200Hz, while the GPS data sampling frequency is only 20Hz. Therefore, in order to get the correct position and attitude information of each of the Laser spot, it is necessary for GPS and IMU data interpolation processing to eliminate certain outside influences. Domestic scholars, Shukai Li (**Li S K 2003** Temporal Remote Sensing Information Integration Technology and Application (Beijing: Science Press)), made full use of pulse time difference 5s, namely track data fitting processing, accuracy up to centimeter level. Generally, the interpolation error depends on weather changes airflow during flight, the error of the time offset impact is between 3 centimeter and 5 centimeter (**Hebel M and Silla U 2012** IEEE Tran. Geoscience Remote Sens.50 2364-79).

4.2. Integrated error

We need to consider the relationship between the axes of the reference coordinate system and the scanner IMU reference coordinate system when each of system is integrated. In general, the installation integrates axes must parallel to each other, but it does not guarantee parallel to each other between themselves in the actual installation process, resulting in the flight direction around the roll angle (Roll) error, about the direction of the wing pitch angle (Pitch) error angle about a vertical navigation (Heading) error. Roll angle error is mainly reflected in the plane of the scan lines having a certain inclination; flight angle error can cause ranging inaccurate, mainly in track route deviation, distorted, broken phenomenon (**Xiong A W and Yang M M 2014** Surveying Mapping 3 75-78). Haikun Yu, Peng Li, Nan Liu (**Sun L M, Deng Q J and Ling X C 2015** Electric Power Survey Design 2 15-18) and other studies of airborne LIDAR collimation calibration method, application of new technology in the Leica Gallery measurement are discussed in detail so that both sides of the roll angle error route inconsistent level phenomenon; pitch angle error will cause the LASer plane position data before and after the dislocation phenomena; flight angle error will cause the strip to the right of the point cloud is shifted forward, the left back offset. In the actual operation of the integrated error elimination generally do calibration experiments can eliminate the corresponding error.

5. Platforms of LiDAR

Since LiDAR is a very powerful technology, it's used in different applications like autonomous vehicular and mapping and topography surveys. LiDAR was originally designed as a fixed-position ground-based device for studying atmospheric composition, structure, clouds, and aerosols, and it is now a strong tool for climate observations across the world. These equipments are operated by NOAA and other research groups to improve our understanding of climate change. LiDAR sensors are also employed to scan objects such as bridges, buildings and beaches, they are installed on fixed-position tripods. Tripod-based LiDAR systems produce point data with millimeter accuracy and are often used for localized terrain mapping applications that need frequent surveys.

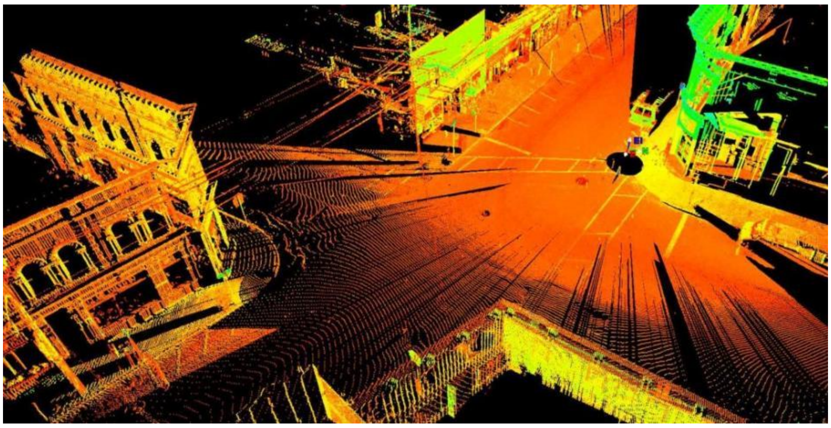

Figure 11 : Dense cloud issued by Terrestrial Laser Scanner (blogsnow.com)

Both land based and water based mobile platforms are used to acquire LiDAR data thanks to modern navigation and positioning systems. These systems may have sensor to target ranges of more than a kilometer and are frequently placed on sport utility and all-terrain vehicles. Since the information gathered from these platforms is so precise, it is frequently used to map specific locations, such as highways, airports, buildings, utility corridors, harbors and shorelines.

Airplanes and helicopters are the most common platforms for acquiring LiDAR data over large, continuous areas. Airborne LiDAR data are obtained by establishing a synchronized system which we introduced in the precious section, inside the aircraft and flying over the target areas. Most airborne platforms can cover about 50 square kilometers per hour and still produce data that meet or exceed the requirements of applications that demand high accuracy data. They are also very efficient in acquiring Bathymetric data in relatively clear, shallow water. Combined topographic and Bathymetric LiDAR systems on airborne platforms are used to map shoreline and nearshore areas to assure the continuous data. They are also used in the mapping of the areas that contains a lot of rivers.

Due to the advancement of the technology nowadays, the drones are efficient as much as planes and Laser scanners, due to its capability of flight lower altitude and surfing in to the roads and around the buildings and bridges, the drones became very stratifying in the quality of the LiDAR data they provide, accuracy and is accessibility in certain cases.

6. Basic principles and techniques

The essential idea about the LiDAR is measuring the time that it takes for pulse of Laser to strike an object and return to the sensor, which itself has a known location due to direct georeferencing system, determining the distance between the sensor and the targeted object using the travel time, record the Laser angle, and then, from this information, compute where the reflecting object (e.g. ground, tree, car, etc) is located in three dimensions.

In the reality, to achieve a high accuracy, this process is a bit more complicated since it is important to know, within a centimeter of precision, where the plane is as it flies at 100 to 200 miles per hour, bumping up and down, while keeping track of thousands of LiDAR pulses per second. Fortunately, several technologies—especially the Global Positioning System (GPS) and precision gyroscopes—came together to make it possible.

The GPS is a ubiquitous satellite-based navigation system renowned for its high-precision geospatial positioning, achieved through satellite signal triangulation. Its characteristic are:

- Accuracy: PPK and DGPS technics can reach sub centimeter accuracy.
- Global coverage: users can obtain location information vertically anywhere in earth
- 24/7 availability

Precision gyroscopes serve as critical sensors for exceptionally accurate angular velocity measurement and stability, with applications spanning aerospace, defense, and consumer electronic. Its characteristics are:

- Frequency: due to the high frequency utilized in the gyroscope we can understand and obtain informations about the angular orientations of the aeronautical vectors. More the frequency is high, the higher precision we obtain.
- Stability: Gyroscopes help maintain stability in various applications by providing feedback for controlling the orientation of equipment or vehicles.

In essence, GPS ensures precise global positioning, while precision gyroscopes provide meticulous angular velocity data and stabilization in diverse contexts.

Major advancements in Inertial Measuring Units (IMU) or Inertial Navigation Systems (INS) have been instrumental in making the exact positioning of the plane possible. These systems are capable of measuring movement in all directions and parlaying these measurements into position. They are, however, not perfect, and lose precision after a short time (e.g., 1 second).A very highly sophisticated GPS unit, which records several types of signals from the GPS satellites, is used to “update or reset” the INS or IMU every second or so. The GPS positions are recorded by the plane and also at a ground station with a known position. The ground station provides a “correction” factor to the GPS position recorded by the plane.

Likewise, the LiDAR systems have advanced considerably. Early commercial units were capable of 10,000 per seconds and were large and bulky. Newer more compact systems have overcame these sensors with a higher angular precision, they can process multiple Laser returns in the air allowing for pulse rates of over 6 million points per second for the new Leica SPL and 3 million points per second for the VQ-1460. The multiple return systems, which are common, can register up to six returns per pulse. As a counterpart, the data has increased by 30% or more in addition to the ability to look at the three dimensional structure of the features above the ground surface, such as the forest canopy and understory.

With this talking we can move to classify the two types of LiDAR

- Discrete the discrete LiDAR basically records individual returns representing the peaks i the waveform curve. It can record up to five returns from each Laser pulse like the figure 12 describes.

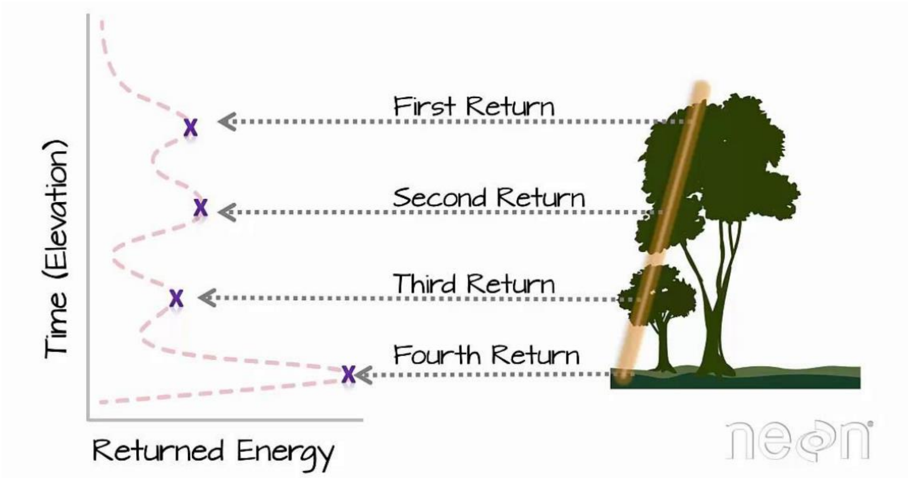

Figure 12 : Discrete LiDAR (NEON)

- Full waveform it records the distribution of returned light, the cons of this technique is its data are more complex to process but can contain more information than the discrete LiDAR sensors. The other cons of this type of LiDAR that they require huge storage in order to store the huge quantity of the data recorded like the figure 16 describes.

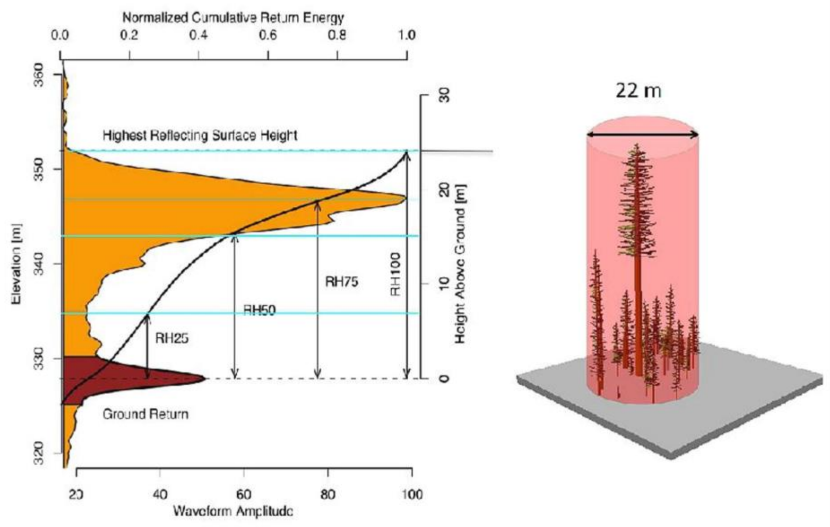

Figure 13 : Full waveform LiDAR (Ralph Dubayah)

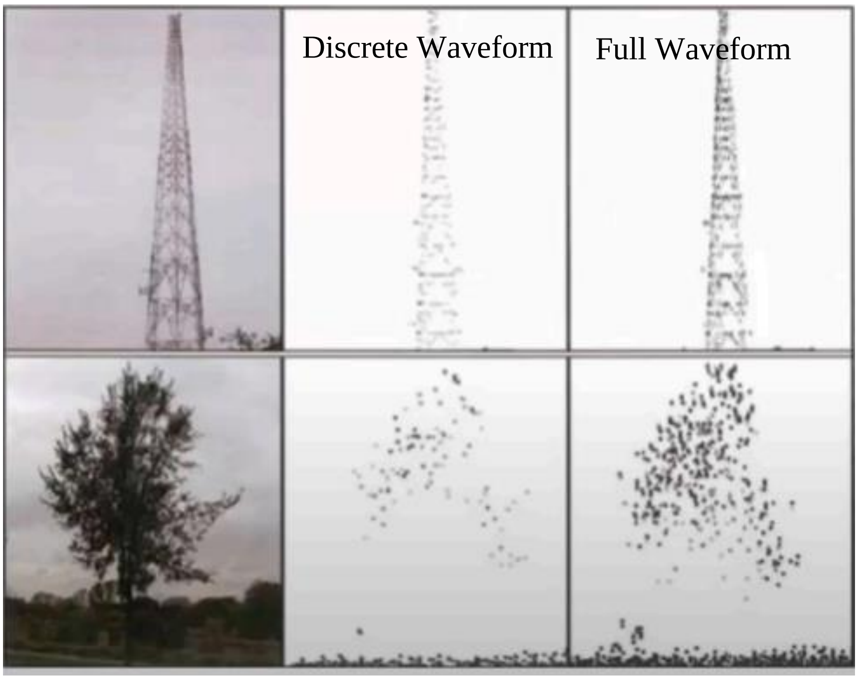

Figure 14 : Difference between Discrete and full Waveform LiDAR (Renslow, 2012)

The figure 14 highlight the difference in point density of the tree and the power tower, in the discrete and full waveform.

III. DSM and DTM

1. DSM

The Digital Surface Model (DSM) represents the elevations above sea level of the reflective surfaces of trees, buildings, and other elevated features above the "bare Earth." In a LiDAR (Light Detection and Ranging) system, pulses of light travel to the ground. When the pulse of light bounces off its target and returns to the sensor, it gives the range (a variable distance) to Earth. Hence, this system earned its name of LIDAR.

In the end, LiDAR returns a huge point cloud filled with different elevation values. But the height can come from the tops of buildings, the tree canopy, power lines, and other features. A DSM captures and displays natural and built features on the Earth's surface.

A DSM is useful in 3D modelling for telecommunications, urban planning, and aviation. Since the objects are extruded from the Earth, this is particularly useful in these examples

- Invaded runway approach area. In aviation, DSMs can determine runway obstructions in the approach zone.

- Vegetation management. Along a transmission line, DSMs can see where and how much vegetation is encroaching.
- Obstruction of sight. Urban planners use the DSM to check how a proposed building would affect the viewpoint of residents and businesses.

Figure 15 : Example of Digital Surface Model from the study area

2. DTM

A complete, high-resolution computer depiction of the earth's naked surface that excludes all vegetation, structures and other above-ground elements is known as a Digital Terrain Model (DTM). In order to create a DTM, elevation data must first be collected from a variety of s, such as LiDAR surveys, satellite and aerial images, and ground based surveying. Due to its capacity to produce accurate dense point clouds by delivering Laser pulses and observing the time it takes for the light to return from the earth's surface, LiDAR in particular is a well-like technique. After collecting the elevation data, it is being processed to eliminate the noise, errors and inconsistencies. While changes are performed to make sure the data align with a common reference system or vertical datum, filtering techniques are used to remove outliers and fix systematic errors.

After that, a continuous depiction of the terrain is produced via data interpolation.

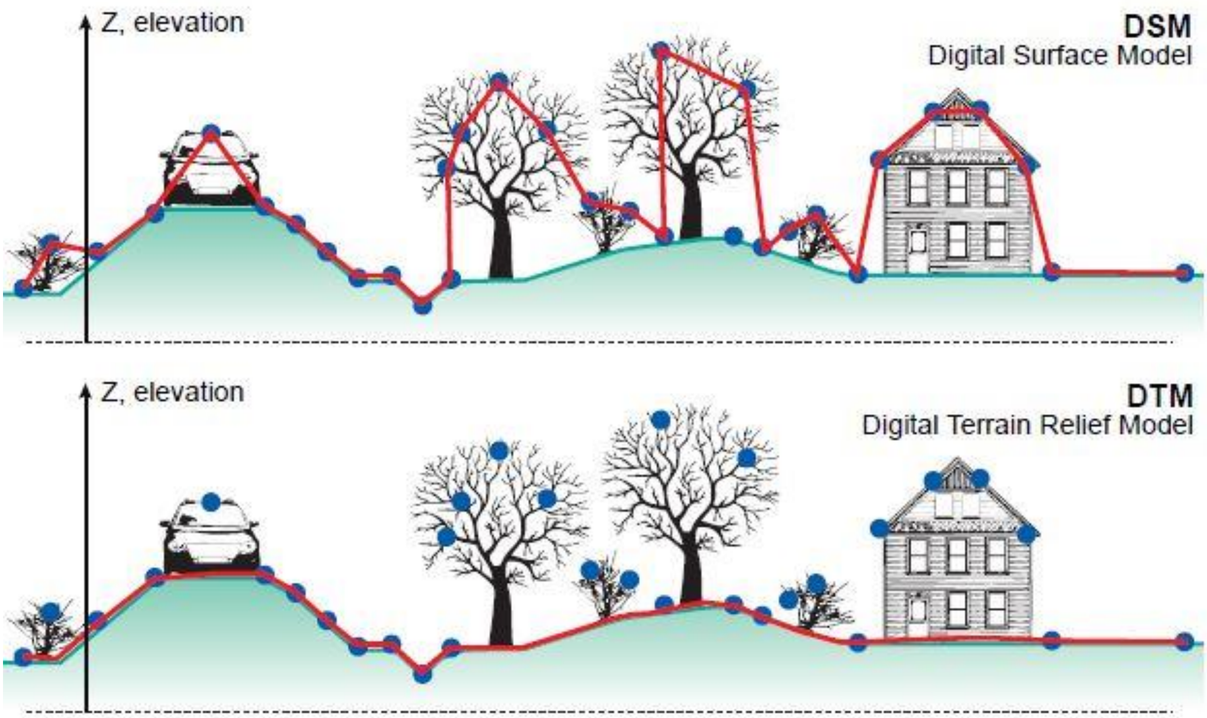

Figure 16 : Difference between DSM and DTM (acolita.com/diferencias-dsm-dem-dtm/)

Data fusion and integration techniques are used to improve the DTM's accuracy and completeness. To provide a more accurate and thorough depiction of the earth's topography, many data s, including LiDAR, aerial photography and ground surveys, are merged. The raw elevation data is subjected to smoothing and filtering algorithms to eliminate noise and anomalies, producing and accurate and pleasing-to-the eye DTM.

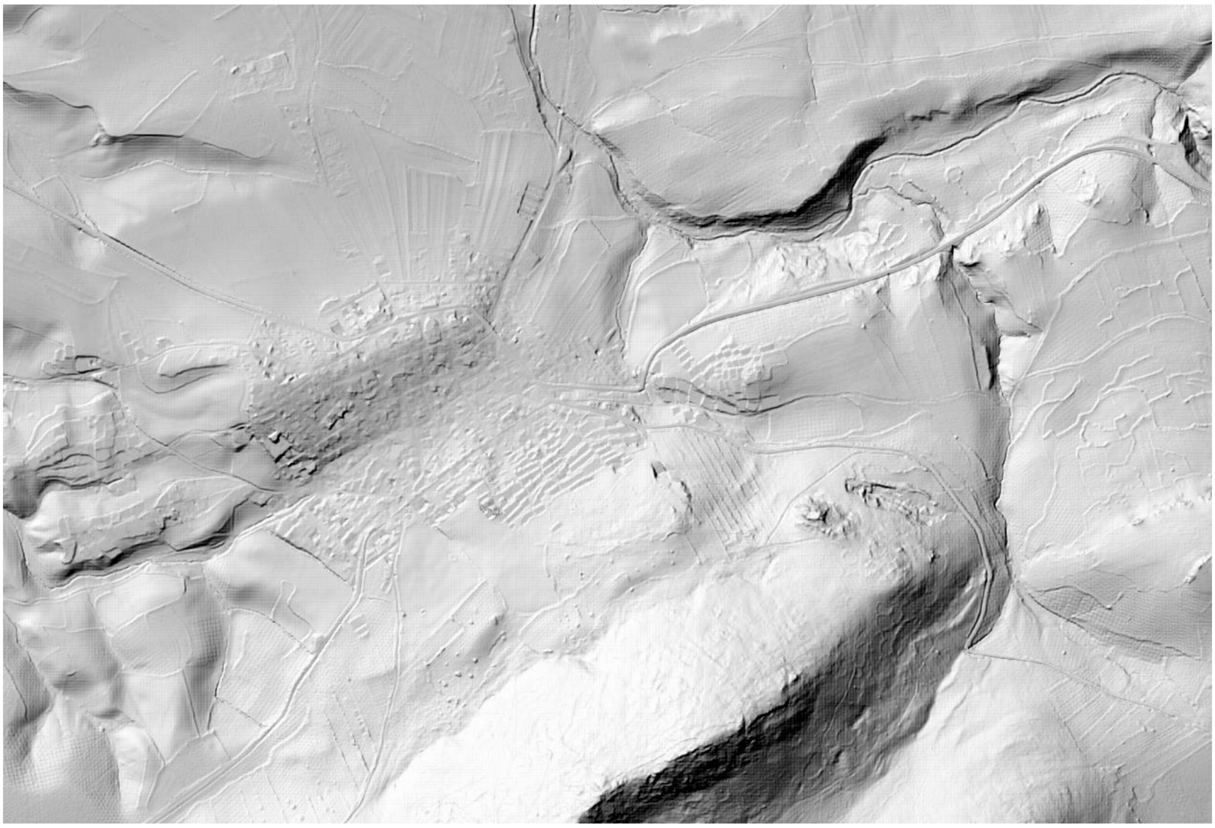

Figure 17 : Digital Terrain Model of the study area

IV. Quality Control

The quality control of the data is a crucial step after proceeding the acquisition phase, in order to deliver accurate and reliable data, we need to respond to the criteria fixed by the IGN of Spain. In this section we have done a bunch of procedures that will help us to criticize the quality of this LIDAR data. We have used for this task a software developed by Dr. Martin Isenberg called LAStools, this software contains many tools which are capable of handling massive LIDAR data and can read and generate LAS,laz and ascii files rapidly (more details in the previous section). To begin with I would like to present the methodology and the philosophy of the quality checking especially with this type of LIDAR sensor (Riegl which contains 2 channels) in the diagram in the figure 18

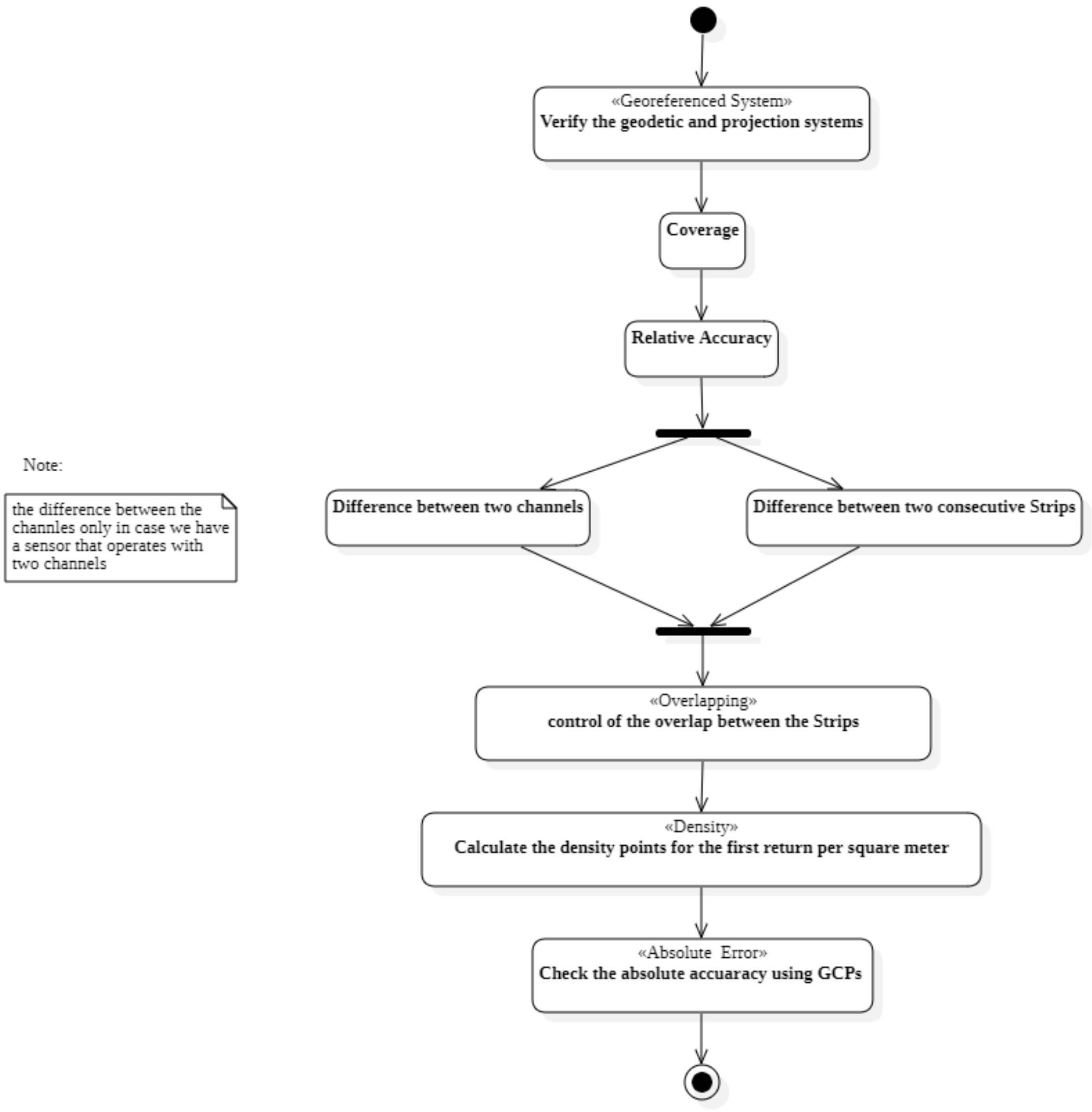

Figure 18 : Activity diagram for quality control

V. Conclusion

To conclude this chapter, the LiDAR is a very powerful technology used in various specialties, like topography, mapping large scale areas, producing a very high dense and accurate point cloud that represents the ground, important vegetation height, buildings, etc.

In the next chapter we will use these theoretical informations to extract the digital products from a LiDAR data acquired under the PNOA project.

Chapter 2 National LiDAR Projects

I. Introduction

This chapter presents the national LiDAR projects starting with their historical evolution, objectives and the technology used for data acquisition. Additionally, we are going to discuss on one hand the data accessibility and dissemination and the applications .On the other hand, we will put on display the benefits, the challenges and the limitations faced by the national LiDAR projects. Finally, we will present the PNOA project as an example.

II. Historical evolution of national LiDAR projects

1. Early initiatives

National LiDAR Projects arose from an awareness of LiDAR technology's promise for gathering accurate and detailed geospatial data. Early adopters in nations such as the United States and Canada began investigating the value of LiDAR in terrain mapping and natural resource management.

2. Motivations

These early attempts were driven by the constraints of traditional mapping technologies and the need for extensive, accurate, and up-to-date geospatial data. LiDAR technology was expected to revolutionize data collection, enabling a wide range of applications ranging from flood risk assessment to infrastructure design.

3. Pioneering projects

Several pioneering efforts arose as examples of the technology's potential as National LiDAR Projects gained traction. These initiatives attempted to collect high-resolution LiDAR data as well as aerial photography of whole regions or nations. The US Geological Survey's (USGS) National Elevation Dataset (NED) effort, for example, intended to produce a continuous, high-resolution elevation model of the whole contiguous United States. Similarly, Canada's Geobase program sought to offer complete geographic data, including elevation data, to aid in the implementation of numerous government programs.

III. Objectives and scope of national LiDAR projects

1. Defining goals

National LiDAR Projects often have well-defined primary objectives. They work hard to build extensive and accurate geospatial datasets for their particular areas or countries. This includes high-resolution aerial images, elevation models produced from LiDAR, and orthoimagery. Overarching aims frequently include improving decision-making processes, better resource management, and supporting various government projects.

2. Sector specific focus

National LiDAR Projects broaden their applicability into a variety of industries. They help with precise land-use analyses and transportation infrastructure design in urban planning. They help with crop monitoring and precision agricultural procedures in agriculture. They aid in flood modeling and catastrophe response operations in disaster management. Because of the adaptability of LiDAR-derived data, it is a significant resource for a wide range of government agencies and enterprises.

3. Geographic coverage

National LiDAR projects often cover the entire country or a specific region. The programs strive for consistency in quality and coverage, ensuring that geospatial data is available and useable across a wide range of landscapes and habitats.

IV. Technology for data acquisition in national LiDAR projects

1. LiDAR sensor types

The deployment of cutting-edge LiDAR sensor technology is frequently critical to the success of National LiDAR Projects. Airborne LiDAR sensors placed on airplanes, capable of producing LASer pulses and recording precise elevation data with extraordinary precision, are widely used in these projects. Sensor technology advancements have enabled projects to continuously increase the quality and resolution of their LiDAR-derived data.

2. Data collection methods

National LiDAR Projects rigorously develop and implement data collecting procedures. Flight plans are meticulously planned to cover the whole project region, including remote and difficult terrain. Ground control points are used to assure georeferencing accuracy, allowing LiDAR data to be seamlessly integrated with other geospatial datasets.

3. Data processing in national LiDAR projects

National LiDAR Project data processing methods are complicated and iterative. They include operations such as data calibration, point cloud production, and quality control. The gathered LiDAR data is meticulously processed to remove mistakes, outliers, and artifacts, yielding high-quality elevation models and point clouds.

V. Data accessibility and dissemination in national LiDAR projects

1. Data accessibility

One distinguishing feature of National LiDAR Projects is their dedication to data accessibility. These initiatives frequently provide online platforms where government organizations, scholars, and the general public may access LiDAR-derived elevation data, orthoimagery, and other geospatial data. This data democratization allows different stakeholders to use the resources provided by National LiDAR Projects for study, decision-making, and commercial applications.

2. Data dissemination platforms

Accessing and downloading geospatial data from National LiDAR Projects is often made simple via user-friendly interfaces. These platforms provide standardized data formats and simplicity of access, which contributes to the wide acceptance of created datasets.

3. Data standards and policies

National LiDAR Projects establish stringent data standards and procedures to manage data access and utilization. These may include license agreements, data sharing methods, and metadata standards to ensure that geographic datasets are used responsibly and ethically.

VI. Applications and benefits of national LiDAR projects

1. Diverse applications

National LiDAR projects have a wide range of applications. They help with precise land-use analyses, transportation infrastructure construction, and smart city projects in urban planning. They help with forest inventory management and wildfire risk assessment in forestry. They enable precision agricultural operations and crop health monitoring in agriculture. They help with flood modeling, landslide detection, and disaster response planning in disaster management. The adaptability of LiDAR-derived data results in a plethora of applications that improve decision-making and resource management.

2. Impact on decision-making

The availability of high-quality geospatial data from National LiDAR Projects has profoundly altered local, regional, and national decision-making processes. Data is used by government agencies, environmental groups, and commercial businesses to influence policy, improve resource management, and increase catastrophe preparedness. The capacity to make educated judgments based on accurate and up-to-date data has resulted in more efficient resource allocation, enhanced infrastructure development, and more effective natural disaster response.

3. Economic and environmental benefits

National LiDAR projects have a significant economic and environmental impact. These initiatives contribute to economic development and sustainability by maximizing infrastructure investments, decreasing environmental consequences, and improving resource efficiency. They promote long-term environmental advantages such as less deforestation and more effective water resource management by promoting sustainable land management and conservation activities.

VII. Challenges and limitations faced by national LiDAR projects

1. Technical challenges

National LiDAR projects face a variety of technological problems in data collecting, processing, and analysis. These include data accuracy, resolution, and noise concerns. To overcome these problems, continual research and innovation in sensor technology and data processing approaches are required.

2. Financial constraints

The breadth and size of National LiDAR Projects necessitate substantial financial commitments. Project budget management, finance acquisition, and cost-effectiveness are continuing difficulties. Governments and organizations must weigh the financial costs of these programs against the possible long-term benefits.

3. Logistical issues

Coordination of National LiDAR Projects, particularly those spanning large and varied geographic areas, involves logistical challenges. Coordinating flight campaigns, ground control surveys, and data processing logistics across a variety of terrains and weather situations is part of this.

VIII. Example: The National Aerial Orthophotography Plan (PNOA)

The Plan Nacional de Ortofotografía Aérea (National Aerial Orthophotography Plan) (PNOA) is a cooperative project involving the General State Administration and the Autonomous Communities. It was initiated in 2004 with the objective of obtaining digital aerial orthophotographs of the entire Spanish territory, with a fixed update period, currently set at 3 years. In 2009, LIDAR technology was incorporated into the PNOA project.

In 2009, after conducting a series of pilot tests and addressing the need expressed by some project partners to have more accurately detailed digital terrain models, the opportunity arose to integrate LIDAR technology into the PNOA project. This gave rise to the PNOA-LiDAR project.

The project's goal is to cover the entire territory of Spain (within a 6-year cycle) using point clouds with X, Y, Z coordinates, and attributes such as classification or color, obtained through airborne LIDAR sensors. The first coverage was captured between 2009 and 2015, and the second coverage began in 2015 and concluded in 2021. The third coverage started in 2023, with the exception of Catalonia, which began in 2022 through an agreement with the Autonomous

Community. This coverage will have a higher pulse density (5 pulses/m²) compared to previous coverages, aiming to provide higher-resolution products capable of addressing a wider range of applications.

The point density is 0.5 points/m² in the first coverage and 0.5-4 points/m² in the second coverage, with exceptions where density is even higher. The achieved altimetric accuracy is better than 20 cm RMSE Z.

The data is distributed for free through the CNIG Download Center in digital files with a size of 2x2 km in LAZ format.

The PNOA-LiDAR project is a collaborative effort involving the Ministry of Transport, Mobility, and Urban Agenda (through the Directorate General of the National Geographic Institute and the National Geographic Information Center), the Ministry of Agriculture, Fisheries, and Food (through the Spanish Agrarian Guarantee Fund), the Ministry of Finance and Public Function (through the Directorate General of the Cadaster), and the Ministry for Ecological Transition and Demographic Challenge (through the Directorate General of Water), as well as the Autonomous Communities. (PNOA).

IX. Conclusion

As we conclude our exploration of National LiDAR Projects, it becomes evident that these ambitious initiatives are driving forces behind the advancement of geospatial knowledge acquisition and utilization. They symbolize the transformative power of technology, policy, and collaboration in shaping our understanding of the world. National LiDAR Projects have not only set new standards for geospatial data acquisition but have also established a paradigm for responsible and open data sharing. Their enduring contributions extend far beyond the realms of science and technology, influencing societal and environmental well-being.

Chapter 3 Generation of DSM and DTM from LiDAR data of Castilla la Mancha SW

I. Introduction

In this chapter, we will utilize the fundamentals of LiDAR technology to generate digital terrain and surface models of a selected area with a 1:50000 area map in the southwestern of Castilla La Mancha, using LiDAR data obtained through the PNOA LiDAR second coverage project. We will begin by introducing the study area and outlining the specifications set by the National Geographic Institute. Additionally, we will discuss the sensor employed in the mission and the software tools utilized for data processing. Lastly, we will present the methodology employed to create the two resulting products.

II. Study area

Castilla-La Mancha, positioned within the heart of Spain, stands as a vibrant testament to the country's rich cultural heritage and geographical diversity. Established as an autonomous community under the Spanish Constitution, the region is a mosaic of 919 municipalities interwoven across the provinces of Albacete, Ciudad Real, Cuenca, Guadalajara, and Toledo. Its significance extends beyond administrative divisions, as Castilla-La Mancha boasts a profound historical legacy, a tapestry of traditions, and breathtaking landscapes that have captivated both locals and global admirers alike. Within its borders lie iconic cities such as the medieval treasure trove of Toledo, the captivating charm of Cuenca, and the dynamic urban center of Albacete.

Nestled within this tapestry, Torre de Juan Abad emerges as a microcosm of Castilla-La Mancha's distinctive character. Located in the province of Ciudad Real, this municipality stands as a testament to the enduring connections between human settlement and natural topography. With a population of 1003 inhabitants as of 2022, Torre de Juan Abad graces the southwestern corner of Ciudad Real, where it finds itself nestled against the gentle foothills of the Sierra Morena to the south. Gazing skyward, the landmark Cabeza de Buey, towering at 1155 meters, accentuates the municipality's elevation and adds to its geographic prominence.

Against this backdrop of historical context and geographical nuance, the present project finds its purpose. Focusing on the spatial expanse outlined earlier, specifically centered around the coordinates corresponding to grid 939 (Torre de Juan Pedro Abad) on a scale of 1:150,000, the project aligns itself with the National Aerial Orthophotography Plan. This meticulously defined scope, visually articulated on the accompanying map, encompasses an array of notable settlements including Cozar, Torre de Juan Abad itself, Almedina, Santa Cruz, Puebla Del

Príncipe, and Villamanrique. As the following pages unveil the project's methodologies and outcomes, they do so within the contextual embrace of Castilla-La Mancha's historical grandeur and geographical allure.

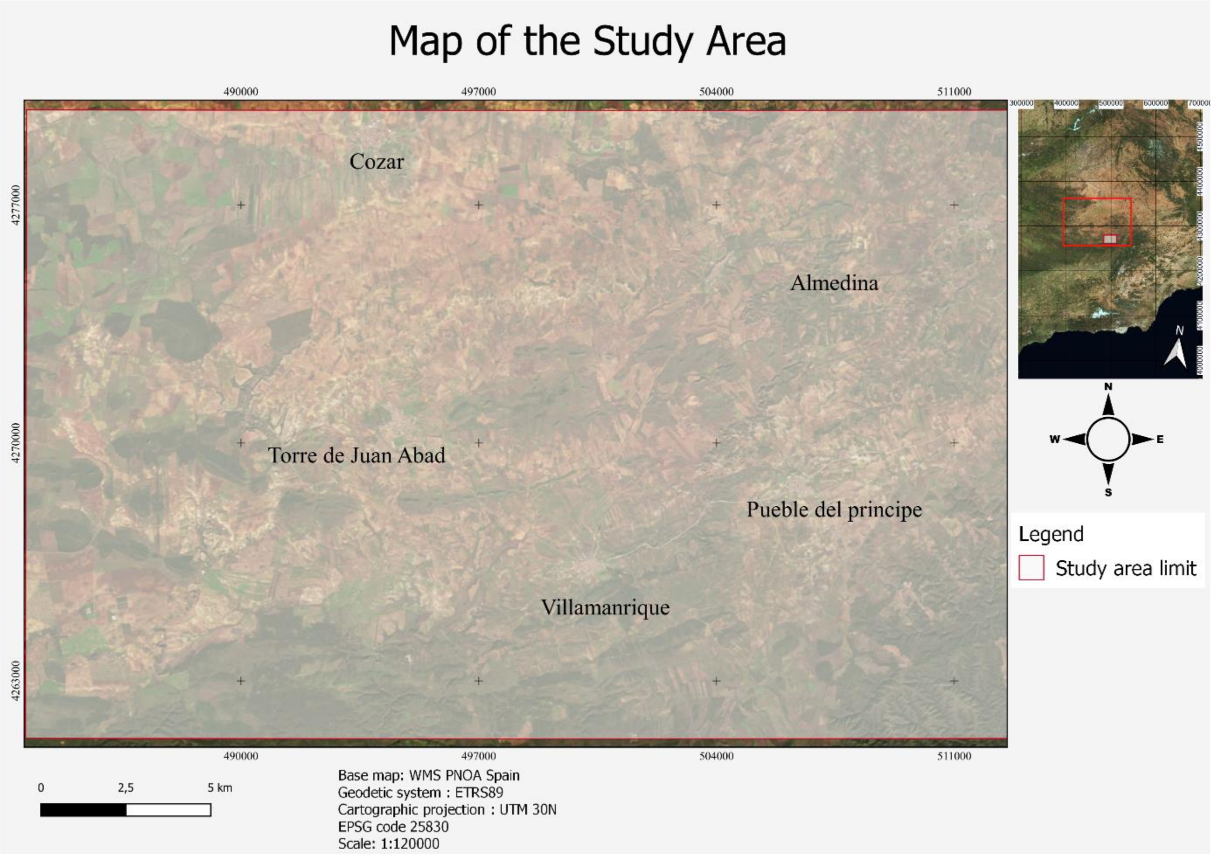

Figure 19 : Study area

Illustrated in Figure 19 are the meticulously orchestrated flight lines that blanket the expansive study area, a configuration that encompasses a total of 15 distinct trajectories spanning across the landscape. These lines, constituting a collective assemblage of 32 individual files, intricately traverse the expanse, resulting in a comprehensive coverage of 538 square kilometers. Characterized by their impeccable alignment, these flight lines trace a harmoniously symmetrical path through the study area, each thread interlocking seamlessly with the next. The regularity of these straight trajectories imparts a sense of precision and purpose, exemplifying the meticulous planning and execution that underlie the acquisition of the invaluable LiDAR data captured over this vast and intricate domain.

III. Specifications

IGN fix the specifications of each area community in Spain according to their specified budget. The table 1 below represents the main specifications.

Table 1 Specifications

Item	Parameter	Specification
1	Geodesic system	ETRS89
2	Ellipsoid altitude	GRS80
3	Cartographic projection	UTM 30N
4	Point density	1pt\m² for the first return
5	Altimetry accuracy	RMSEz < 0.15 m
6	Planimetric accuracy	RMSExy < 0.30 m
7	Overlapping	> 15% in areas of little orography

IV. Equipment

1. Sensor

The company had used Riegl LMS Q-1560 LiDAR sensor in order to fulfill the needs that the IGN has specified. The sensor is equipped with two scanners that produces two channels that scan forward and backward. The figure below explains how the sensor works

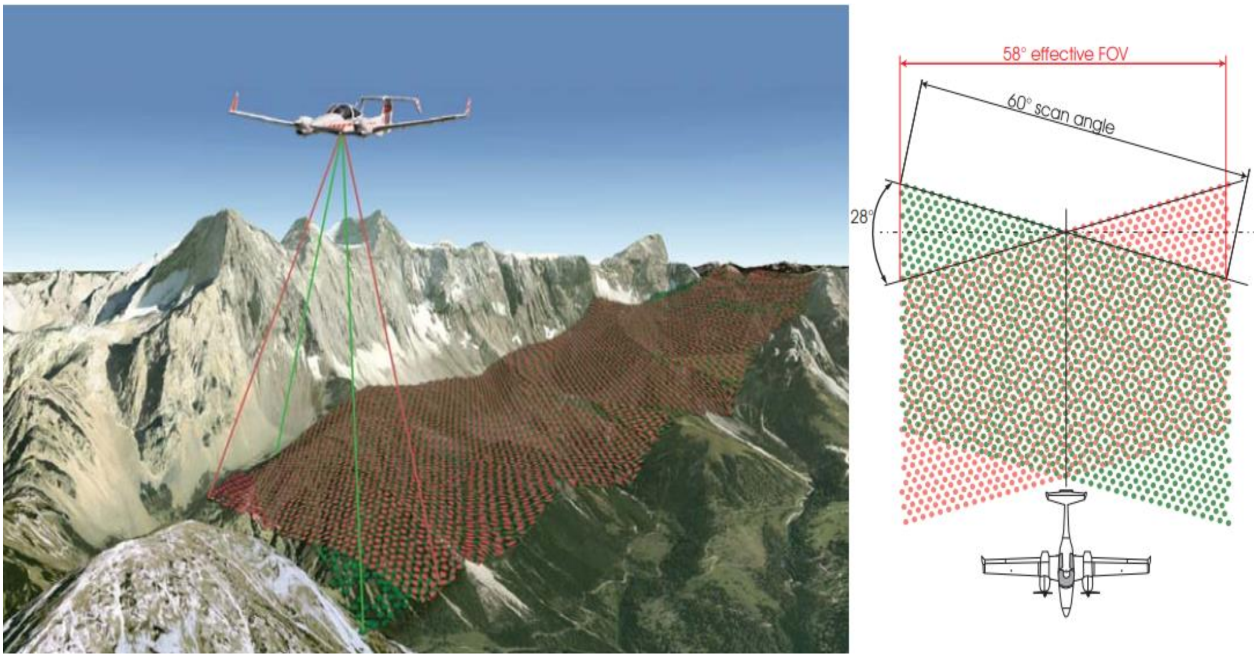

Figure 20 : Schema of the channels of the Riegle Q1560 (Riegle.com)

This sensor proves exceptionally adept at mapping extensive landscapes from elevated altitudes, a prowess attributed to its remarkably high operating frequency. This capability is harnessed to its utmost potential owing to its adeptness in accommodating high altitudes. Augmenting its mapping efficacy, the sensor is fortified with an Inertial Measurement Unit (IMU) that achieves a remarkable accuracy level of 0.005°, complemented by an impressive sampling rate of 200 Hz.

Furthermore, the sensor's capabilities are fortified with digital medium format and infrared cameras, while its two Laser channels demonstrate a pulsating vigor with a remarkable pulse repetition rate that can surge to 800 kHz. Adding to its sophistication, the sensor is further enriched with the inclusion of an IMU and a Global Navigation Satellite System (GNSS) receiver, collectively ensuring a comprehensive capture of geospatial data with an astute emphasis on precision and accuracy.

However, it's the sensor's distinctive attribute that truly sets it apart—the fusion of two sensors within a singular device. This ingenious integration translates into a twofold advantage, producing a dual yield of LiDAR files per individual flight line. Channel one and channel two manifest as distinct streams of data, each encapsulating a unique perspective that contributes to an enriched comprehension of the surveyed terrain. This duality amplifies the sensor's versatility and underscores its pioneering role in expanding the horizons of geospatial data acquisition and analysis.

This sensor is very efficient for mapping ultra wide areas in high altitude due its very high frequency, it is equipped with IMU unit with a 0.005° of accuracy and 200 Hz of sampling rate.

It is equipped with digital medium format and infrared cameras and two Laser channels with a high pulse repetition rate up to 800 kHz. It is equipped with an IMU and a GNSS receiver. The sensor is unique because it uses two sensors in one device, which produces two LiDAR files per flight line (channel one and channel two).

The table 2 illustrates the characteristics of Riegl LMS-1560 sensor.

Table 2 Characteristics of the sensor (Riegle.com**)**

Eye safety class	Laser Class 3B
Max Range target reflectivity 60%	5 800 m
Max Range target reflectivity 20%	4 100 m
Minimum range	50 m
Accuracy	20 mm
Effective measurement rate	Up to 532 000 meas./sec
Scan angel	60°
Max operating flight altitude	4 700 m
Number of channels	2
Formats	LAS

2. Software

2.1. LAStools

For this project we have used LAStools for the reading, compression and analyzing the data (quality control). This software was developed by Dr. Martin Isenberg, a data science engineer born in Germany and worked in the United States. The journey of this development began with the need of this engineer for a tool that can read and open massive Laser file in ASCII file or LAS file, also he needed to compress this massive data in order to reduce its storage. He looked up for a tool that fulfill his requirements and unfortunately he didn’t found one, and as he is a software engineer and a data scientist, he decided to code his own software for the current job and for another time. He named this bunch of tools «LASTOOLS» and he published it on the internet with that name. Dr. Martin ISENBEURG coded and designed the software with C++ language and with a methodology that make it easy to deal and to work with massive data, he also developed a better code for compressing LiDAR data. The best way t handles and to work with LASTOOLS is to use the command line, with it we can create a batch file that contain the whole procedure that we need to do, with that way we can save time and define pre-defined processing tasks.

2.2. QGIS

For GIS application we have used QGIS software 3.22 because its open Source, and he reply to our needs.

QGIS, short for Quantum GIS, has developed as a major open-source software solution in the field of Geographical Information Systems (GIS). QGIS 3.22, the most recent version at the time of writing, is a capable tool for manipulating and analyzing geographic data. QGIS serves to a varied range of users, ranging from governmental institutions to environmental organizations and independent researchers, thanks to its user-friendly interface and extensive feature set. It distinguishes itself by supporting a wide range of vector and raster data types, aiding data visualization and mapping, enabling geoprocessing, and providing expansion via plugins and Python scripting. Its interoperability and cross-platform compatibility add to its allure. QGIS, as an essential component of the current GIS environment, is critical in supporting geospatial research.

We have used it for analyzing the results generated by LAStools (the ASCII files) and to create maps for our projects.

Figure 21 : QGIS logo (qgis.org/fr/site/)

2.3. Stripalign

By swiftly and methodically completing the alignment of broad aerial LiDAR strips, we introduce a revolutionary software solution whose capabilities exceed those of its contemporaries. It represents a paradigm shift in efficiency and precision, leveraging the capability of modern, completely automated algorithms to fulfill its primary goals. Surprisingly, this program eliminates the requirement for data pre-processing, categorization, and filtration, demonstrating its ability to streamline operations.

This program is further distinguished by its compatibility to a wide range of LiDARs, not only extending its benefits to aerial surveys but also accommodating UAV scanners and some Sonar point clouds. It performs the difficult process of recording crossing LiDAR swaths and correcting both relative and absolute geometric abnormalities as an automated strip alignment tool. This complex program acts as a bridge, adeptly reducing the distance between neighboring strips and correcting difficulties caused by IMU attitude and positioning imperfections.

This program excels at harmonizing corrections, which is a procedure that properly combines changes to minimize both relative and absolute mistakes. The algorithmic framework is built on a time-dependent approach that takes use of an in-depth understanding of the temporal dynamics inherent in LiDAR data. It delivers a holistic solution that surpasses the constraints of traditional sensor calibration methodologies by tolerating complex phenomena such as IMU drifts and oscillations.

In essence, this software emerges as a transformative tool, a pioneer in the realm of LiDAR data alignment. Through its integration of state-of-the-art algorithms, it not only ensures the seamless fusion of expansive datasets but also instills a level of precision that redefines expectations. The software's dedication to accuracy, adaptability, and innovation heralds a new era in airborne LiDAR strip alignment, where advanced technology converges with meticulous methodology to yield results that resonate with unparalleled reliability and fidelity.

V. Methodology

Within this dedicated section, a comprehensive exposition of the procedural framework enacted to transform the raw LiDAR data, directly from the Riegl LMS Q-1560 airborne sensor, into the refined outputs of digital surface and terrain models shall be unveiled. The intricate processes that underpin these transformations are intricately delineated within the confines of the activity diagram presented below. This diagram serves as a visual compass, guiding us through the intricate landscape of tasks, methods, and methodologies that collectively orchestrate the metamorphosis of intricate data streams into tangible and invaluable geospatial representations. It is within this framework that the alchemy of technological innovation converges with meticulous methodology, culminating in the creation of digital models that faithfully mirror the complex nuances of the natural terrain.

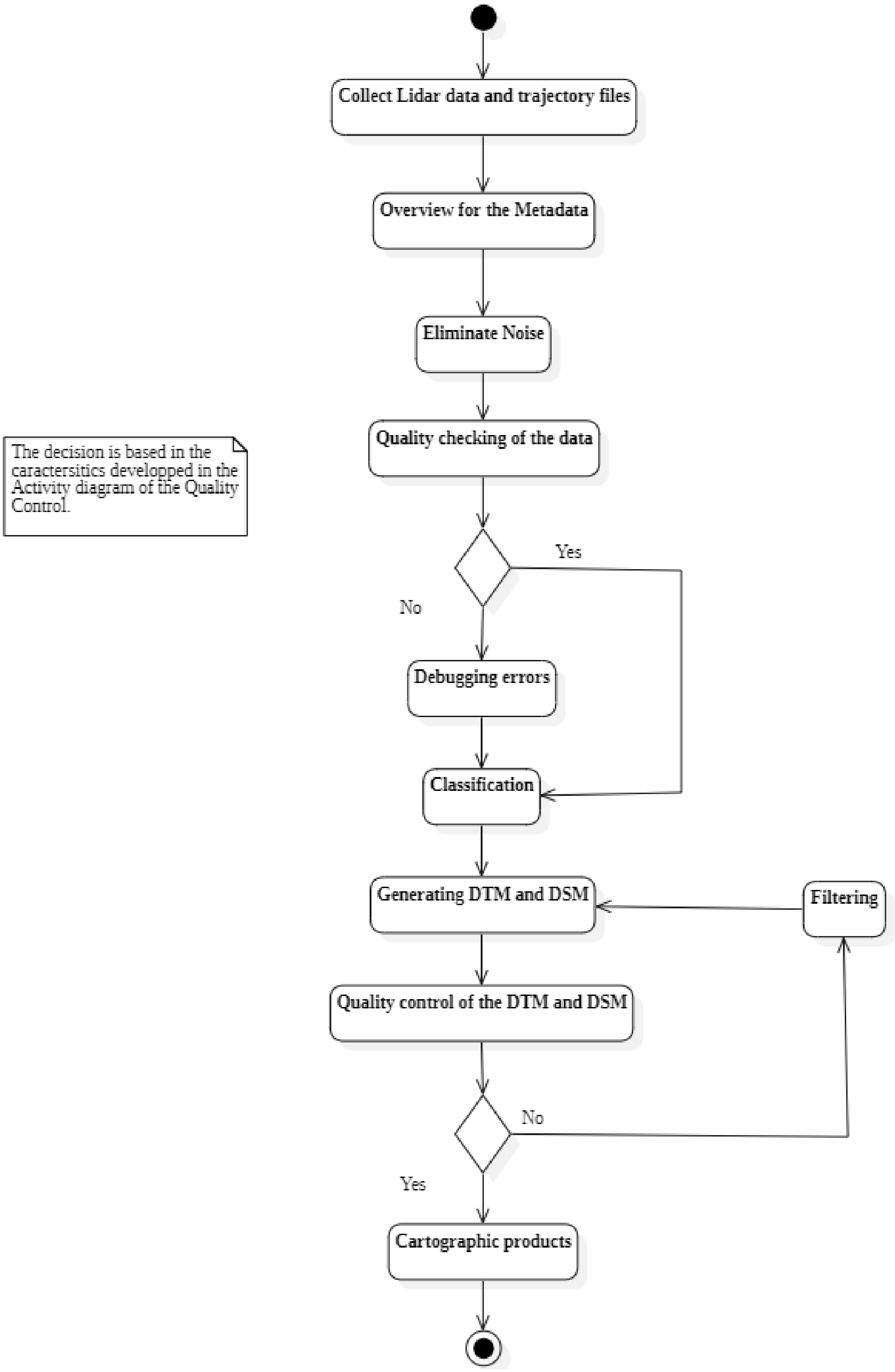

Figure 22 : Activity diagram for the Process of the data

1. Collect Data information

Gathering informations about the laz files that you are going to work with is considered an important step, in which you can learn about whether the files are projected or not, whether they have the correct projection or not, the number of points and the number of returns.

The information that are reported are multiple, we can site for example file signature, file ID file creation date, header size, number of points and number of records, projection systems, return numbers, scan directions and angles, gps time and the georeferenced system of the file.

Now from this file we verified the projection system which is **ETRS89** as a geodetic system and **UTM 30N** as a cartographic projection with the **EPSG code 25830** and we had an insight about the density points for the Last return only which is for this file 1.06 pt/m^2.

LASinfo

The LAStools package includes a command-line program called "LASinfo" that may be used to learn more about LAS/LAZ LiDAR files. It produces a report that includes information on the file format, header information, point characteristics, statistics, histograms, and summaries when used with the correct file parameter. This application is useful for swiftly evaluating the content and features of LiDAR datasets, assisting users in comprehending the quality, properties, and distribution of the data. In LiDAR data processes, it helps with data exploration, quality evaluation, and planning following processing stages.

Our files are generated from LASzip tool, which amazingly reduce the volume of the LiDAR file without changings. This tool made a significant revolution in the LiDAR technique for its powerful propriety. Imaging recording 6 million points per second on an aircraft and you are scanning a large area, where are you going to record all the data? That’s where the compressed type (LAZ) interfere.

2. Eliminate noise:

It is critical to remove noise from LiDAR data before doing quality control to ensure the accuracy and reliability of future analysis. Noise, which might include erroneous or outlier points, can add errors and artifacts that jeopardize the data's integrity. By reducing noise, the resultant point cloud portrays the real features and properties of the studied environment more precisely. This is especially critical during procedures such as data alignment, when noiseinduced misalignments can deform the overall structure and introduce mistakes. Additionally, noise points impair the overall coherence of the data, making it difficult to distinguish between genuine and erroneous characteristics. The removal of noise increases the performance of automated classification algorithms, enabling them to concentrate on significant ground, vegetation, and building points.

Furthermore, during data processing, noise points cost storage space and computing res. By removing them, you can improve storage and computational efficiency. Because noise can cause misregistration with ground control points and reference data, proper georeferencing of the point cloud relies on consistent and trustworthy points. Preventing noise guarantees that the georeferencing process is built on firm ground. This method also simplifies later quality control efforts, allowing you to focus on legitimate data points rather than wasting time on noise concerns. Finally, noise reduction improves visualization and understanding by presenting the LiDAR data in a cleaner and more accurate manner. To summarize, removing noise as an early preprocessing step in LiDAR data management dramatically improves data accuracy, usability, and overall success of subsequent analyses and applications.

We proceed this task with LASnoise which is a strong tool for finding and eliminating noise from LiDAR point cloud data. LASnoise improves data quality and usefulness by identifying and filtering out noise points, which are often generated by variables like as sensor artifacts, ambient interference, or scanning variances. This stage is critical because noise can skew analysis results, cause misalignments, and impede feature extraction. Users can improve the performance of classification, registration, and modeling algorithms by using LASnoise to focus future studies on trustworthy and coherent data. This tool aids in the creation of cleaner, more accurate point clouds, which are better suited for a variety of applications such as mapping, urban planning, and environmental monitoring.

LASnoise

This algorithm allows to classify as low or high noise (noise, class 7) the points that meet the isolation criteria based on the step (step) that is imposed. These points can be removed or in the following steps ignored with the ignore_class option.

It is based on the geometry of the points and based on a defined radius of action, the cloud points are tracked and the heights between neighbors are compared, if no points are found at the same height or at a defined height interval, it is assumed that the point is wrong, that is, class 7 (noise).

Example:

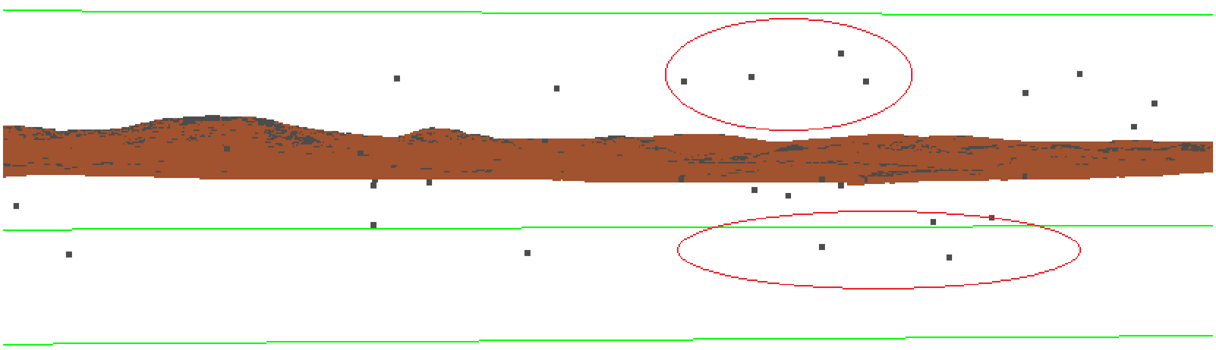

Figure 23: Example of the noise points from our study area

3. Quality Checking

The quality checking is a fundamental phase in our field and has a very importance because we will deliver data that are going to be a reference for the scientific researches and for producing cartography products such as digital terrain and surface models and contour lines for the topographic maps.

The company had used Riegl Q-1560 for the acquisition, the sensor, as described in the equipment section, is composed of two channels that scans backward and forward, equipped also with a GPS and IMU unit inside the sensor. The calibration of the sensor had been done before at least six months before the mission.

The acquisition of interested area had been done on three non-consecutive days, the area covers 537.35 km², it contain 13 flight lines with a 16 LiDAR files for each channel, totally 32 files.

We are going to proceed the quality control with having an overview on the laz files and check the georeferencing system, number of points and number of returns.

3.1. Overlapping

In the field of surveying we always seek to create a single, comprehensive representation of the terrain or landscape being surveyed. To do so, it's essential to have a unified and complete dataset of the terrain. Unfortunately, in practice, achieving a perfectly seamless and error-free representation of the terrain can be challenging, on one hand, we always could have inaccuracies or discrepancies that can occur during the data collection process. On the other hand, these errors can be caused by various factors, including the limitations of the surveying equipments, environmental conditions, or technical issues. That's why we need to asses and evaluate these differences or errors.

As a solution we control the overlap and the alignment between the LiDAR files by looking for the voids, misalignment, and to assure the overlap needed is attended in order to have a dense and a unify point cloud data.

We used for this task LASoverlap and we delivered and ASCII file that contains the real value from the calculation that has been done by the software, we should note that we can deliver a .PNG file that represent a color coded value to facilitate the interpretation.

LASoverlap

The LASTools software package includes the LASoverlap command, which is frequently used for LiDAR data processing. It computes the overlap ratio between points in two LiDAR datasets. The overlap ratio indicates how well two LiDAR point clouds agree with each other in a given location.

The mathematical procedure underlying LASoverlap entails calculating the number of points that fall within a given distance threshold (often chosen by the user) between the two point clouds. The overlap ratio is then determined as the proportion of overlapping points to total points in one of the datasets. This indicates how closely the two datasets geographically match in the given area. The formula for computing overlap ratio is as follows

Overlap Ratio = Total Number of Points in One Dataset / Number of Overlapping Points

This formula is used by the LASoverlap tool to offer insights into the alignment and coverage of two LiDAR datasets, which can be valuable for quality control, accuracy evaluation, and other geospatial analytic applications.

The most important parameter '-step n' specifies the n x n area that of LiDAR points that are gridded on one raster (or pixel) that are then used for doing the overlap and/or difference calculations.

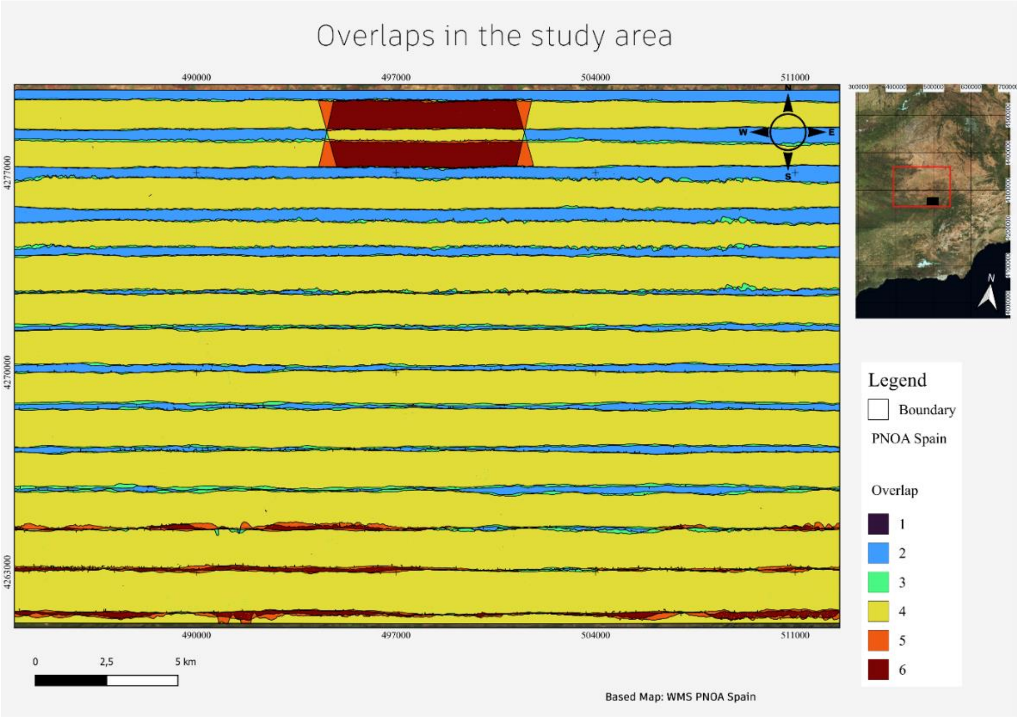

Figure 24 : Map that represents the number of overlaps in our study area

The figure 27 shows us the overlapping in the area. The overlap ratio confirm with the specifications which is > 15%. Free of voids and presented a coherent and single representation, the overlap is verified.

The 5 and 6 overlaps in the south and the north are present, it's due to the control flight line.

3.2. Alignment

As a critical part of the quality control procedure, the alignment verification is a crucial step. The control consist of verifying and evaluate the alignment between the LiDAR data to assure a continuous and coherent information.

The sensor used is Riegl Q-1560. It has a reputation for delivering a bad alignment in LiDAR data. This control was run in both methods:

- Residual analyses
- Visual interpretation.

Residual analyses

Residuals, which are the differences between corresponding points after alignment, are analyzed. Large residuals can indicate misalignments or errors that need correction.

Our point cloud data are collected from different sources (different channels 1 & 2) and different times (3 non consecutive days), so its common problem is to exhibit variations or differences. These differences can manifest as inconsistencies in the elevation of the terrain points, slight misalignment, or other discrepancies.

We interfere to asses and to evaluate these differences and errors by calculating the difference in elevation between the points from different source on two levels:

- Passes
- Channels

The difference is calculated with LASoverlap using the difference option. The most important parameter in this tool is the step size were the software is going to make a grid of n*n unit (step) and calculate the difference between the points in the overlapping areas.

LASoverlap calculate the difference between the lowest elevation of LAS files in the overlapping areas (we cannot calculate the difference if there is nothing to compare with) in a grid size of 1*1 m or 0.5*0.5 m, and that allows us to criticize the quality of the alignment of the flight lines and to estimate their errors. We noticed a very large error randomly distributed across our study area.

We choose the flight line 200831_1434 as a start and we calculate the difference between the two channels. The figure 25 represents a color coded result the colors red and blue for the values (-0.5 and 0.5).

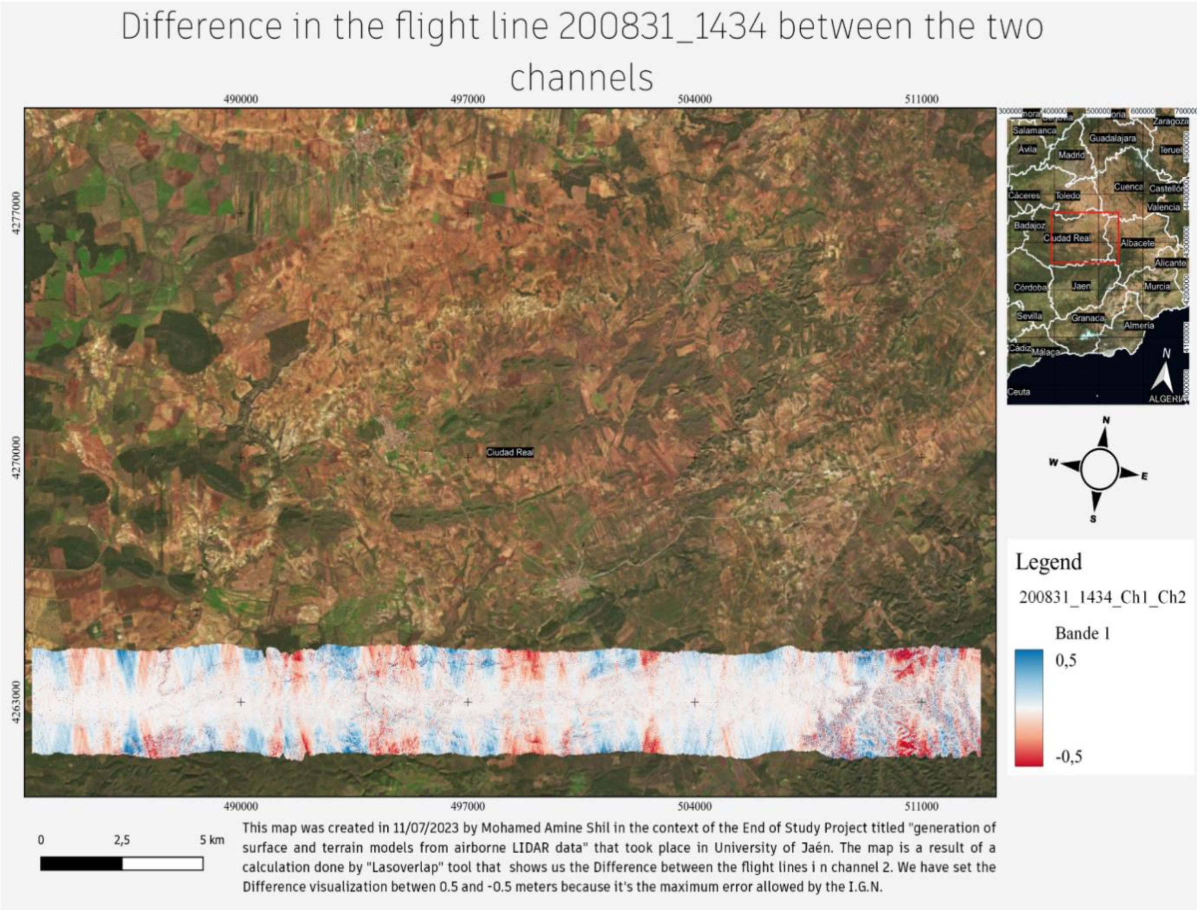

Figure 25 : Difference between the 2 channels for flight 200831_1434

As indicates in the figure 25, with the color red and blue, there is a difference between LiDAR points that belongs to channel one and the channel two that overcame the limit (0.5m) in the edges of the strip. This kind of the difference is typical and it’s expected due to the wide angle of the sensor.

The histogram in the next page, describe an important number of pixels that has an error between 0.3 m to 1 m.

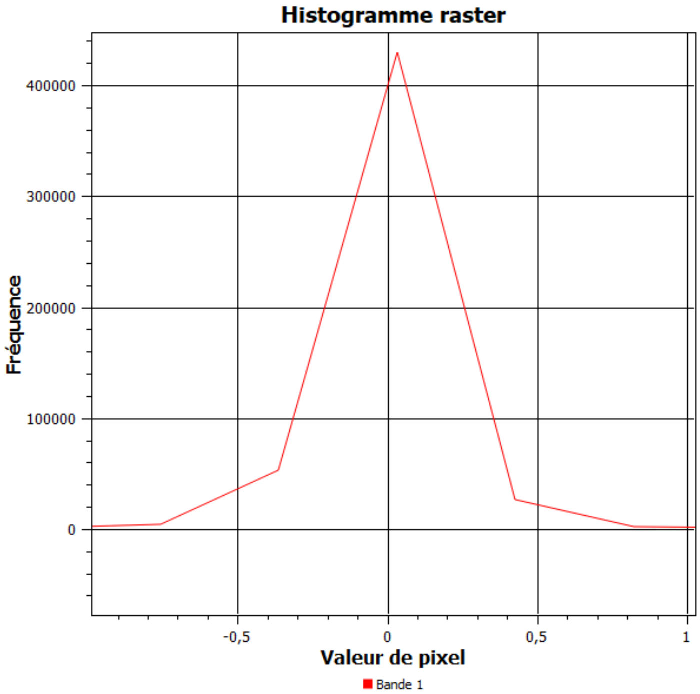

Figure 26: Histogram of the Pass 200831_1434

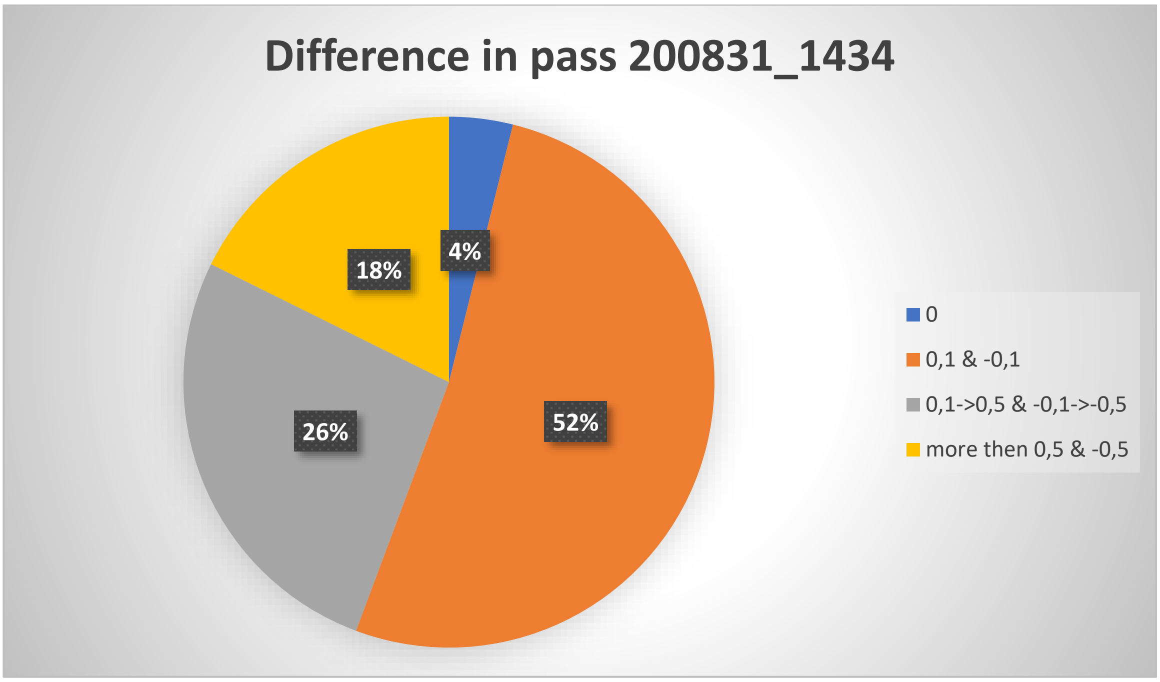

Figure 27: Chart for difference in 200831_1434 pass

This pie chart illustrate the statistics of the number of pixels that contain the difference values. As shown, we divided the chart in four parts:

- 0 m difference: contain 1 054 122 pixels.
- Between 0.1 and -0.1 m of difference: 14 071 884 pixels. We considered this as a safe zone.

- Between 0.1 and 0.5, -0.1 and -0.5 m: 7 235 446 pixels.
- The rest which is above 0.5 m and -0.5 m of difference: 4 799 726 pixels.

Table 3: Statistics of the difference calculation in strip 200831_1435

Range (difference in m)	Difference
0	1054122
0,1 & -0,1	14071884
0,1->0,5 & -0,1->-0,5	7235446
more then 0,5 & -0,5	4799726

We calculate the difference between the two channels for the next strip is 200831_1105. Which is considered the successive strip of the 200831_1434. The figure 28 shows us the result

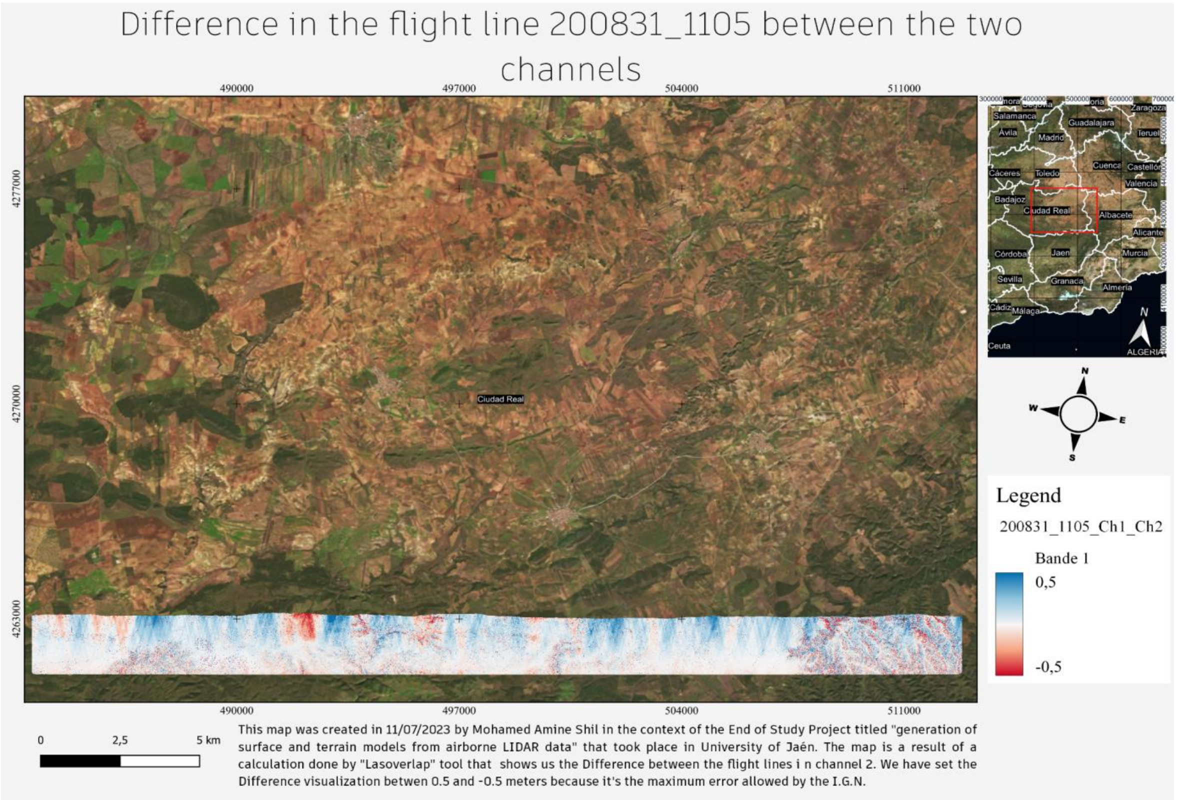

Figure 28 : Difference in the strip 200831_1105

This figure shows us a difference again at the limit in the edges.

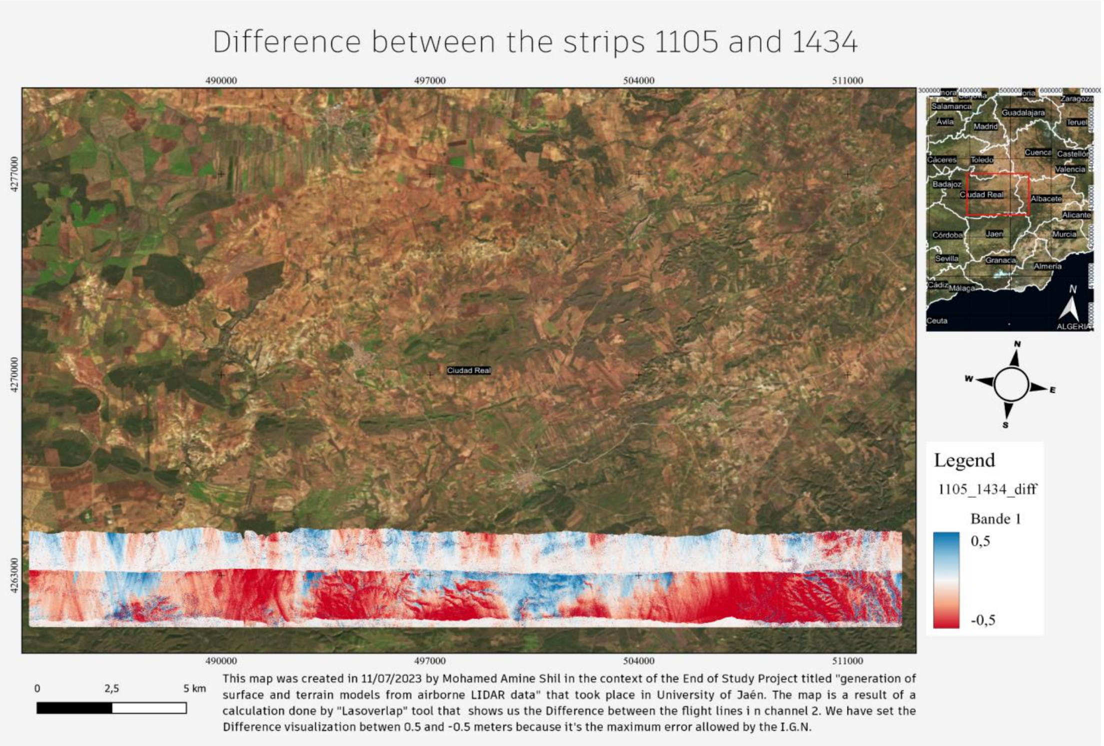

Figure 29 : Difference between the strips 200831_1105 and 200831_1434

The next move is to calculate the difference between the two consecutive strips 200831_1105 and 200831_1434 for the both channels (four files in total) and the result is represented in the figure 29.

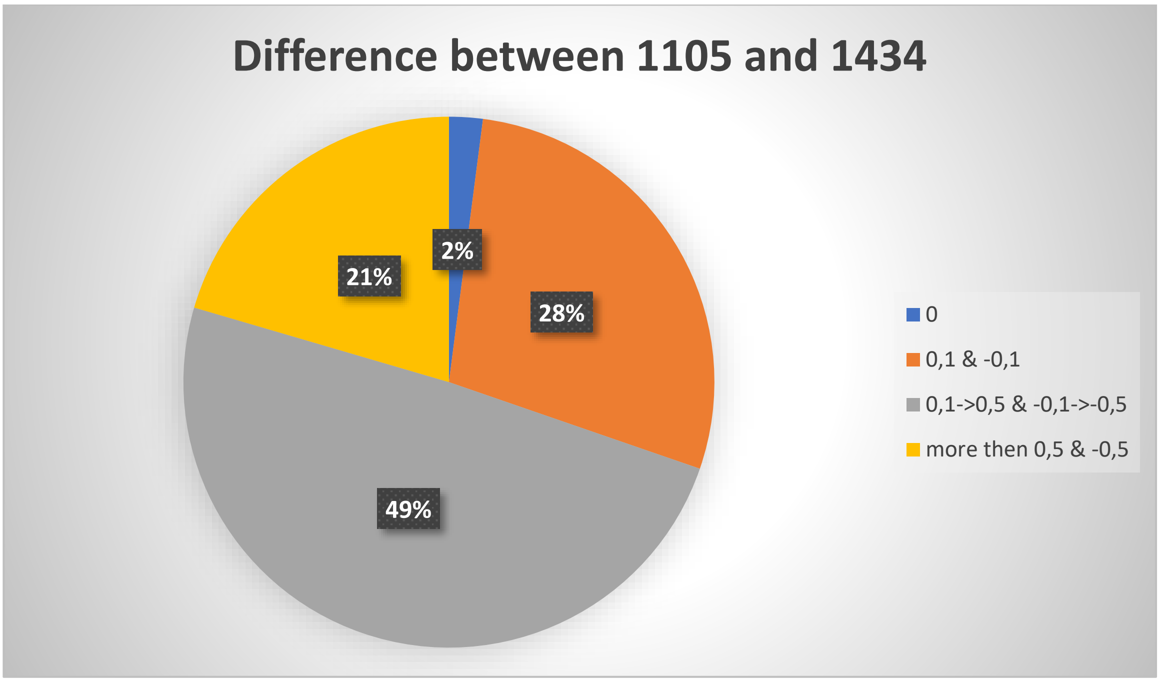

Figure 30: Chart for the difference between 1105 and 1434 passes

This pie chart in figure 30 illustrate the statistics of the number of pixels that contain the difference values. As shown, we divided the chart in four parts:

- 0 m difference: contain 525 297 pixels.
- Between 0.1 and -0.1 m of difference: 7 232 116 pixels. We considered this as a safe zone.
- Between 0.1 and 0.5, -0.1 and -0.5 m: 12 611 221 pixels.
- The rest which is above 0.5 m and -0.5 m of difference: 5 242 393 pixels.

Table 4: Statistics for the difference calculation between the strips 1104 and 1435

Range (difference in m)	Pixel numbers
0	525297
0,1 & -0,1	7232116
0,1->0,5 & -0,1->-0,5	12611221
more then 0,5 & -0,5	5242393

As an interpretation, the difference is so huge between the strips and the channels, as a result, we calculate the difference between the channel one in all the strips.

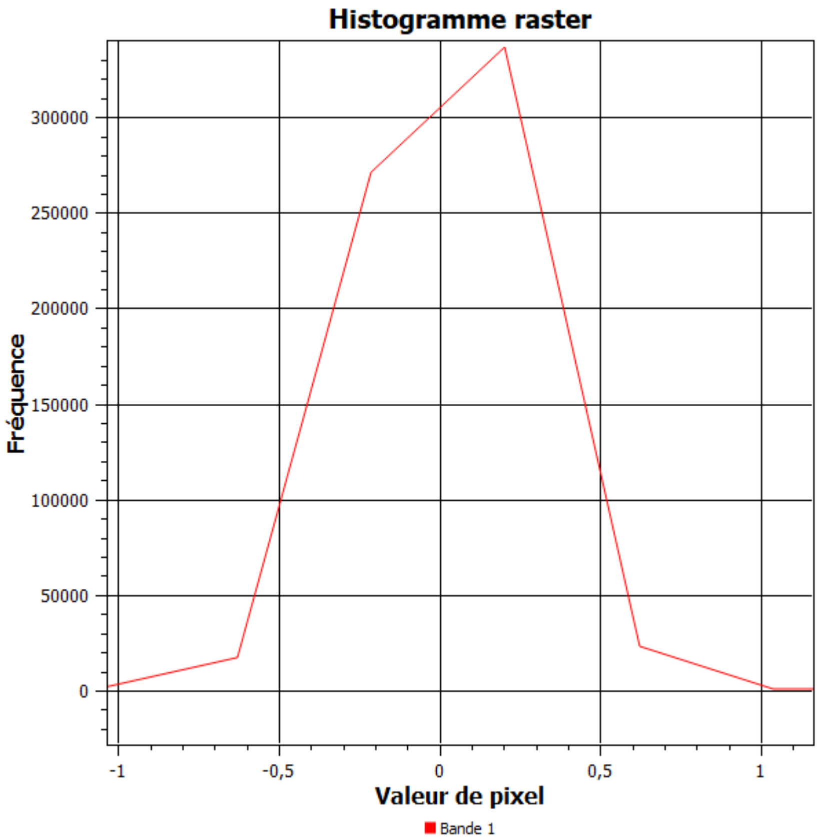

Figure 31 : Histogram of the difference for the first channel (pixel Value is in meter)

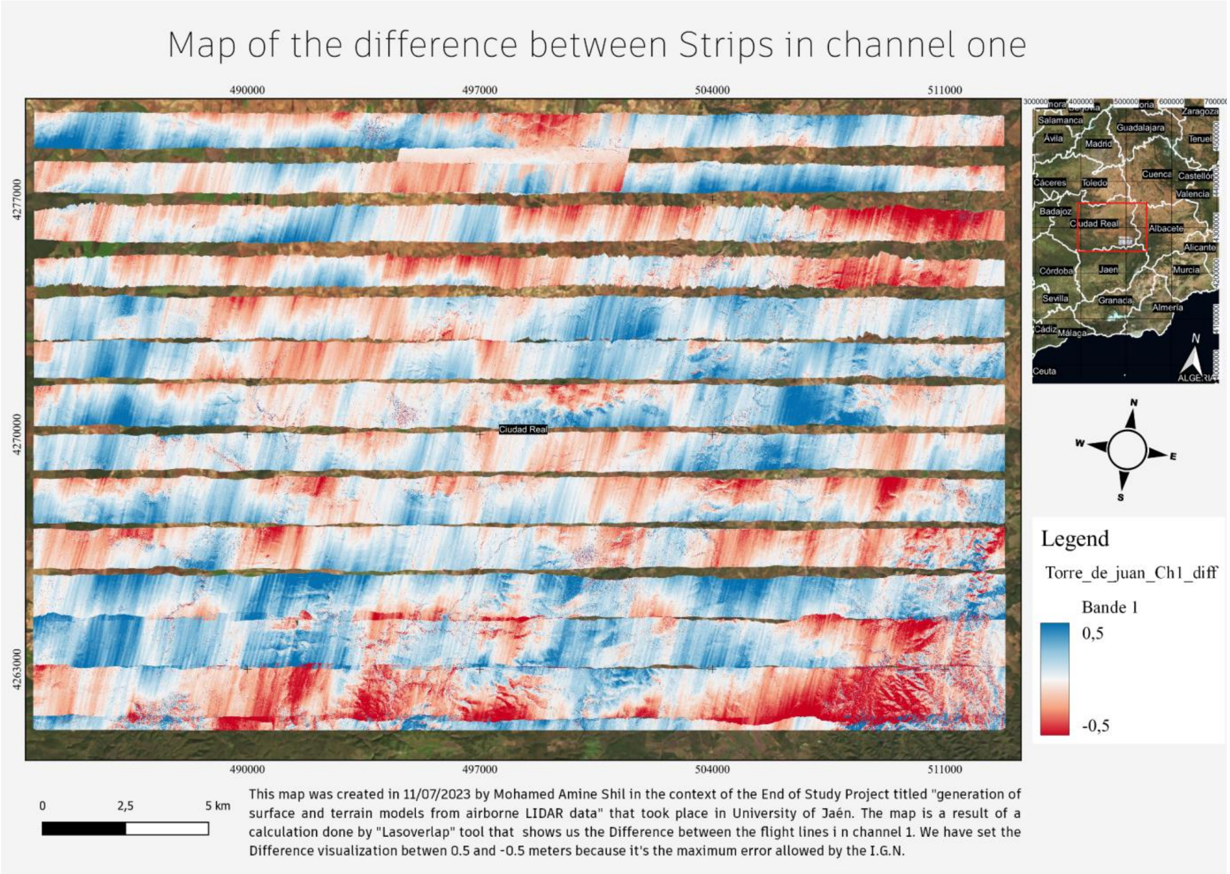

Figure 32 : Difference between the strips in channel one

The figure 31 and 32 shows us the difference all over the study area (the color red and blue is on over the study area). The difference is above 50 cm in all over the area.

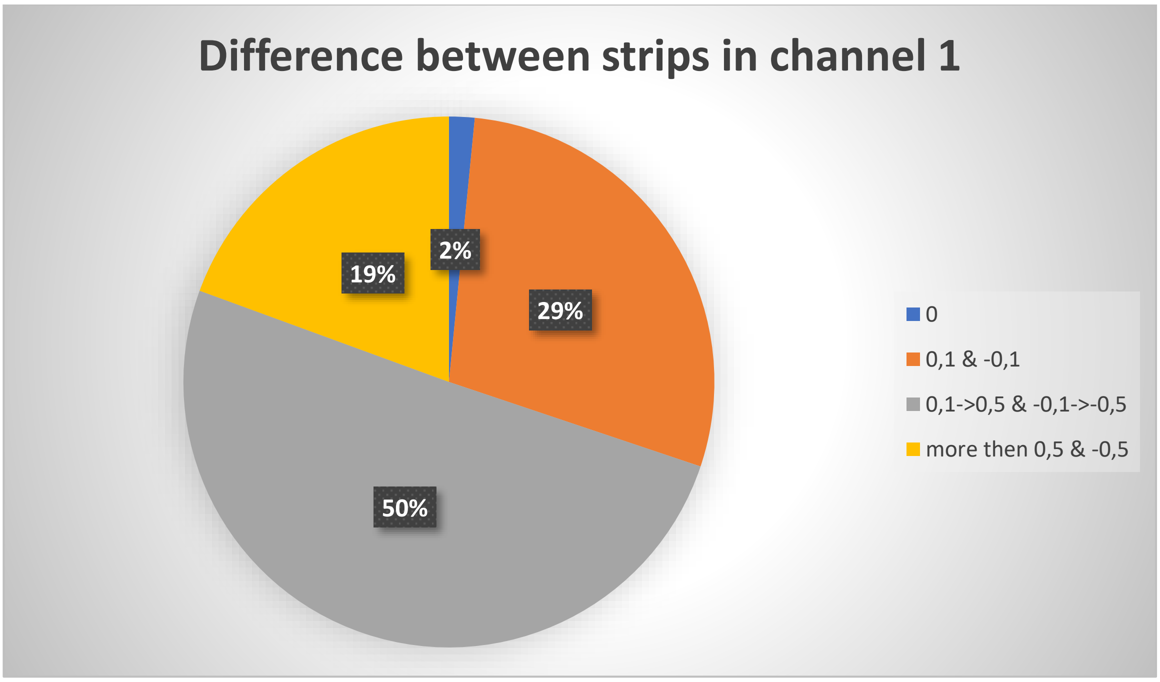

Figure 33: Chart of the difference between strips in channel 1

This pie chart in figure 33 illustrate the statistics of the number of pixels that contain the difference values. As shown, we divided the chart in four parts:

- 0 m difference: contain 932 922 pixels.
- Between 0.1 and -0.1 m of difference: 17 140 237 pixels. We considered this as a safe zone.
- Between 0.1 and 0.5, -0.1 and -0.5 m: 30 216 283 pixels.
- The rest which is above 0.5 m and -0.5 m of difference: 11 635 564 pixels.

Table 5: Statistics for the difference calculation between strips in channel 1

Range (difference in m)	Difference
0	932922
0,1 & -0,1	17140237
0,1->0,5 & -0,1->-0,5	30216283
more then 0,5 & -0,5	11635564

The next figures (34 and 35) shows us the result of the calculation of the difference between the strips in the second channel.

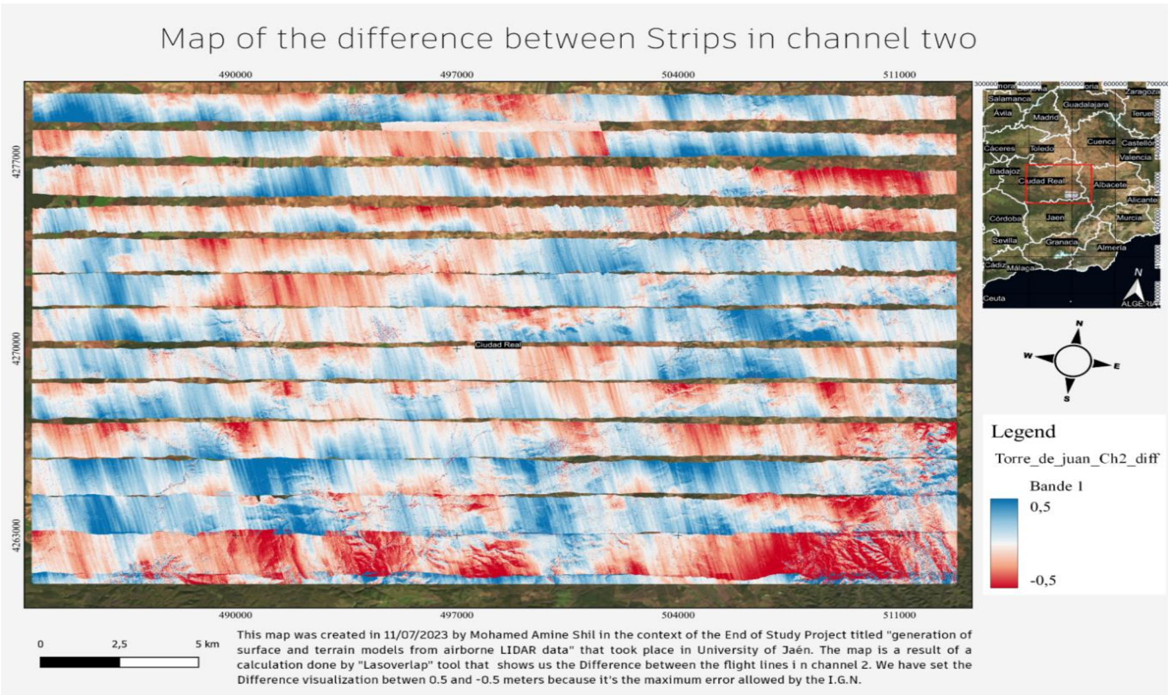

Figure 34 : Difference between the strips in channel two

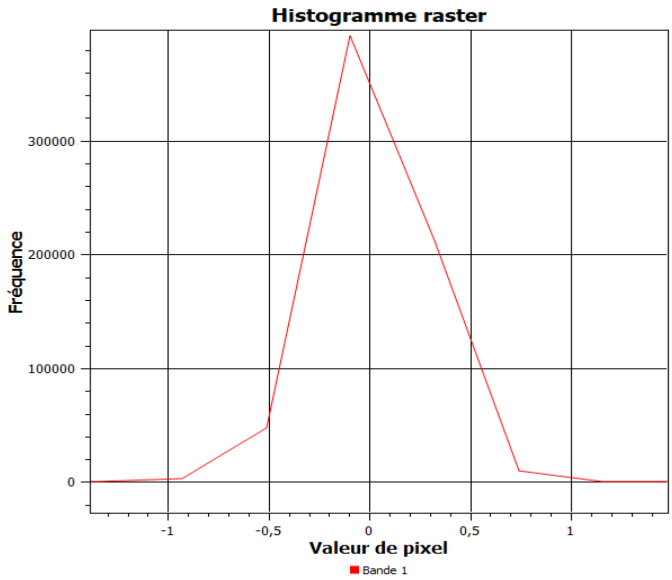

Figure 35 : Histogram of the difference between the strips for the channel two (pixel value is in meter)

The first and the second channel have the same gross difference spots (0.5 m and above).

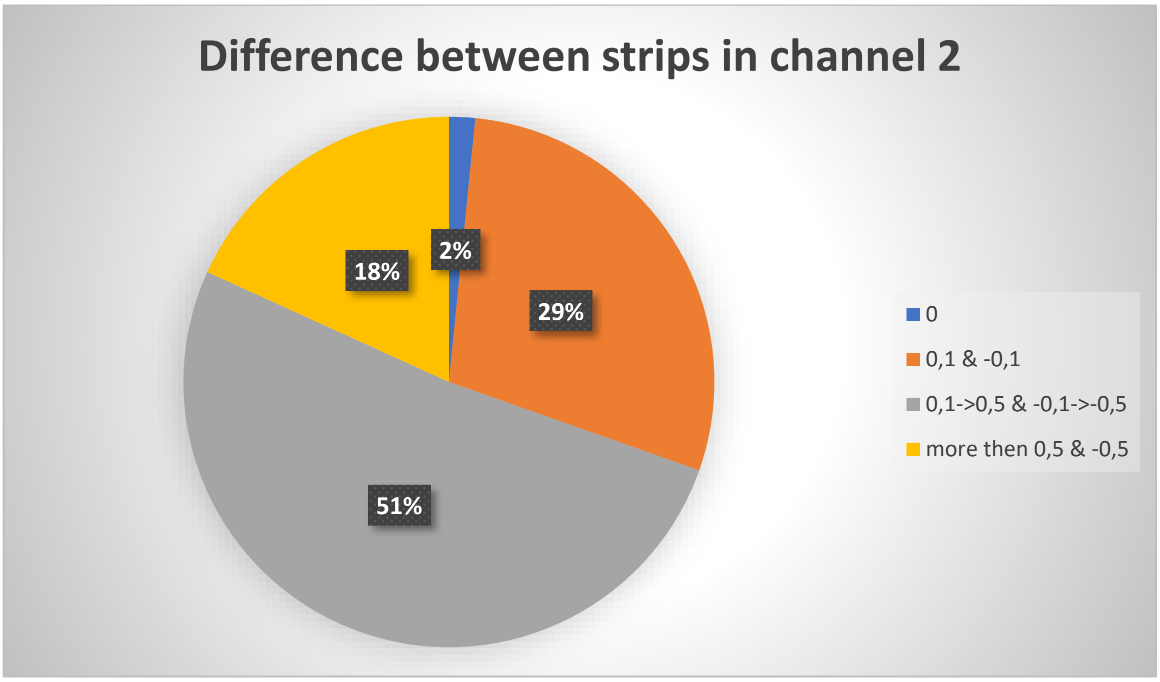

Figure 36: Chart of the difference between strips in channel 2

This pie chart in figure 36 illustrate the statistics of the number of pixels that contain the difference values. As shown, we divided the chart in four parts:

- 0 m difference: contain 953 110 pixels.
- Between 0.1 and -0.1 m of difference: 17 261 484 pixels. We considered this as a safe zone.

- Between 0.1 and 0.5, -0.1 and -0.5 m: 30 788 642 pixels.
- The rest which is above 0.5 m and -0.5 m of difference: 10 901 582 pixels.

Table 6 : Statistics for the difference calculation between strips in channel 2

Range (difference in m)	Difference
0	953110
0,1 & -0,1	17261484
0,1->0,5 & -0,1->-0,5	30788642
more then 0,5 & -0,5	10901582

We took it further and we calculated difference in all the strips and all the channels (all the 32 LiDAR files).

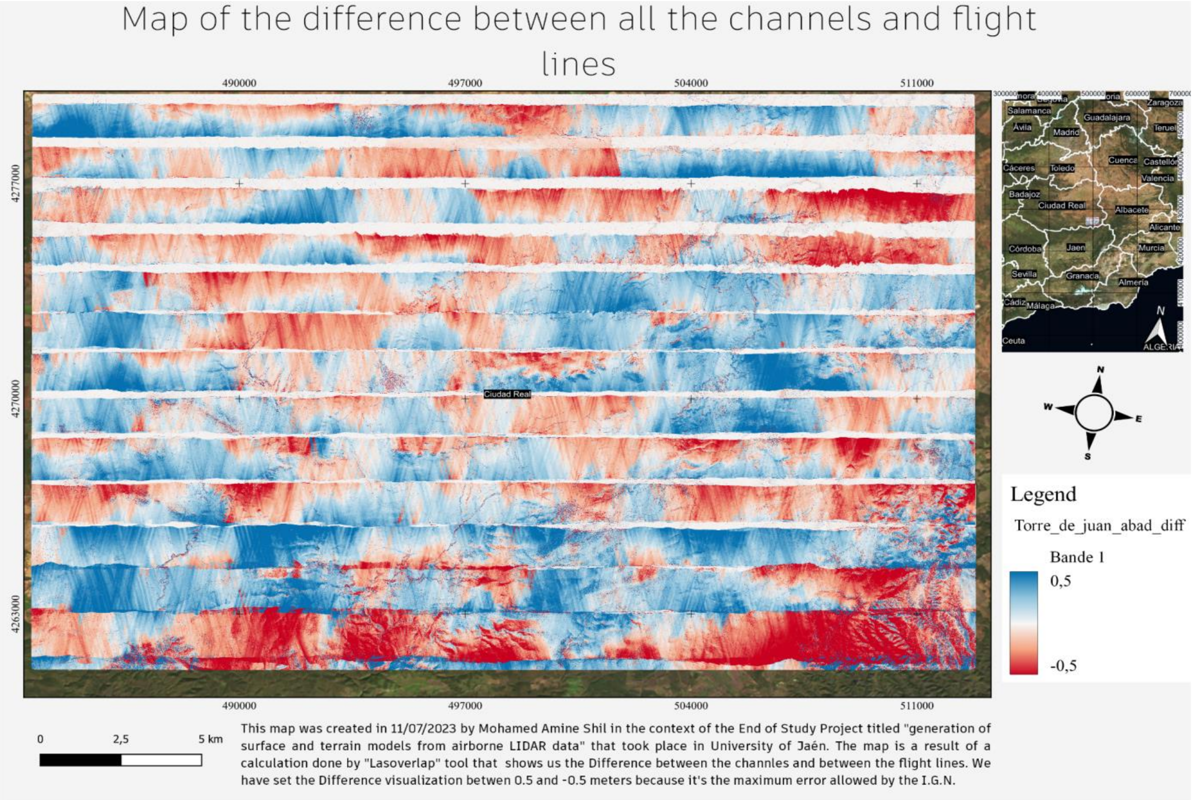

Figure 37 : Difference between the strips for the two channels

As it is obvious in the figure 37, we have an irregular gross error in all over the area of study. This type of error is generally due to GNSS problems, sensor calibration or an IMU misbehavior.

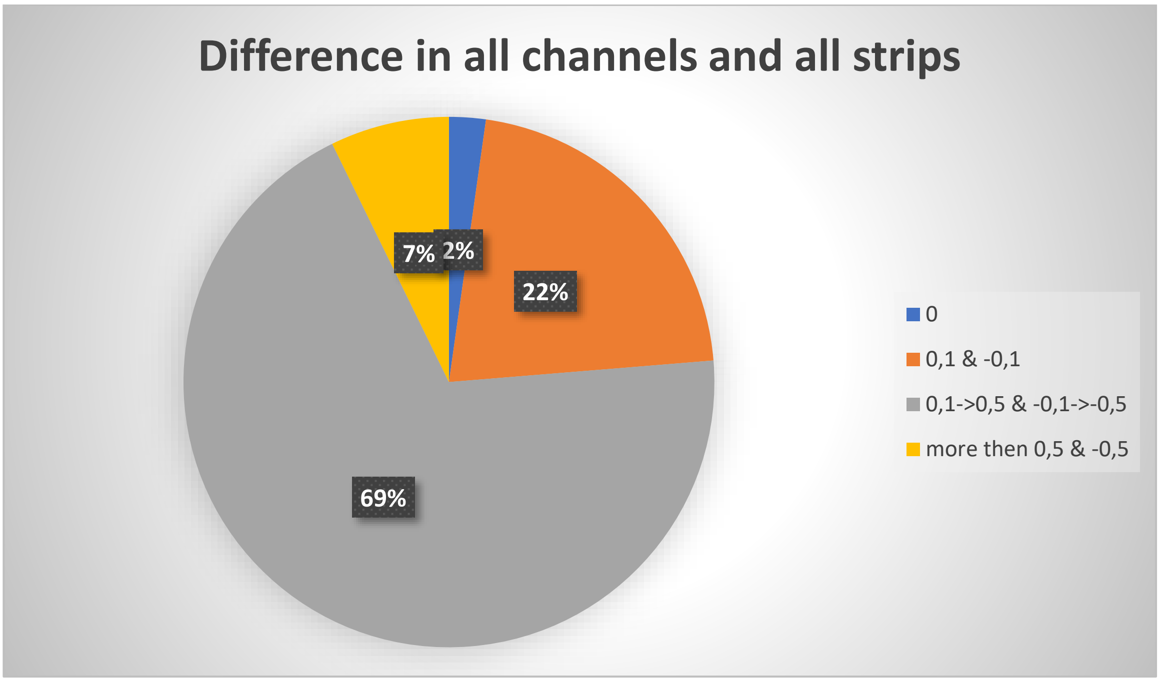

Figure 38: Chart of the difference between the strips in the two channels

This pie chart in figure 38 illustrate the statistics of the number of pixels that contain the difference values. As shown, we divided the chart in four parts:

- 0 m difference: contain 1 329 354 pixels.
- Between 0.1 and -0.1 m of difference: 12 781 891 pixels. We considered this as a safe zone.
- Between 0.1 and 0.5, -0.1 and -0.5 m: 41 103 468 pixels.
- The rest which is above 0.5 m and -0.5 m of difference: 4 313 861 pixels.

Table 7: Statistics for the difference calculation between the strips in two channels

Range (difference in m)	Difference
0	1329354
0,1 & -0,1	12781891
0,1->0,5 & -0,1->-0,5	41103468
more then 0,5 & -0,5	4313861

The IMU plays a crucial role in providing orientation and motion data of the plane. However, the instances of IMU misbehavior can lead to significant disparities in the LiDAR point cloud, when the gyroscope readings are corrupted or drift over the time, it can result an inaccurate data of the sensor's position and orientation. As a consequence, the point cloud will have a difference especially when the sensor work with two separate channels like the Riegl Q-

1560, where the point clouds of its channel should be cooperative and complete each other on a certain level, it will be so different which cause a he error.

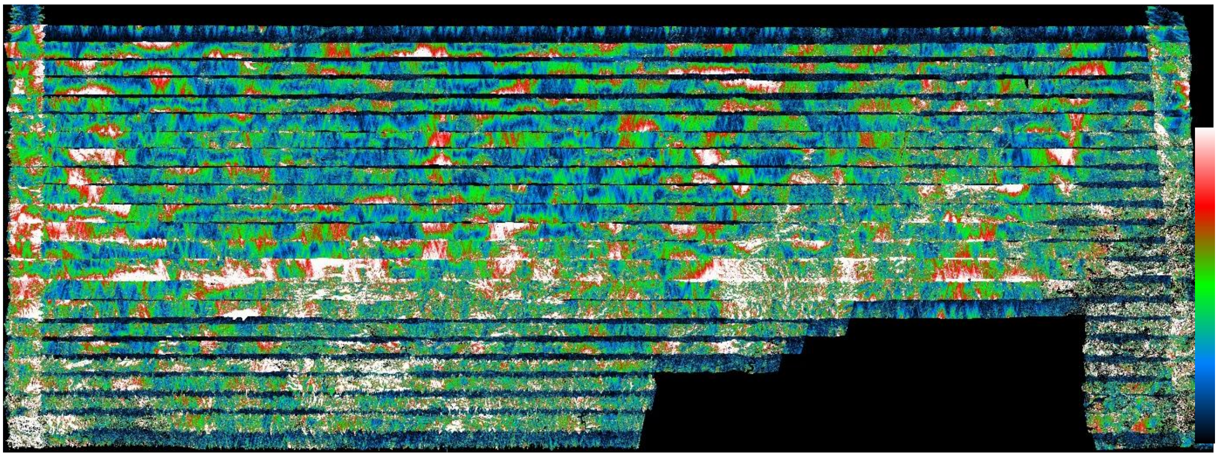

Figure 39 : Difference calculation for the flight compane of 2728 km²

Visual inspection

We completed the control of the alignment and took it to another level, the visual inspection, which serves as a pivotal component within the alignment control paradigm of LIDAR data, facilitating the meticulous evaluation and adjustment of spatial congruence. We utilized global mapper for this task, with uploading all the files, we were capable of having an overview of the points of each LIDAR channel (which is represented by a specific color) in a path profile.

We focused in the buildings to interpret the alignment as shown in the figure 40 and 41.

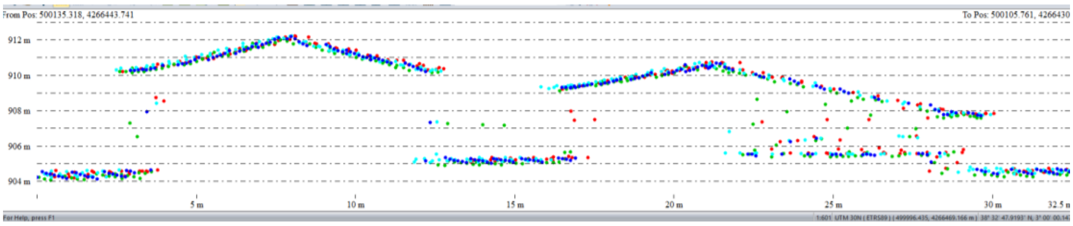

Figure 40 : Path profile for a building in an overlapping area

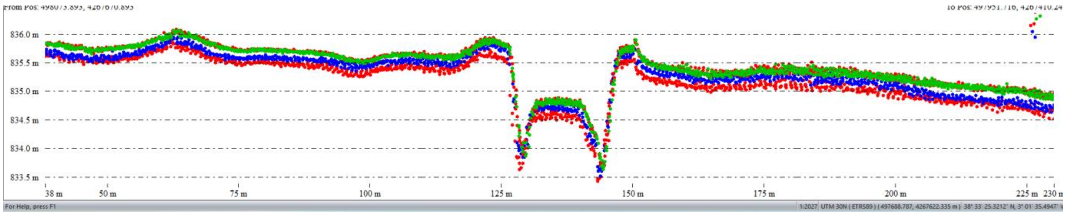

Figure 41 : Line profile of a rural area

3.3. Point density

The point density is a critical parameter that affect the quality, the accuracy and the level of detail of the study area. It refers to the number of points in a square meter.

There is a multiple parameters that influence on the point density, like

- Flight altitude the altitude have a direct impact on the point density. Flying lower will result in higher point density as the Laser beams are more focused and cover a smaller ground area.
- Pulse repetition rate a higher pulse repetition rate allows more laser pulses to be emitted and collected within a given time frame, leading to higher point density.
- Scan pattern multiple swaths can be used to achieve higher point density by overlapping adjacent flight lines.

- Ground Speed The spacing between laser pulses along the flight path is influenced by the speed of the aircraft. Denser point spacing may be the effect of slower ground speed.
- Similar to UAV LiDAR, the characteristics of the terrain and the objects being scanned might affect how many laser pulses are sent to the ground.

Balancing point density with project requirements, survey area size, and res is essential, higher point density provides more accurate and detailed data but also requires more flight time, data processing, and storage capacity, on the other hand, lower point density is acceptable for larger survey areas where high levels of detail are not required.

The task is done with LASgrid and as it is specified in the specification, it should be above 1 pt/m² for the first return only.

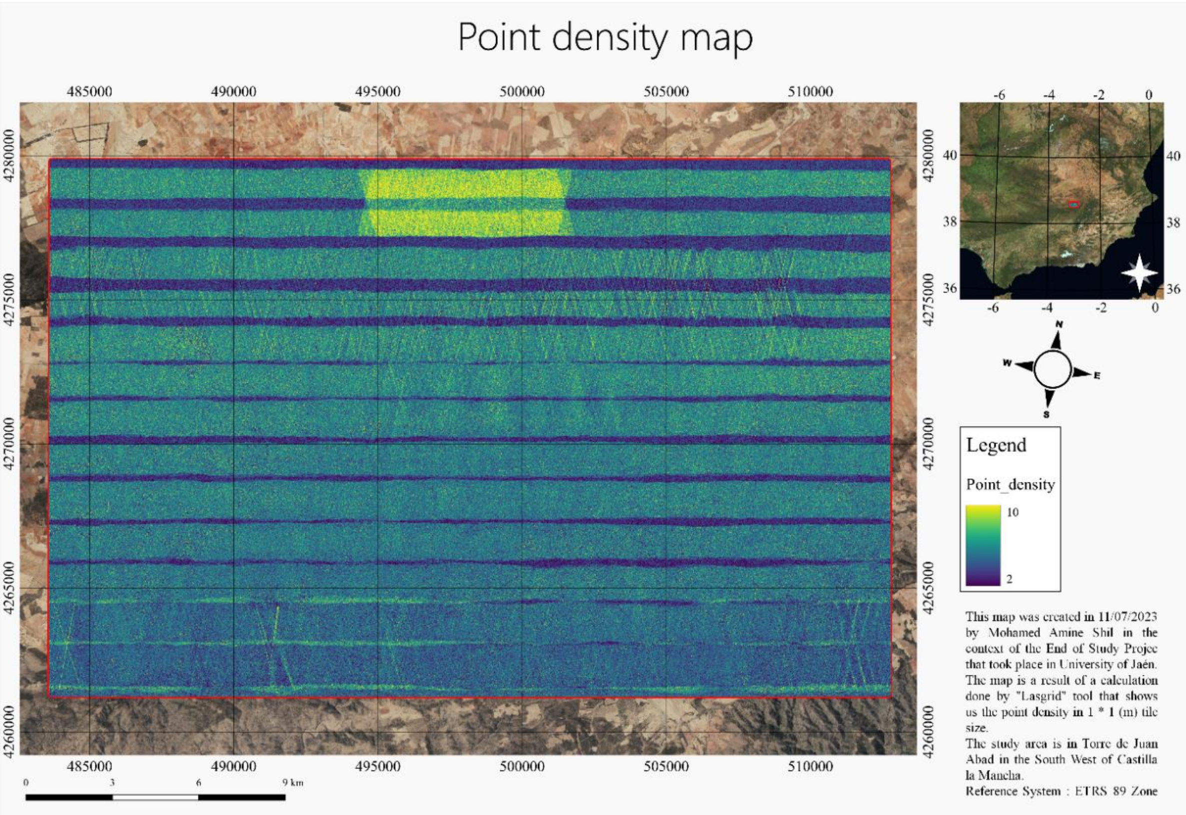

Figure 42 : Map of the point density

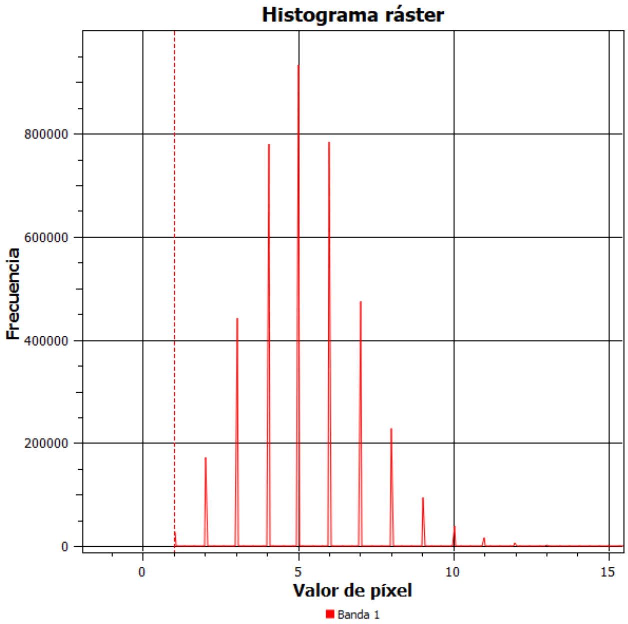

Figure 43 : Histogram of the point density per m²

The figure 42 represent the a color coded map from that represents the density of the points per square meter, the color is degraded from dark blue to yellow. As a Remarque, we notice that we have a lot values around 2 and 5 points/m².

In the figure 43 we made sure of our analyses, the figure represents an histogram that contain information of the number of pixels of each values, in that case the values are the density points, and as we can notice, the minimum value is 2 and the most are around 5.

As a conclusion, the density points are confirm to the specifications.

4. Debugging errors

For this task we used Stripalign from the Bayesmap solutions. The software has been developed to deal with this kind of errors (IMU drifts and error) and to use a specific mathematics formula to make an approach.

The overall accuracy and uncertainty obtained from the LiDAR technology depends on the assembly and calibration of the three system components the GNSS, the IMU (Inertial Navigation System) and the Laser scanner device.

Bore-sight angles are the angular offsets in X, Y and Z directions between the scanner frame and the IMU frame measured at the center of the IMU body frame. The software used a novel method based on the Bayesian inference to address this problem.

The first contribution is to use not only the 3D points extracted from the raw waveforms but their uncertainty as well, and to apply a probabilistic surface matching with spatially variable point accuracy in order to obtain the attitude corrections. The second contribution consists of using all the flight lines, where most methods only use the calibration cross. This way we can also estimate the attitude drift and correct for temporal attitude variations as well. Finally, the software uses the probabilistic framework for error propagation and propose a probability distribution of the calibrated bore-sight angles.

This capture shows us the drift and the bore-sight effect on the LiDAR points. In the figure 44, we have a line profile of a building, in which we distingue a lot of points on the roofs with different colors. Each color represent the ID of the point, it means the file that the point belongs to. We notice the planarity and the miss alignment between the different points that have different ID’s. The same thing for the figure 45.

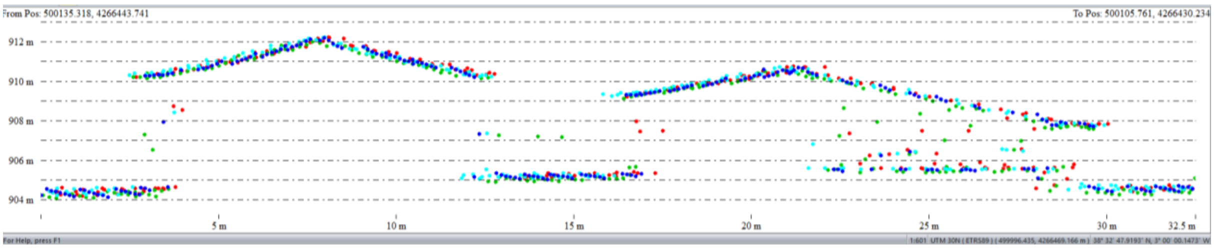

Figure 44 : Path profile of building before correction

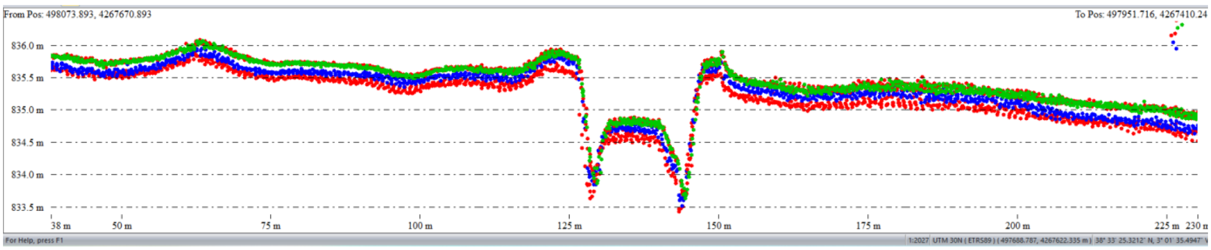

Figure 45 : Line profile for a hazard place before correction

The proposed Bayesian approach that the software uses

It consists of using all the strips at once in a Bayesian framework and compute directly the probability density function of the bore-sight angles, by performing an iterative reconstruction of the surface z(x,y) from all the observations. In this way we don’t use any Delaunay triangulation or any kd-tree for spatial search. A fast gridding method optimally integrates all the point data, taking into account the vertical uncertainty of each point when available (eg. from waveform processing). This gridding is performed via Bayesian fusion of N strips providing a mean zp and a variance σp. A specialized Gaussian Loopy Belief Propagation algorithm is used to achieve a fast, approximate fusion. Then, we integrating out the mean and variance variables (marginalization), yielding a function U that only depends on the bore-sight angles. This function U can be minimized using a gradient technique, and the low number of variables allows for numerical derivatives to be used. This method provides optimal values and a covariance matrix, and can use arbitrary strip configurations. Calibration lines are not necessary if we can use 3 strips (two in opposite directions) of the regular flight.

1. Waveform processing extract the ground peaks P and range accuracies σr
2. Numerical derivatives 4 evaluations of U(<״,<˳,<ˡ)
   A. Fast Gridding Gaussian Loopy Belief Propagation (GLBP) using P, σp for each strip.
   B. Marginalization compute the energy U summing over pixels p and strips n
3. Gradient descent step to update the bore-sight angles
4. Repeat (go to 2) until convergence.

After applying the correction we obtained the following result that represented in the figure 46, 47 and 48

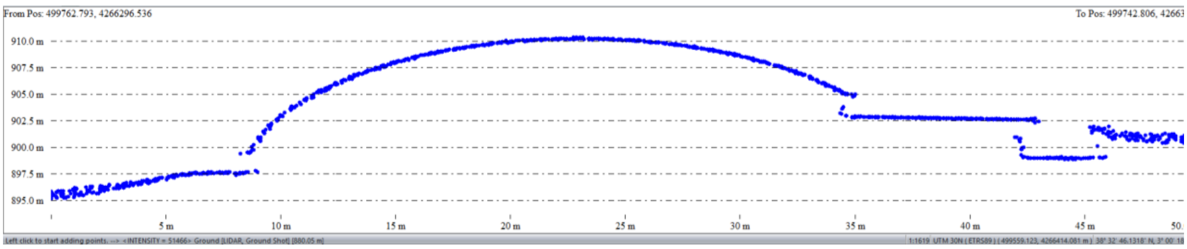

Figure 46 : Line profile for a warehouse after correction

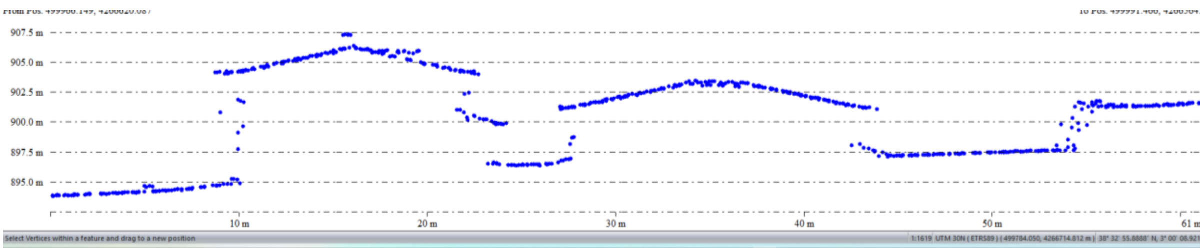

Figure 47 : Line profile of buildings after correction

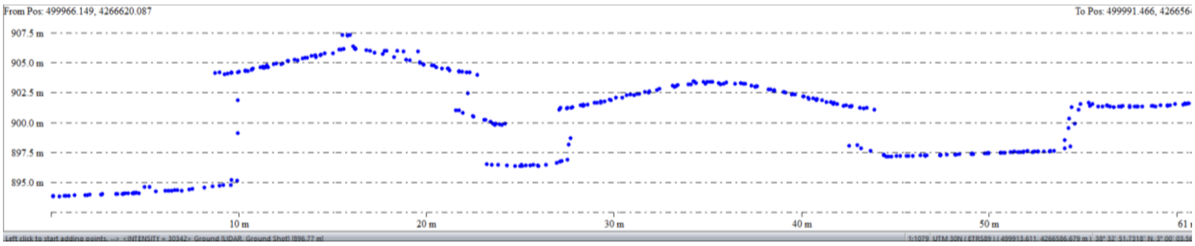

Figure 48 : Line profile of buildings with a 0.5m wide after correction

These figures shows a perfect coherence and alignment between the points of the different strips.

As we inspect the difference between the strips and channels with LASoverlap tool, we recalculated the difference between all the channels and all the strips in our study area after the correction using this command line:

```
:: Difference between Strips in Channel 1 & 2
lasoverlap      -i *.laz -merged -faf -fill 3 -values -no_over -elevation -lowest -odir difference   -o "Difference_strips_allchannels.asc"
```

Figure 49: Parameters of the software

The figure 50 represents the result

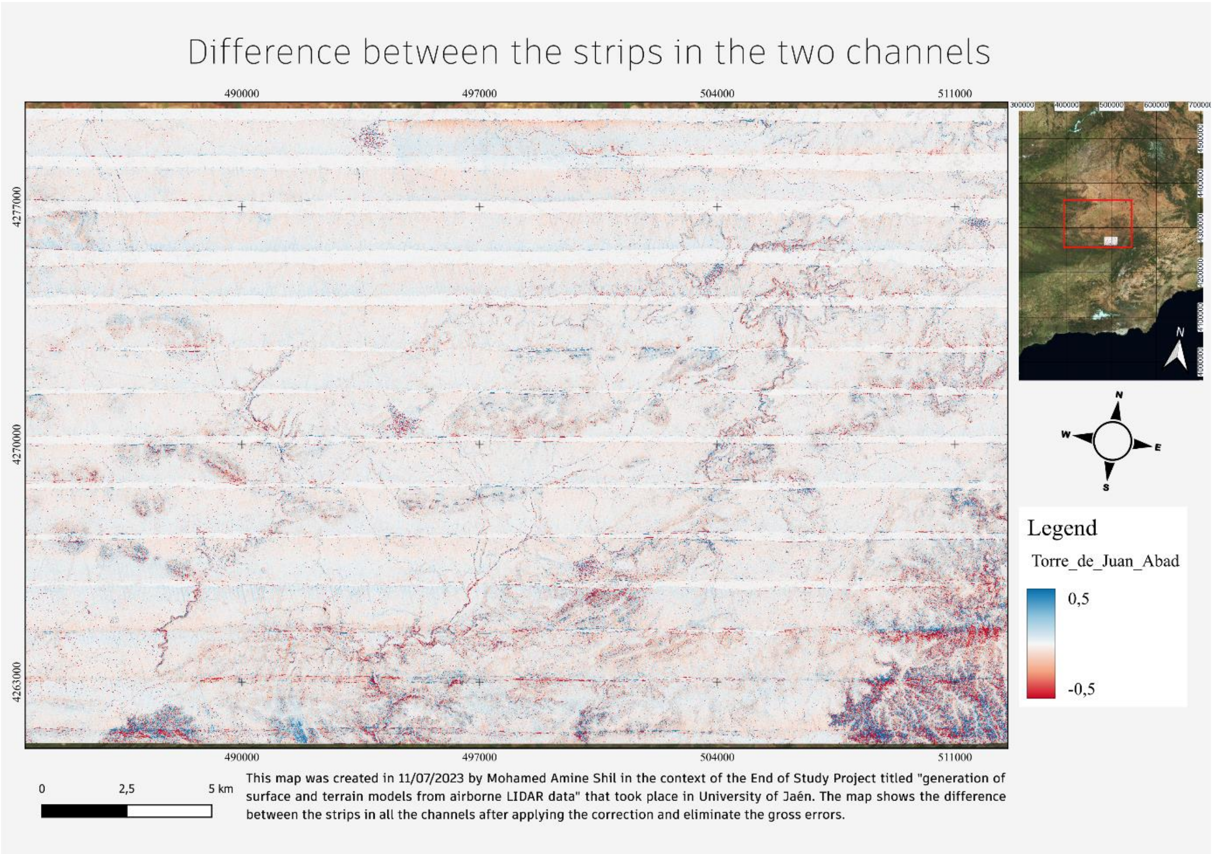

Figure 50 : Map of the difference between all the channels in all the strips after correction

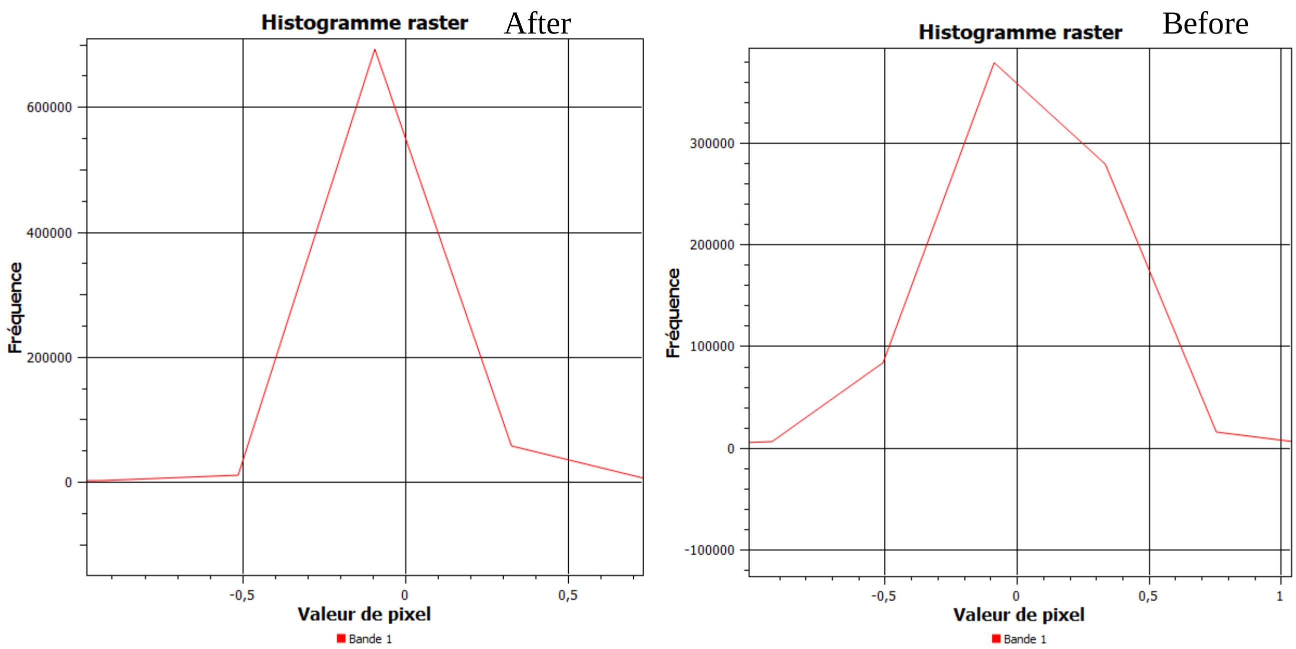

Figure 51: Before and after correction histograms

In the Histogram on the right, which represent the values of difference before the correction, has a large number (almost 200000 pixel on the positive side and 100000 on the negative one) of pixels that surpass the 0.5 m of error. On the different side, the number is remarkably reduced (almost 0 pixel at the 0.5 m difference).

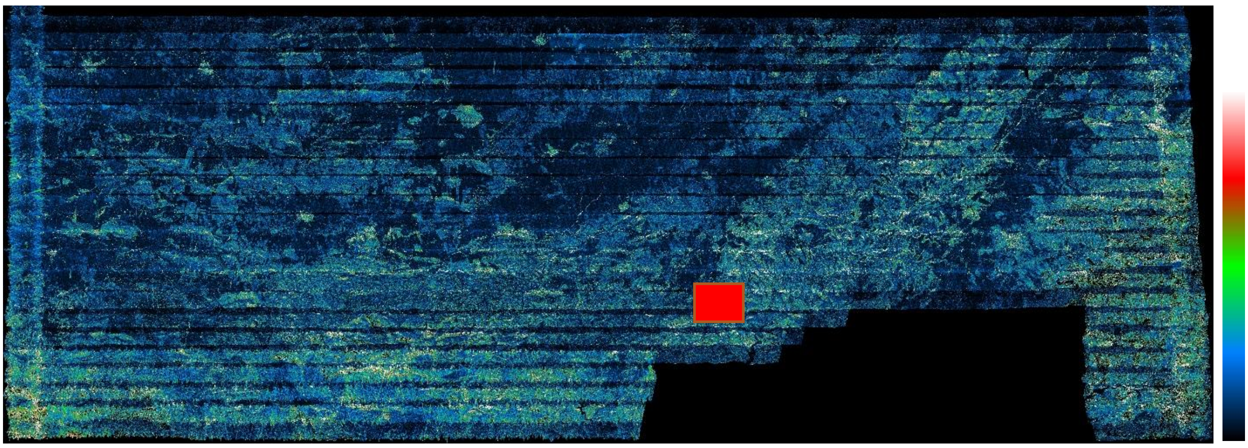

Figure 52 : Difference in the flight compane of 2728 km²

A very important Remarque is that we applied the process to all the available data which cover 2728 km².

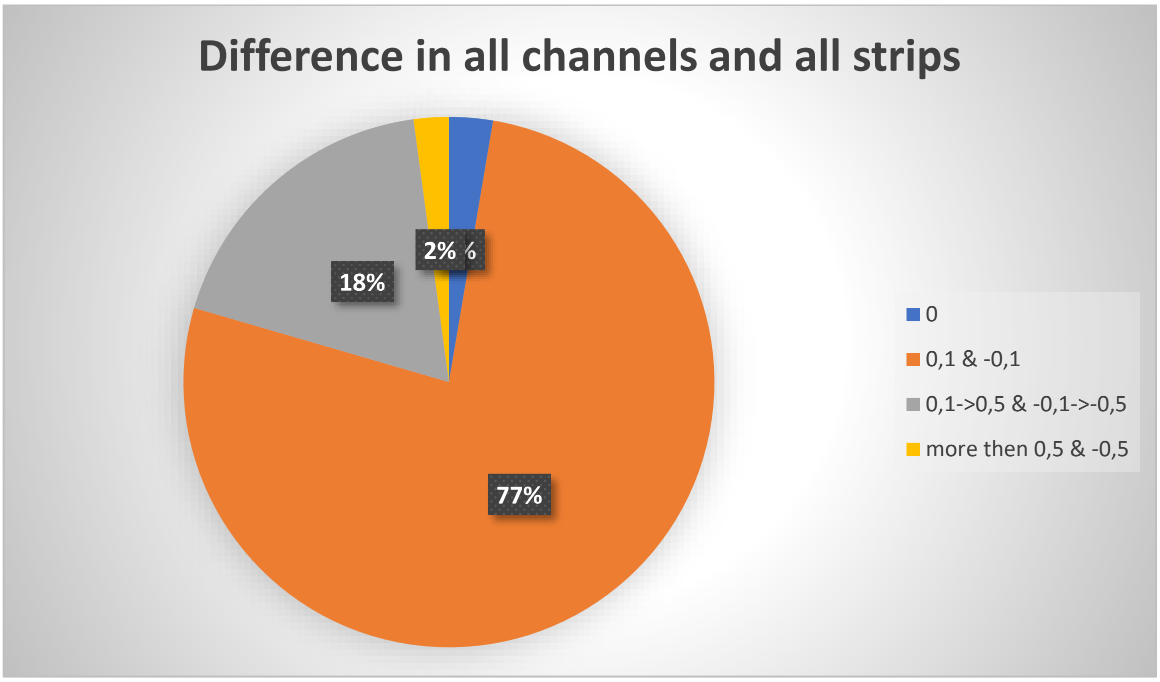

Figure 53: Chart of the difference between the Strips in the two channels after correction

This pie chart illustrate the statistics of the number of pixels that contain the difference values. As shown, we divided the chart in four parts:

- 0 m difference: contain 1 581 514 pixels.
- Between 0.1 and -0.1 m of difference: 45 548 262 pixels. We considered this as a safe zone.
- Between 0.1 and 0.5, -0.1 and -0.5 m: 10 882 316 pixels.
- The rest which is above 0.5 m and -0.5 m of difference: 1 264 322 pixels.

Table 8: Statistics for the difference calculation between the strips for the two channels after correction

Range (difference in m)	Difference
0	1581514
0,1 & -0,1	45548262
0,1->0,5 & -0,1->-0,5	10882316
more then 0,5 & -0,5	1264322

Figure 54: Line chart that shows the difference before and after correction of the data

In the figure 54, we had a line chart that represent the variation and the significant change in the difference between the channels and the strips, at the level of 0.1 and 0.5 we had a drop in counts of pixels, furthermore a correction in the error, and in the opposite direction a level up in the 0.1 and -0.1 count.

5. Absolute accuracy:

After controlling the relative accuracy and debugging the error that occurs, we checked the absolute accuracy using the GCPs.

We used for this task LAScontrol with the following command line:

```
lascontrol -i *.laz  -odir "E:\uja\Corrected_LAZ_files" -cp "E:\uja\Corrected_LAZ_files\gcp\control_points_BufferZone.txt"
-parse xyz -cp_ignore_diff_above 1 -cp_out controlOfCh1.txt
```

```
avgabs/rms/stddev/avg of elevation errors are 0.1384/0.142338/0.0333021/0.1384 meter. skew is -0.166016.
took 1010.35 sec.
```

We have RMSE= 0.14m < 0.15m. Condition verified.

6. Filtering and classification

The objective of this phase is to separate the points that refer, present the bare earth surface and the points that represent the vegetation and the buildings.

Due to the huge surface and point number of the LiDAR files (over 3 billion points and 527 km² in total), we tiled them in order to facilitate the calculation and better interpret each result in each step.

6.1. Tiling

Due to the huge surface and number of points, we tiled the files in a 1500*1500 m with a 20 m of buffer using LAStile tool, but as a first step we merged all the files.

LAStile

LAStile is a LAStools command-line program for quickly tiling big LiDAR point cloud data into smaller, manageable chunks while keeping spatial coherence. This tiling approach improves data organizing, display, and analysis. LAStile breaks large LiDAR datasets into smaller, non-overlapping tiles or blocks that may be processed or shown independently. These tiles preserve geographic context, allowing users to operate with specific locations while controlling memory consumption effectively. This tool is useful for streamlining data handling, speeding up data access, and enabling parallel processing of LiDAR point cloud data. It is frequently utilized in applications ranging from forestry management to urban planning, easing and improving the usability of large-scale LiDAR data handling.

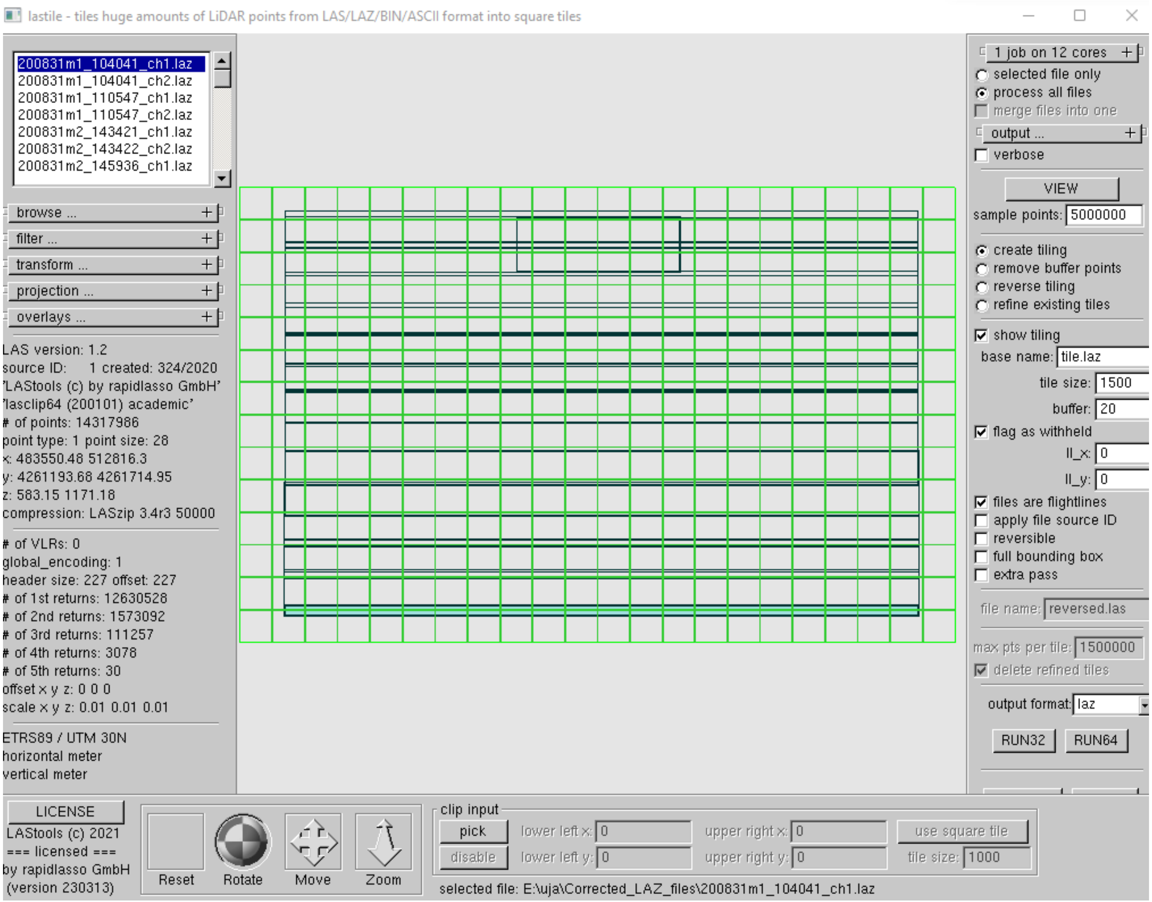

Figure 55 : Tiling the data with LAStile

6.2. Ground classification

After creating the tiles of our study area, we proceeded the ground classification with LASground_new from LAStools.

- LASground_new allows us to classify the points belonging to the ground on the basis of the criteria to establish. It is based on the progressive reconstruction of the terrain. First, an approximation of the terrain is generated considering the lowest points. They are triangulated and establishes an angle criterion and distance, that if it is fulfilled by the points that are inside each triangle, it will be classified as land. This process is iterative, so points that meet the membership conditions.

LASground_new has several options that adjust depending on what terrain the player is on project. In this case, there are areas with a large number of buildings which is why the Metropolis option that has a step size of 30 meters and with it allows to eliminate all or almost all the buildings in the area. Compute Height has also been selected so that the algorithm to calculate the height of each point to the ground and LASclassify can be used without having to use the LASheight option.

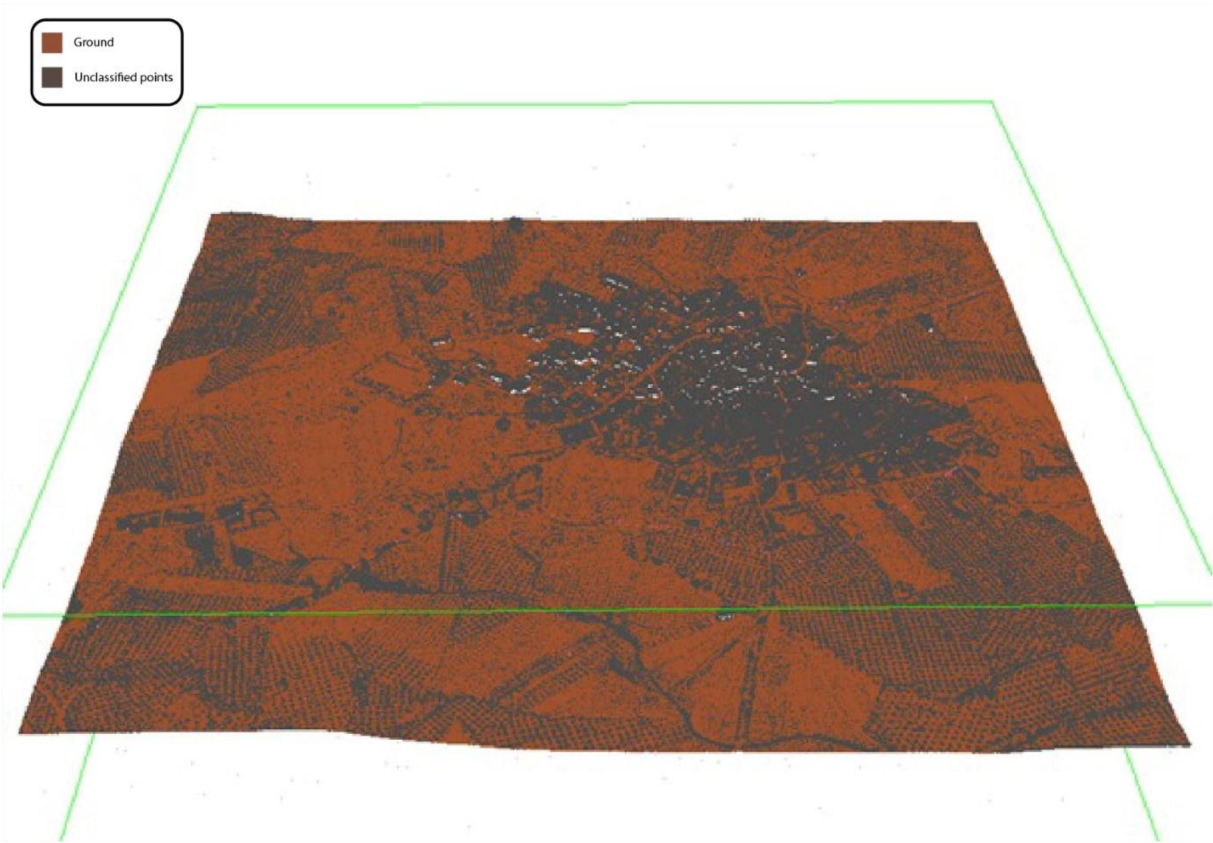

Figure 56 : Part of the ground classification of the study area

Due to the very large area we usually control the classification by triangulating the points using the LASview by pressing the ‘t’ alphabet; it’s a quick quality control to validate the work, for a detailed quality control we proceed by generate the hill shade of the DTM.

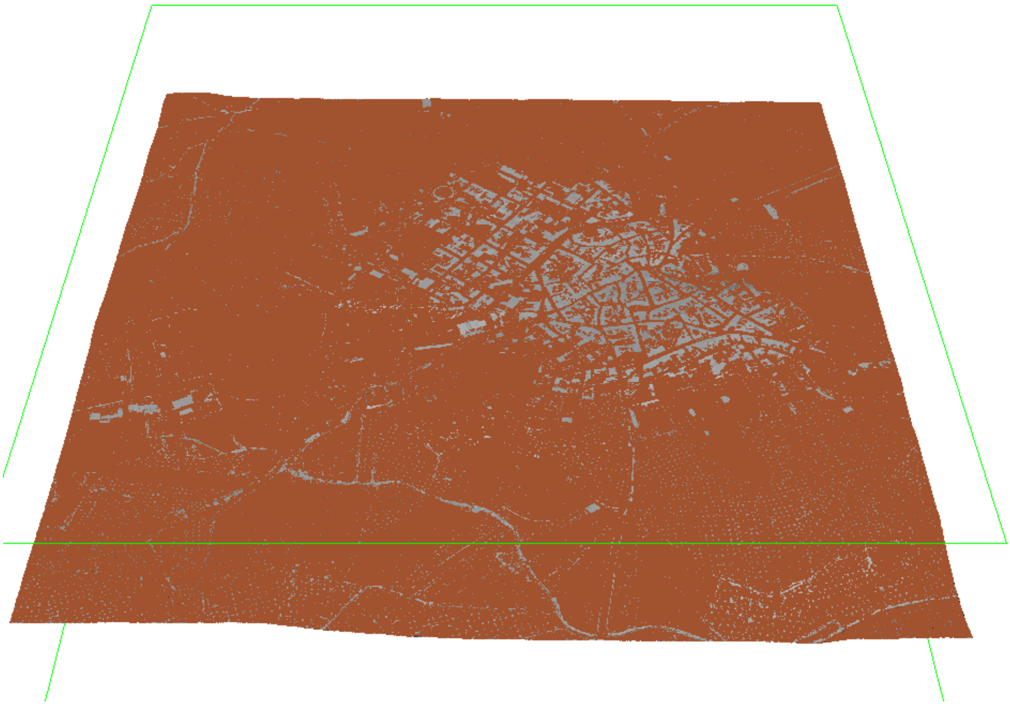

Figure 57 : Fast gridding for the ground point of a part of the study area

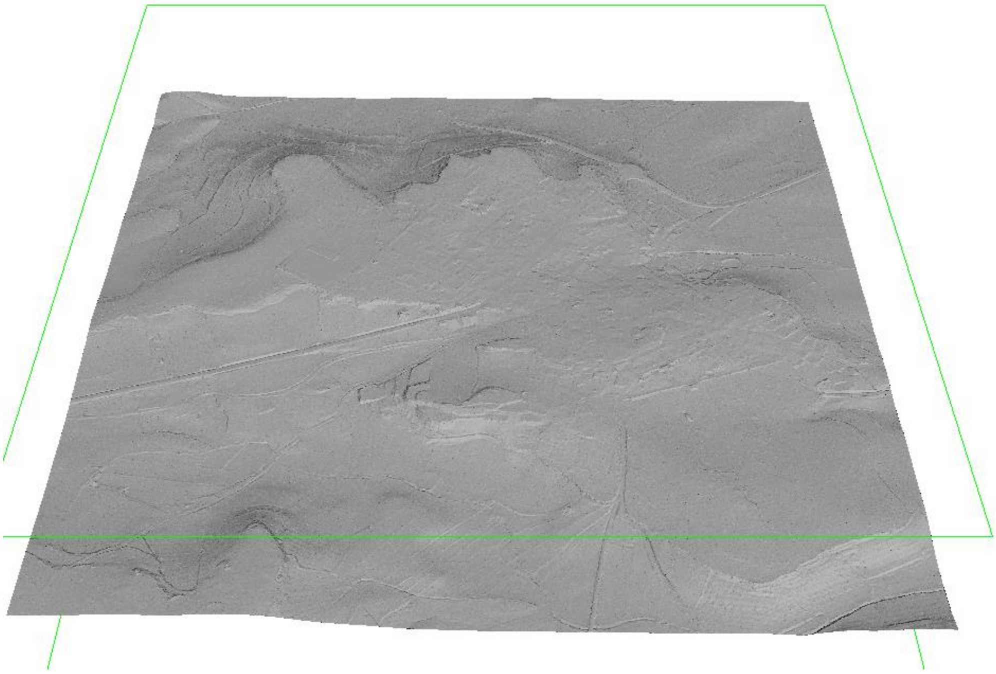

Figure 58 : Quality check of the Ground classification

6.3. Classification of buildings and vegetation

After had classified the ground, we had used the LASclassify to classify the vegetation and the buildings. We have tried to focus our classification on the buildings, after that we had used the LASheight to classify the rest of the points into vegetation.

While classifying the ground, which represent the base reference, we calculated the height of the points above the ground and store it so we can use in the classifications of the buildings and vegetation.

LASclassify uses an algorithm that classifies the buildings and the vegetation in a specific area size with a specific parameter like building planarity, forest ruggedness and it give you the hand to specify whether you have tiny buildings in the study area or not.

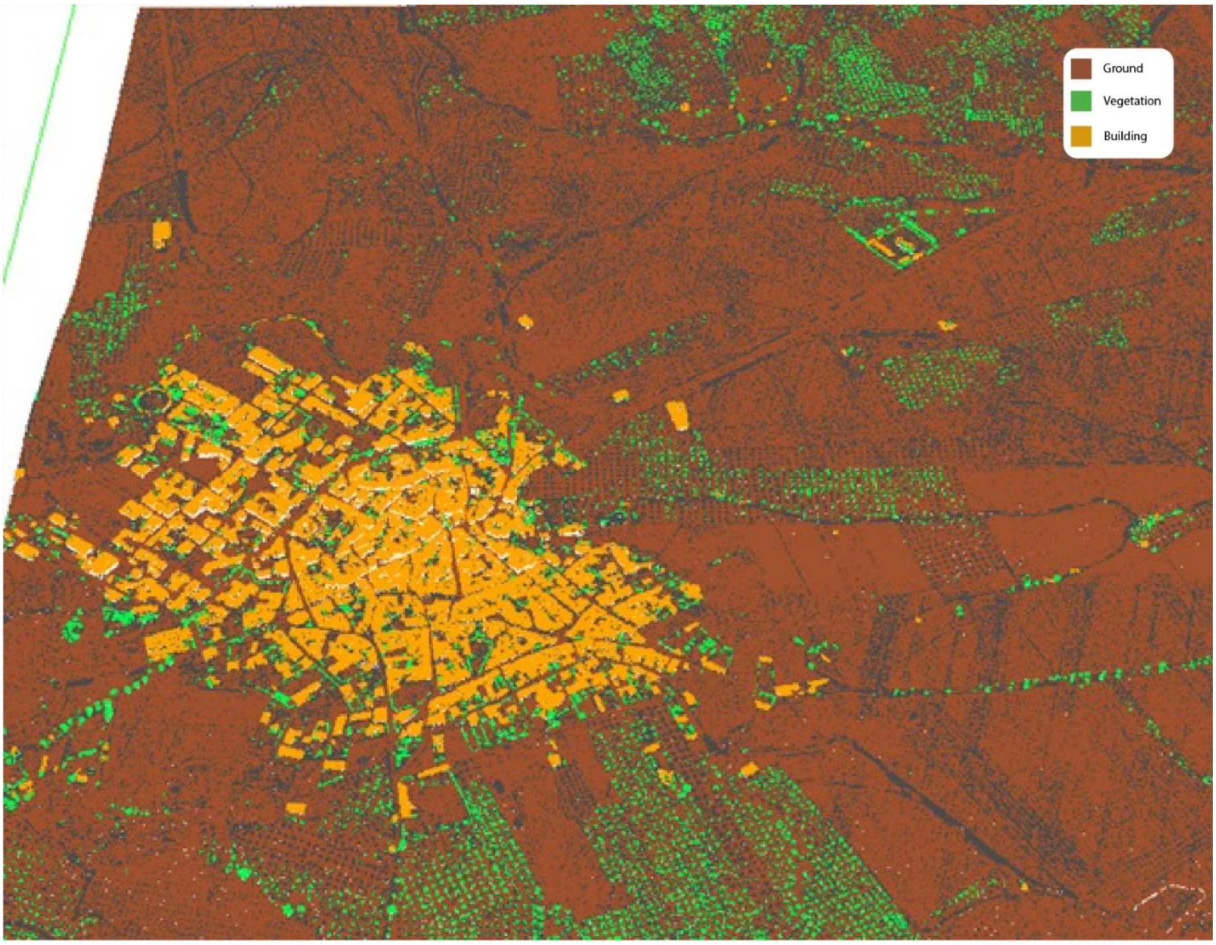

Figure 59 : Visualization of ground, buildings and vegetation classes

7. Generation of DSM and DTM

7.1. DTM

As we filtered and classified the point cloud, we obtained a class ground (2) which contain all the points that represents the ground, the next step is to generate the digital terrain model using only this class.

For this task we used bLASt2dem which is significant for dealing with a large number of LiDAR points (up to 2 billion point).

BLASt2dem

"BLASt2DEM" is a software tool commonly used in the field of geospatial analysis and remote sensing. It serves as a bridge between LiDAR (Light Detection and Ranging) data and digital elevation models (DEMs). BLASt2DEM facilitates the process of converting raw LiDAR point cloud data into accurate and detailed DEMs, which represent the elevation values of the Earth's surface. This tool employs various algorithms and techniques to handle LiDAR data preprocessing, filtering, and interpolation, resulting in a seamless and high-resolution representation of terrain. Researchers, environmental scientists, and professionals in fields like cartography and urban planning often utilize BLASt2DEM to extract valuable topographical information from LiDAR data, aiding in applications such as flood modeling, land management, and infrastructure planning.

Our mean density is 3 pts/m² so we generated the DTM with a Cell size will be 1 * 1 m in ASCII format with **ETRS89** as a geodetic system and **UTM 30N** as a cartographic projection with the **EPSG code 25830.**

Result

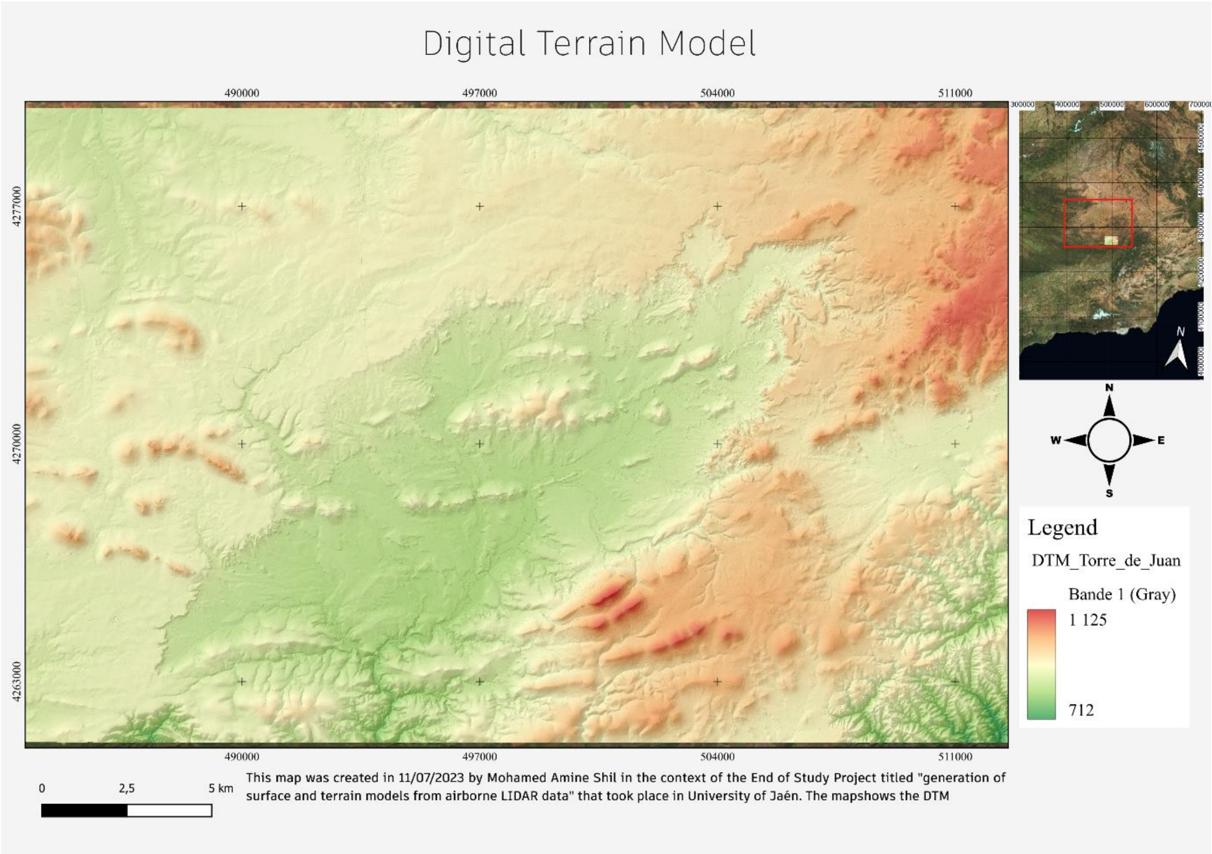

Figure 60 : DTM of the study area

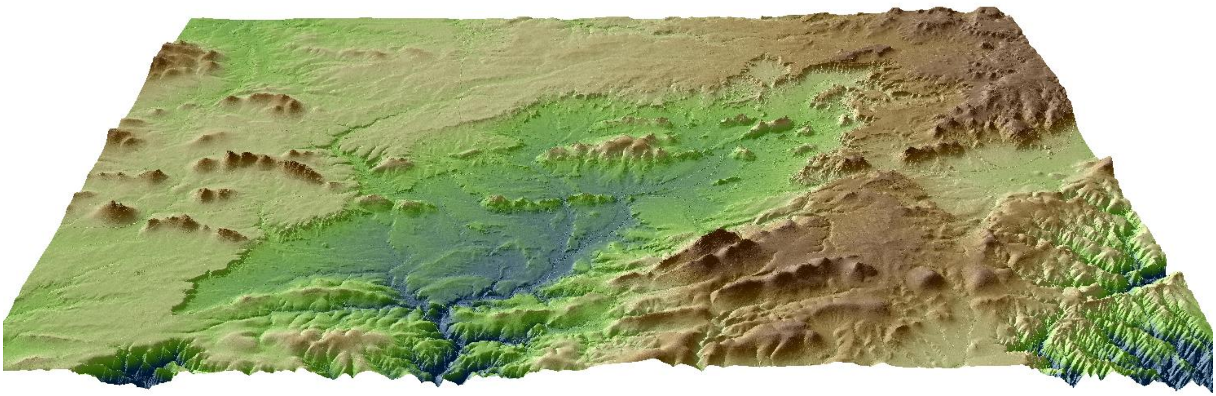

Figure 61 : 3D view of the DTM of the study area

Quality control of the DTM

The quality control of the digital terrain model consist of looking for errors and voids, miscalculation of the raster or some artifacts in the pixels. This procedure is done by hand and its precision depends on the qualification and the quality of the interpreter.

The meticulous evaluation of the digital terrain model (DTM) constitutes a pivotal phase in ensuring the reliability and accuracy of geospatial data. This multifaceted process is primarily centered on the meticulous identification and rectification of anomalies that might compromise the DTM's integrity. These anomalies encompass a spectrum of potential issues, including but not limited to errors stemming from data acquisition, voids resulting from incomplete data coverage, miscalculations in the rasterization process, and subtle artifacts that may manifest as aberrations within individual pixel values.

In this quality control endeavor, the interpreter assumes a pivotal role as the sentinel of data fidelity. Armed with their nuanced understanding of geospatial dynamics and topographical intricacies, the interpreter undertakes a painstaking examination of the DTM. This process often involves a systematic visual inspection, manual cross-referencing against ground truth measurements, and the application of advanced computational techniques for error detection.

The precision of this evaluation procedure is contingent upon a dual interplay the interpreter's professional qualifications and the caliber of their discernment, along with the overall quality of the dataset under scrutiny. Proficiency in geospatial analysis, cartographic conventions, and an astute awareness of potential artifacts are vital attributes that empower the interpreter to navigate the complex landscape of potential discrepancies effectively. Simultaneously, the quality of the underlying dataset, encompassing data acquisition methodologies, sensor calibration, and post-processing workflows, significantly influences the potential for errors or artifacts to emerge.

In an era increasingly dominated by automated data processing, it's imperative to acknowledge that the human interpreter remains an indispensable component of the quality control framework. Their ability to fuse scientific expertise with contextual awareness culminates in a comprehensive assessment that transcends algorithmic limitations, ensuring the fidelity of the digital terrain model in critical applications ranging from environmental modeling to infrastructure planning. And to fulfill this devious need, we used the hillshade.

The hillshade technically is a simulation for the orientation of the sun and the shade reflection on the terrain, with this hillshade and using different angles of the sun, we can detect the artifacts in the digital terrain model.

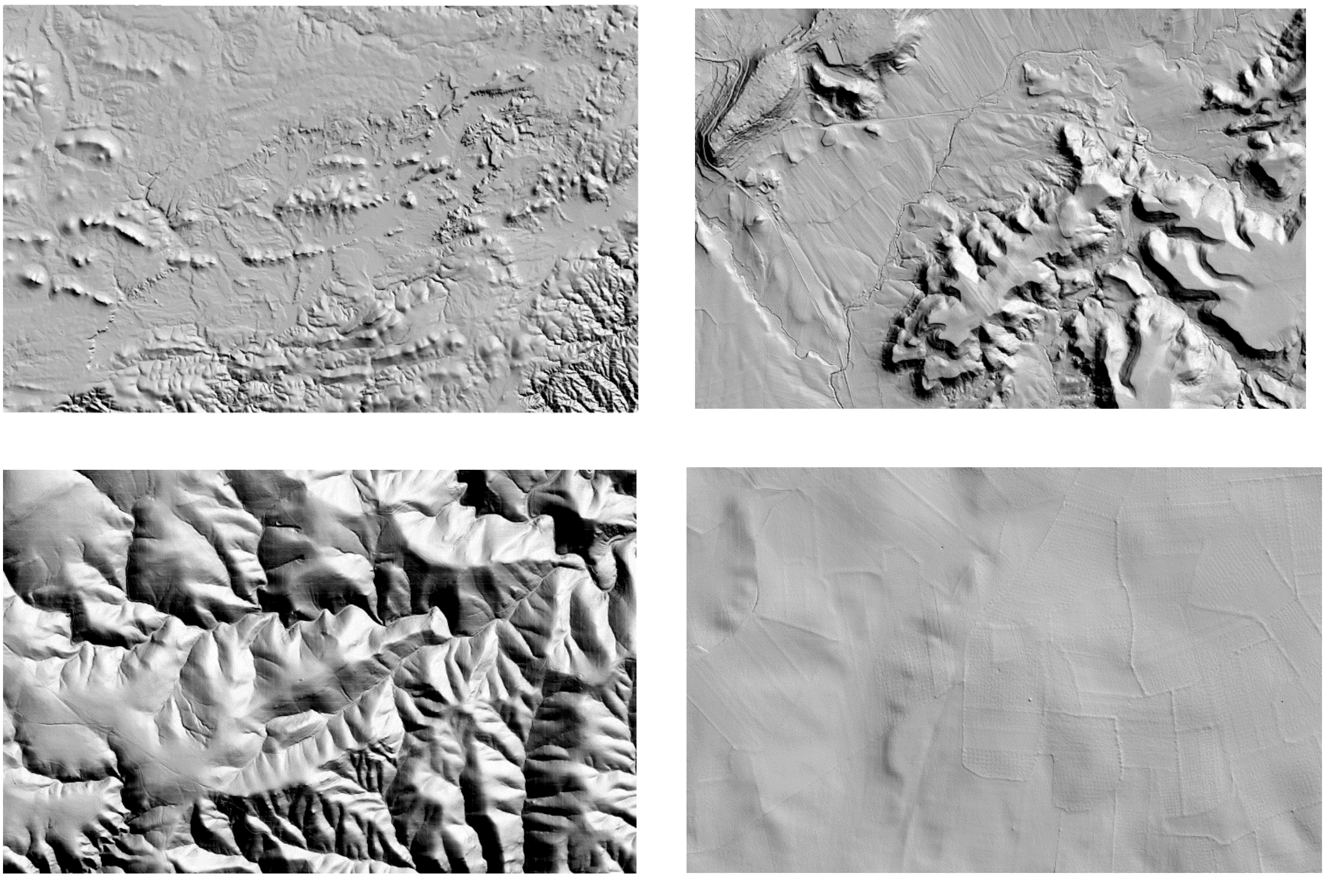

Figure 62 : Hillshade representation of the Digital Terrain Model

The figure 55 represents four images that are captured from the hillshade used to analyze the DTM, the first picture represents the whole area, the second represents a mountain as the same as the third picture, while the fourth represents an almost flat area that obviously contain a trace of agriculture lands. The results are perfect which indicate the quality of the treatment and the filtering used during the process.

7.2. Contour

The derivation of contours from the Digital Terrain Model (DTM) engendered by LiDAR data assumes a critical role in the context of topographic mapping and scientific inquiry. The contours harvested from this process not only offer a remarkable level of granularity but also extend their utility to realms such as topographic cartography and the scientific domain at large. For this intricate endeavor, the SAGA Geographic Information System (GIS) software emerged as the instrument of choice, enabling the aggregation of ASCII-formatted files from the mosaic of tiles and subsequently facilitating the contour generation process.

However, the precision inherent to LiDAR-derived contours introduces a unique set of challenges in their assimilation within topographic maps. Their intrinsic detail, while invaluable for analytical depth, necessitates a finesse in presentation. To bridge this gap, the application of smoothing and filtering algorithms becomes imperative, harmonizing the contours into a format that is comprehensible and visually coherent within the framework of a topographic map.

Central to this contour refinement process is the deployment of the improved Simplified Isohyetal Adjustment (SIA) model, selected for its inherent prowess in enhancing the smoothness of contours. Executed with a sensitivity level calibrated at three, along with a sequence of ten iterative iterations, the algorithm was finessed with ten preservation steps, as expounded in Figure 61. This sophisticated algorithmic approach serves as a linchpin in realizing a harmonious synthesis between the precision of LiDAR data and the contextual requirements of topographic cartography.

In conclusion, the extraction of contours from the DTM, stemming from LiDAR datasets, embodies a convergence of precision, software dexterity, and algorithmic finesse. The contours harvested from this process carry intrinsic scientific value, providing a nuanced depiction of the Earth's surface. Their refinement and assimilation within topographic maps exemplify the delicate interplay between data precision and cartographic representation, a synergy that elevates the comprehension and communicative potential of geospatial information..

We had used the improved SIA model as an algorithm of smoothing with level 3 of sensitivity and 10 iteration and 10 preservation as indicates in the figure 61

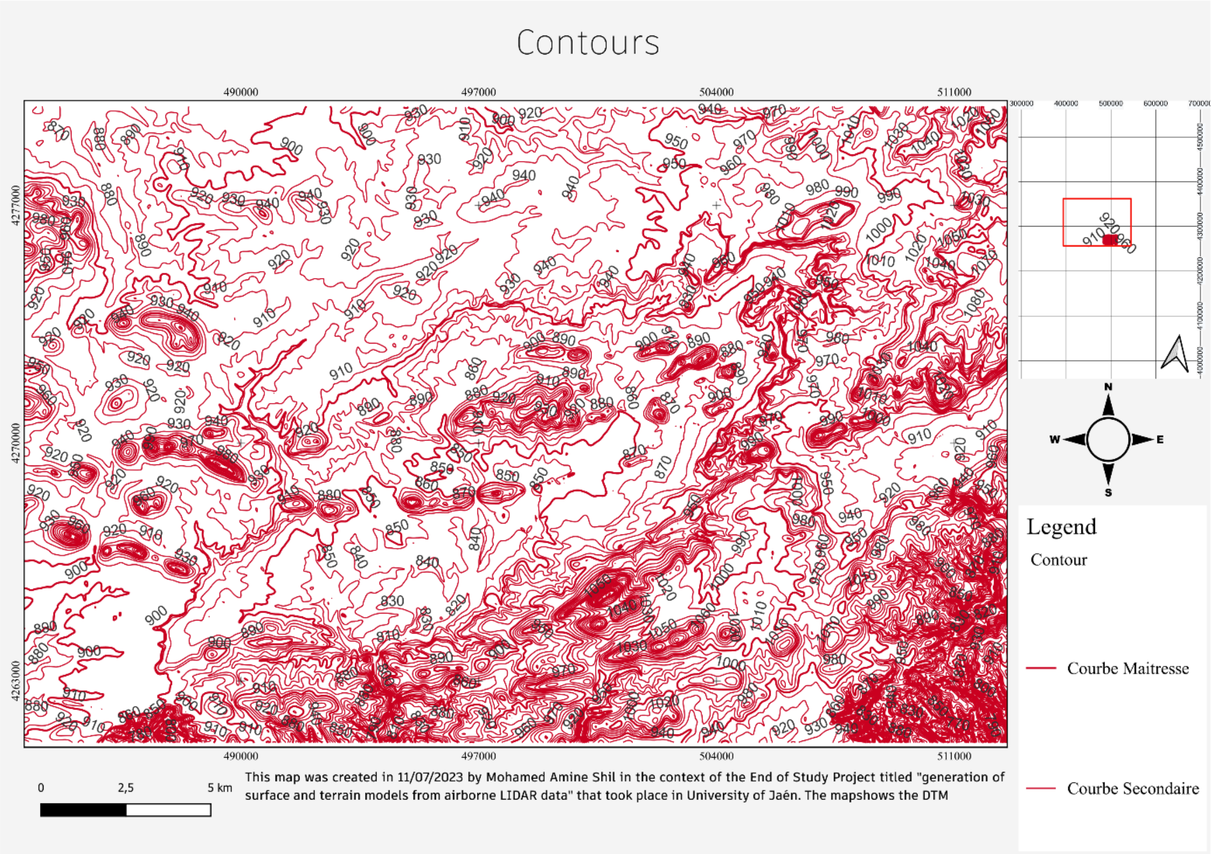

Figure 63 : Contours

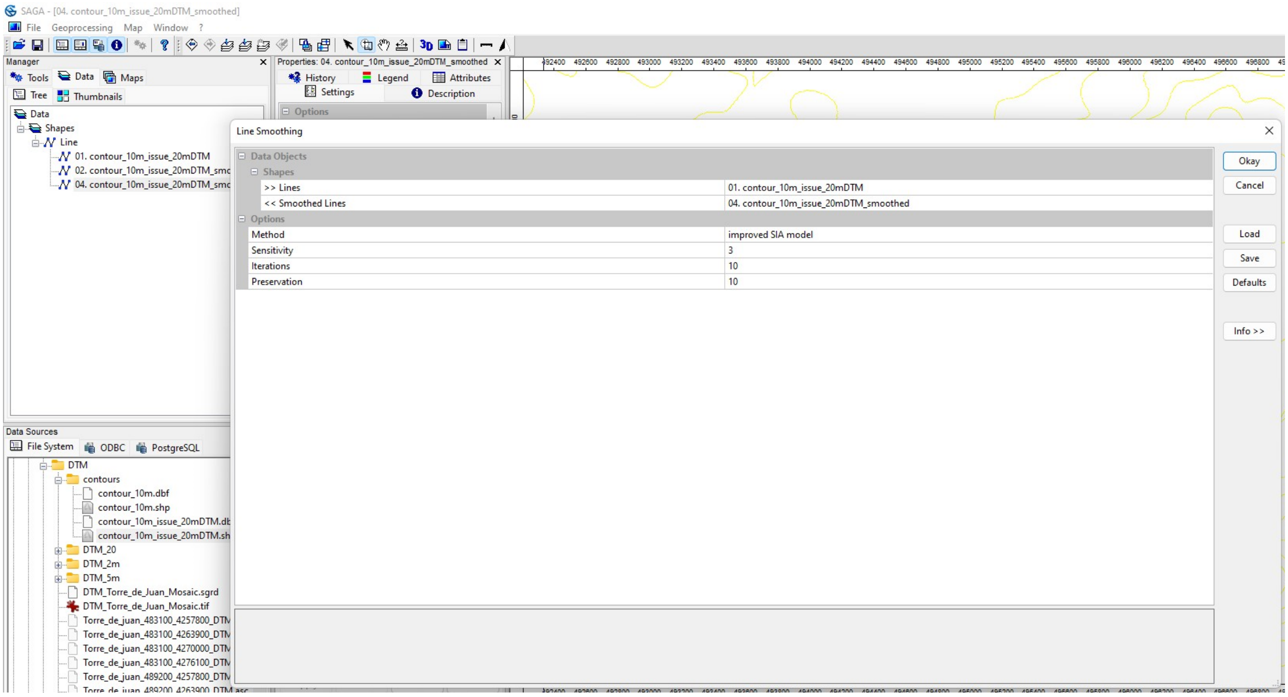

Figure 64 : Smoothing parameters

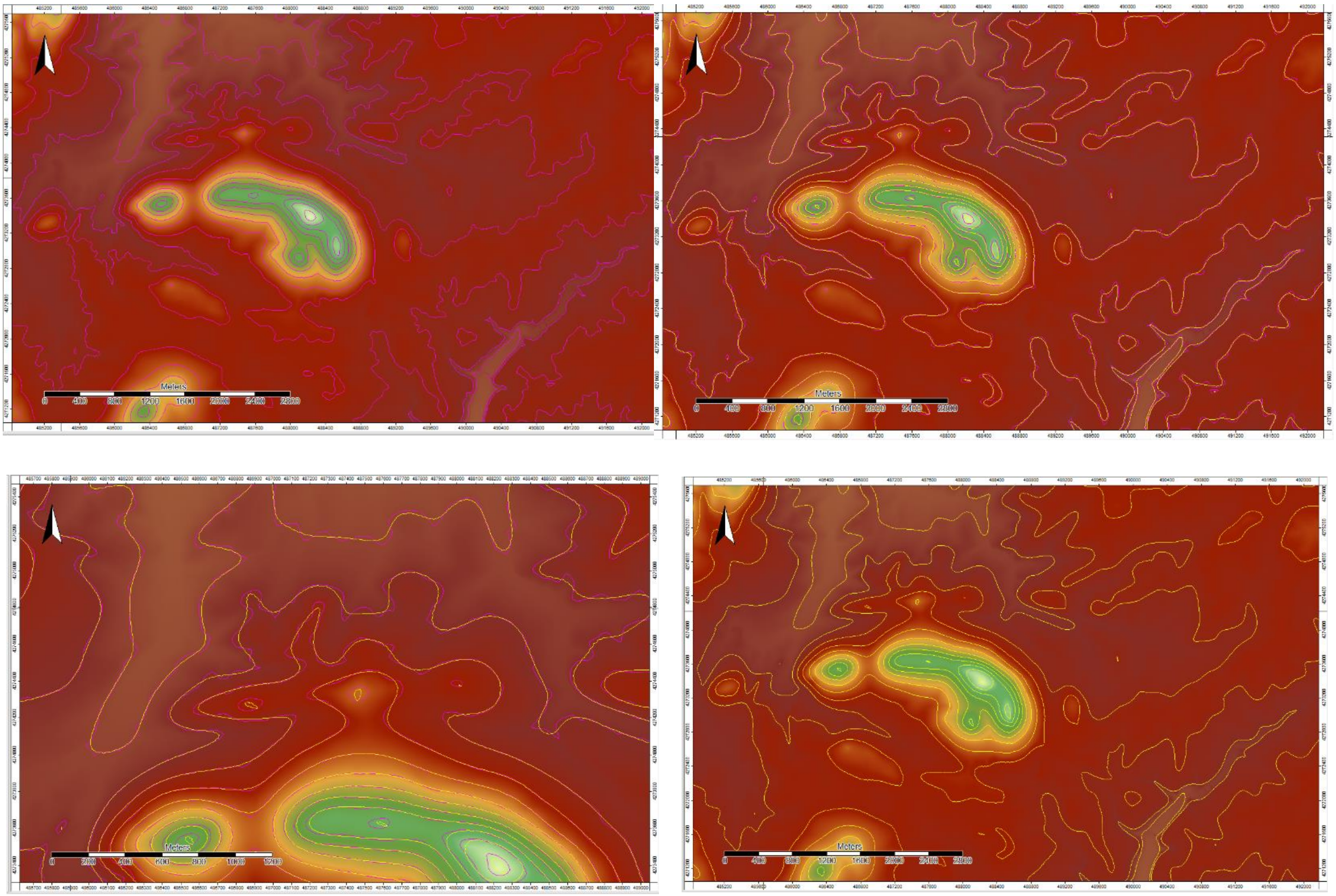

Figure 65 : Contours before and after smoothing

The figure 58 shows us a four different images, the first represent the contours before smoothing. The second and the third shows the two contour before and after smoothing, the fourth shows the contour after smoothing. The smoothing and the filtering of the contours lines is necessary, because the scientific and the normal people that deal with the topographic maps, when you usually find the contours, cannot interpret and work the original data.

7.3. DSM

The Digital Surface Model (DSM), derived from aerial LiDAR sensor data, embodies a pivotal advancement in the realm of geospatial analysis. This intricate model serves as a high-resolution representation of the Earth's surface, encompassing both natural terrain and all superimposed objects. It manifests as a result of meticulously processing point cloud data acquired by the LiDAR sensor, where each point carries precise elevation information. Through the employment of advanced algorithms, point clouds are classified and filtered to eliminate non-ground points, thereby isolating the terrain elements. The remaining ground points form the foundational basis for the DSM, rendering an elevation model that distinctly delineates surface variations, whether they arise from natural topography or anthropogenic features.

The DSM encapsulates not just elevation but a multi-dimensional representation of the landscape. This invaluable asset is foundational to a multitude of applications, spanning from urban planning and environmental monitoring to disaster management and precision agriculture. Urban planners leverage DSMs to assess the impact of infrastructure development, while ecologists utilize them to model water flow patterns and monitor changes in land cover. Furthermore, the DSM's capacity to distinguish terrain features facilitates flood modeling, helping anticipate inundation areas and enabling emergency response preparedness.

The generation of DSMs from aerial LiDAR sensor data is underpinned by a complex interplay of technologies. Airborne LiDAR systems, equipped with high-frequency Laser scanners and precise Global Navigation Satellite System (GNSS) receivers, capture millions of elevation measurements per second, furnishing the point cloud data essential for model creation. Post-acquisition, robust data processing pipelines are deployed, encompassing point cloud filtering, classification, and interpolation techniques. The fusion of these steps culminates in a DSM that holds a mirror to the Earth's topography, enabling stakeholders to not only analyze the terrain's spatial attributes but also interpret intricate patterns that underlie the environmental dynamics.

In essence, the Digital Surface Model derived from aerial LiDAR sensor data is an embodiment of precision, computational prowess, and scientific innovation. It stands as a testament to the convergence of cutting-edge technology and meticulous methodology, bestowing upon geospatial analysis an invaluable tool to comprehend the Earth's contours and features with an unparalleled level of detail and accuracy.

DSM, stands for Digital Surface Model, is a triangulation of all the LIDAR points in all returns, its calculated with BLASt2dem too in a 1m cell.

Result

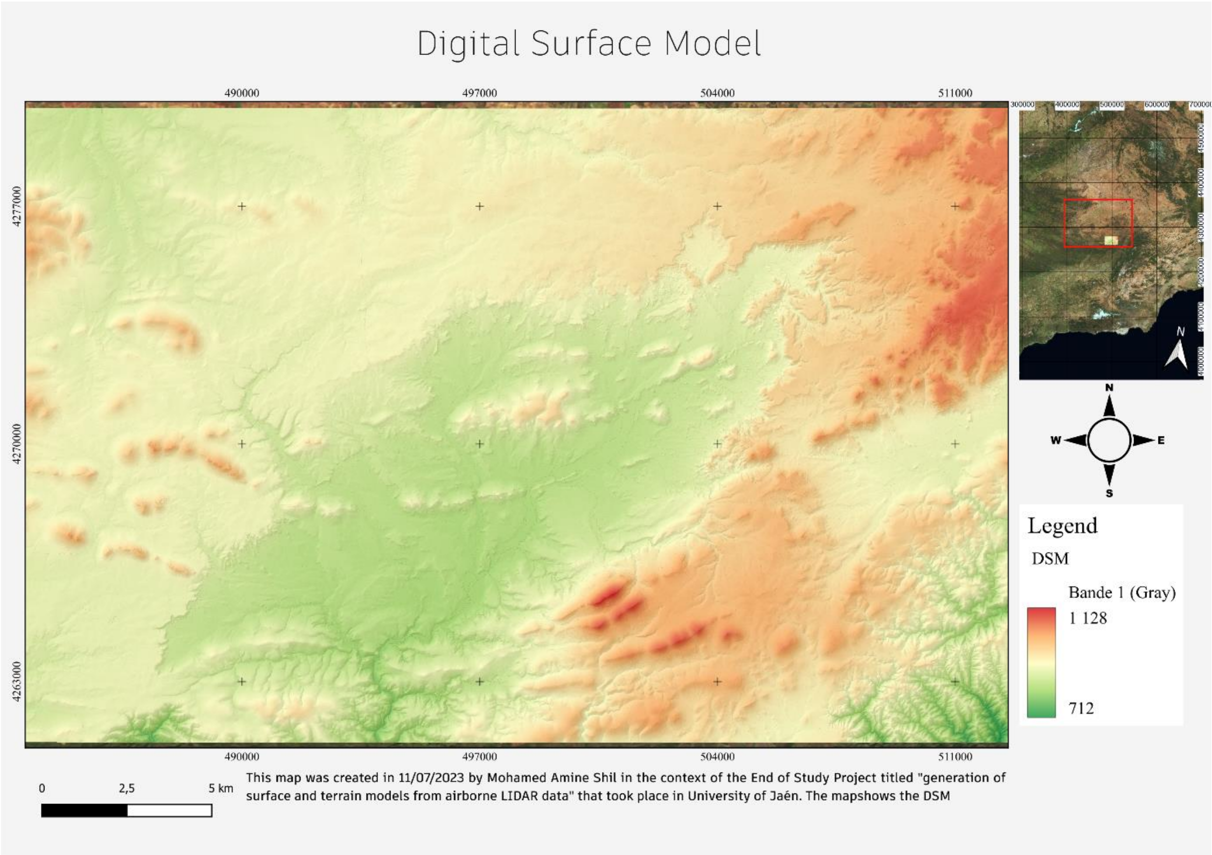

Figure 66 : DSM map

Using the Digital terrain model we could generate other products like terrain slope (figure 59) and terrain aspects (figure 60).

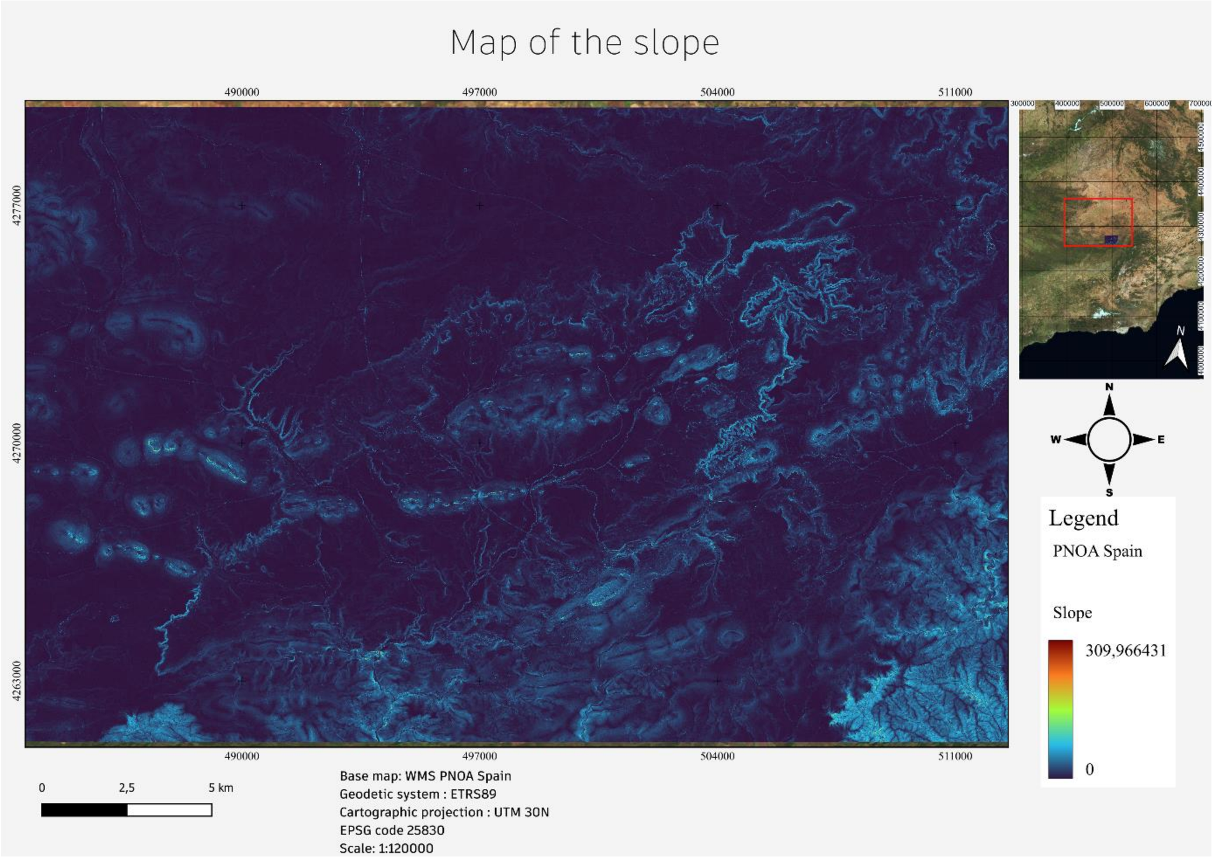

Figure 67: Slope map of our study area

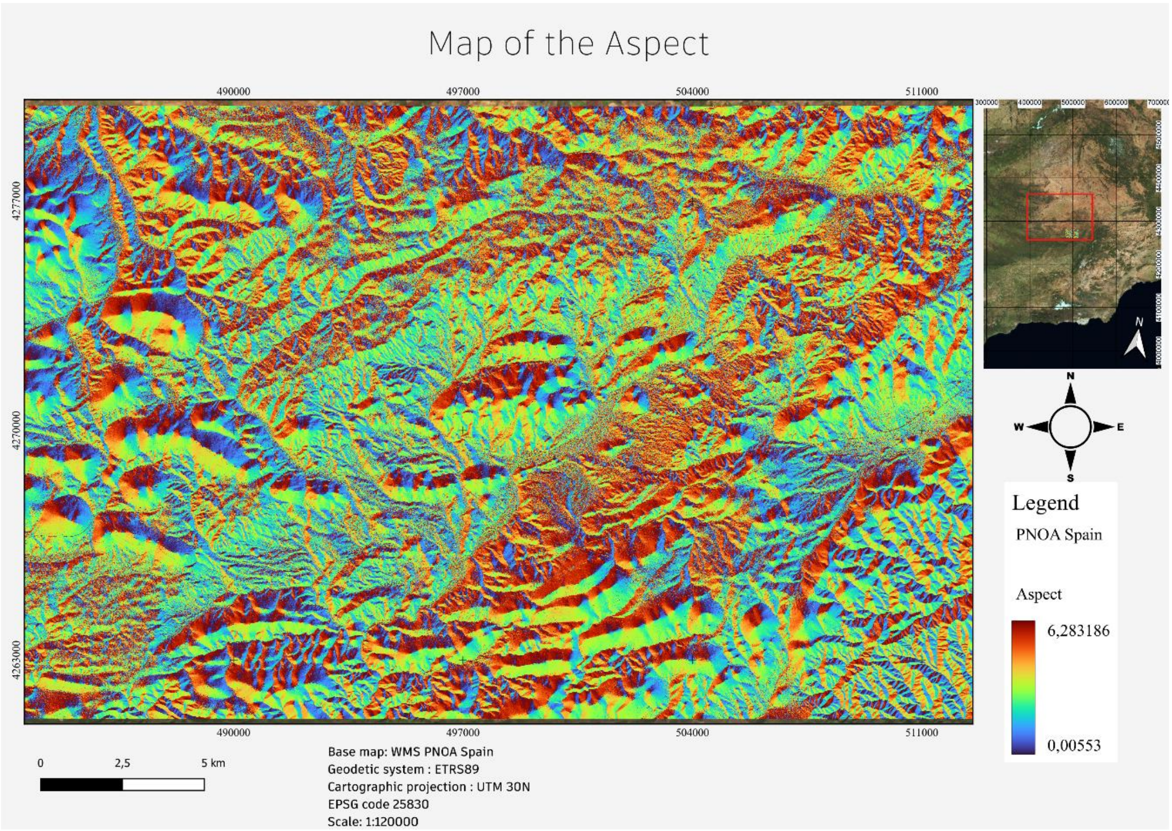

Figure 68: Aspect map of our study area

VI. Conclusion

In this chapter we presented the study area of our project and engaged and detailed the different steps to treat the LIDAR point cloud from the receiving them, passing by the quality control, to the generation of the DTM and the DSM and controlling their quality control.

General Conclusion

During this project, we set a methodology to deal with LIDAR files and treat them passing by the quality control and finally generating the digital terrain and surface models.

We have dialed with a large amount of data which have a different perspective as a workflow and as a method of working. During the quality control we detected a huge error represented by a difference in the strips and in the channels of each strip, using the LASoverlap, difference option, we have been capable of calculating the massive data that cover 527 km² and count over 3 billion points in a matter of minutes. The judgement is based on the specifications set by the IGN of Spain. The gross error identified as a malfunction in the IMU unit that records the behavior of the plane during the acquisition, which causes a misalignment in the data. The error was corrected by the Stripalign software from Bayesmap solutions, it used a different perspective of iterative calculation and a faster gridding algorithm that enclose the correction of the large data in just over an hour of time. We proceeded the quality control of the work by verifying the overlap and detecting the voids.

After the quality control we filtered and classified our point cloud and generated the digital surface and terrain models using the BLASt2dem tool. The Digital terrain model had been under control too, using the hillshade, we controlled the whole area manually in order to detect any anomaly in our product.

This project has been unique for me, with this experience I gained knowledge in the innovative and powerful system LiDAR, and I discovered the other side of handling a real data and encounter a real errors, the error was the keystone of discovering the deep specification and the function of the LiDAR system, which is a necessary to correct the error. Additionally, the quality control represents a huge importance In the process of any LIDAR data use. It also guarantees a trustful data delivery.

Finally, the objective of this project has been attended and the products needed are well delivered, and for it I would like to highlight the importance of the quality control that plays an important role to have a smooth and easy work.

Bibliography

Florant Petit The beginning of lidar- a time travel back in history [Journal] // blickfeld.

National Oceanic and Atmospheric Administration (NOAA) Costal Services Center Lidar introduction [Report]. - 2012.

PNOA Introduction to PNOA [Article].

Wachowicz, M. (2013). *New Frontiers for Geomatics*. Canada: Recuperado de: https://www.gim-international.com/content/article/new-frontiers-for-geomatics

Andre Jalobeanu, Strip Alignment - BayesMap Solutions Guide of Software.

Zhang X H 2007 Airborne Laser Radar Measurement Technology Theory and Method (Wuhan: Wuhan University Press)

Jiang Y S 2001 Remote Sens.5 241-6

Zhang Y T 2012 Airborne LIDAR systems integration and precision calibration error assessment (Qingdao: Shandong University of Science and Technology)

Li S K 2003 Temporal Remote Sensing Information Integration Technology and Application (Beijing: Science Press)

H C Ren et al 2016 IOP Conf. Ser.: Earth Environ. Sci. 46 012030